C.P. No. 955

MINISTRY OF TECHNOLOGY

AERONAUTICAL RESEARCH COUNCIL

CURRENT PAPERS

Measurements at Transonic Speeds of the Side Force and Yawing Moment on Various Store Arrangements Mounted Beneath a 45” Swept Wing-Fuselage Model

BY

P. Marsden, B Sc. (Eng). and A.B. Haines, B.Sc.

LONDON HER MAJESTY'S STATIONERY OFFICE

Price El 0s Od net

C.P. No. 955*

June, 1964.

MEASUREMENTS AT TRANSONIC SPEEDS OF THE SIDEFORCE & YAWING MOMENT ON VARIOUS STORE ARRANGEMENTS MOUNTED BENEATH A 45° SWEPT WING-FUSELAGE MODEL

By

P. Marsden B.Sc(Eng)

A.B. Haines B.Sc

SUMMARY

Tests have been made in the A.R.A. 9ft x 8ft transonic tunnel on a streamlined store-pylon arrangement mounted in various locations beneath a 45° swept wing-fuselage model. Six-component measurements of both the loads on the store including pylon-induced effects, and of the total store plus pylon loads have been obtained for Mach numbers from M = 0.60 to M = 1.41. This note presents the full sideforce and yawing moment results. These are analysed in detail and related to the likely sidewash field beneath the wing at both subsonic and supersonic speeds, as obtained from other sources. The experimental sideforce results are compared with estimates based on the empirical method presented in A.R.A. Report No.5. These comparisons show that certain changes in the empirical method are desirable and appropriate suggestions are made in this note; a final revision will be made when further experimental results are available showing in particular, the effects of changing the depth of the store beneath the wing.

The unpublished results of some ad hoc tests at transonic speeds on winged missiles mounted beneath both a 60° delta and a 40° sweptback wing are given in order to emphasize the dangers in using the empirical method for stores which have significant wing-type lifting surfaces.

---

*Replaces A.R.A. Wind Tunnel Note No. 49 - A.R.C.26 204

LIST OF CONTENTS

/9 I......

LIST OF CONTENTS ctd.

LIST OF FIGURES

LIST OF FIGURES ctd

1. INTRODUCTION

A general review of the-present state of knowledge on the aerodynamic loads on pylon-mounted external stores has recently been published as R. & M.3505 (Ref.?). This showed that much of the existing experimental data had been obtained either at low subsonic speeds or at supersonic Mach numbers such as M = 1.6 - 2.0, with relatively few tests at intermediate speeds, e.g., in the trsnsonic range. This omission is particularly serious since analysis of the data actually available suggests that for many store arrangements, the maximum loads may well occur at transonic speeds. A systematic series of tests has therefore been made in the A.R.A. 9ft x 8ft transonio tunnel on a pylon-mounted external store configuration located in various alternative positions beneath a 45° swept wing-fuselage model. Tests have been made with a store consisting of a simple body of revolution both with and without small tail fins mounted at three alternative chordwise positions at the wing mid semispan station; also, the store without its tail fins was tested at two other spanwise stations. For all these positions, the store was at the same depth below the wing and the store/pylon geometry remained the same throughout, e.g., a change in the store chordwise position meant a change in where the pylon was attached to the wing lower surface. Six-component measurements of both the loads on the store including the pylon-induced effects, and Of the total store plus pylon loads have been obtained for Mach numbers from M = 0.60 to M = 1.41.

The present note gives the full store/pylon sideforce and yawing moment results, together with some indication of tho depth of the side-load centres as deduced from the measured rolling moments. The side load data aro analysed in detail and related to the local flow fields and in particular the local sidewash that is likely to exist beneath the swept wing-fuselage combination. No actual measurements of this local sidewash field were made during the present tests but fortunately, data for both subsonic and supersonic speeds wore availablo, from other sources for a very similar wing-fuselage configuration.

The note also includes comparisons between the measured sideforce data and predictions using the empirical method put forward in Ref.1. These comparisons confirm that the basic features of the empirical method are sound but several of the factors need to be revised in order to improve its general accuracy. Some tentative suggestions as' to how this should be done are included but in this respect, the note should merely be regarded as an interim statement. The experimental programme is to be extended in the near future and it would be preferable to wait for the results of the new tests before making any final revision of the method. In particular, the new tests will include measurements of the loads on stores mounted at different depths below the wing and also at a chordwise position ahead of the wing leading edge at mid semispan; also, comparison will be made between the loads on a store at a given position but supported by pylons of widely differing sweepback.

Despite the need for changes in the empirical method, the present analysis has confirmed the view that there is a place for empirical methods of this type. When finally revised, the method should be useful and reliable in indicating the general trends of the variation of store loads with Mach number and store position but clearly, the accuracy of the results obtained by the method will decrease according to the complexity of the geometry of either the store or the aircraft. In order to emphasise the dangers of using the empirical method outside its proper range of applicability it was thought worthwhile including in the present note some results of store load measurements made in the A.R.A. transonio tunnel on various ad hoc configurations. These are discussed in section 10. In particular, they show that much more thought is needed before the method can be applied to estimate the loads on winged missiles.

Also, an example is included showing how the particular features of the wing-fuselage junction shape on an actual aircraft and the flow around the fuselage can materially affect the loads on stores mounted at least beneath the inner part of the wing. This is a good illustration of how factors that cannot be allowed for easily in an empirical method may nevertheless be very important in practice.

A comment at this point on the justification for generalised programmes such as that described in this note is perhaps opportune. The complex nature of the flow fields beneath swept wing-fuselage combinations at transonic speeds and as just noted, the many factors that can affect the aerodynamic store loads imply that to obtain really accurate quantitative data for a specific installation, wind tunnel tests on the particular layout will probably always be required. Such specific test data are however unlikely to be available at an early stage in the design and it is than that an approximate empirical method based on an analysis of general data is likely to be most useful. A generalized test programme can be justified on three main counts. viz, the extra systematic data that it adds to the literature, the increased accuracy and range of applicability that it brings to the empirical type of method and finally and perhaps most important, the fact that analysis of systematic data should help in understanding what factors are likely to be important and how the store loads are likely to depend on these factors. For example, the analysis in the present note in which the measured store loads are related to the local flow fields beneath the wing of the present tests, coupled with a knowledge of the likely flow fields beneath a wing of different design, e.g., of different sweepback or thickness/chord ratio, should enable one to predict at least qualitatively the loads on similar stores placed in similar positions beneath the other wing. In passing, it may be noted that this may be an easier type of extrapolation than reading across from one store to another beneath the same wing.

2. NOTATION

b	=	wing span
c	=	local wing chord
$\bar{c}$	=	mean aerodynamic chord
c_p	=	pylon chord
C_Y	=	sideforce/q_oF, positive towards fuselage
C_{Y_o}	=	store/pylon sideforce coefficient at $\alpha = \beta = 0^o$
$(C_Y)_\alpha$	=	store/pylon sideforce coefficient at incidence α^o
$(C_Y)_\beta$	=	store/pylon sideforce coefficient at sideslip β^o
$(C_Y)_{\alpha\beta}$	=	store/pylon sideforce coefficient at combined incidence (α^o) and sideslip (β^o)
$dC_Y/d\alpha$	=	rate of change of store/pylon sideforce coefficient with incidence (per deg)
$dC_Y/d\beta$	=	rate of change of store/pylon sideforce coefficient with sideslip (per deg)
C_n	=	yawing moment/q_oFl_s, positive nose inwards, referred to store mid point
C_{n_o}	=	store/pylon yawing moment coefficient at $\alpha = \beta = 0^o$
$dC_n/d\alpha$	=	rate of change of store/pylon yawing moment coefficient with incidence (per deg)
$dC_n/d\beta$	=	rate of change of store/pylon yawing moment coefficient with sideslip (per deg)
C_p	=	pressure coefficient $= p_l - p_o/q_o$
d	=	store maximum diameter

/F = store maximum . . . . .

F = store maximum frontal area = $\frac{\pi d^2}{4}$

K_{n_1}, K_{n_2} etc. = empirical factors for sideforce estimation in Ref.1.

l_s = store overall length

M = freestream Mach number

M_L = local Mach number

p_l = local static pressure

p_o = freestream static pressure

q = local dynamic pressure

q_o = freestream dynamic pressure

R = local store radius

t = wing maximum thickness

x_s = chordwise position of store mid-point from local leading edge, fraction of local wing chord = x/c, positive aft

x/d = chordwise position of store/pylon centre of pressure from store mid-point, expressed in store diameters, positive forward

Y_1 = $\frac{\text{sideforce/unit length}}{q_o \cdot d/2}$

y_s = spanwise position of store mid-point from wing-fuselage centreline, fraction of wing semispan = 2y/b

z_s = depth of store centreline from wing chord plane, expressed in store diameters. For present tests z_s = 1.40d

z/c = vertical distance from wing chord plane, fraction of local wing chord

z/z_{max} = depth of store/pylon centre of pressure from wing chord plane, fraction of store centreline depth z_{max} = 2.22 ins.

α = angle of incidence (degs.), positive nose up

β = angle of sideslip (degs.), positive nose to port.

σ = angle of sidewash (degs.), positive towards wing tip

$\Delta C_{Y_{FINS}} = C_Y$ (fins on) $- C_Y$ (fins off) for (SP) or (S) cases

$\Delta C_{n_{FINS}} = C_n$ (fins on) $- C_n$ (fins off) for (SP) or (S) cases

$\Delta C_{Y_{GAP}} = \Delta C_{Y_{FINS}} (SP) - \Delta C_{Y_{FINS}} (S)$

$\Delta C_{n_{GAP}} = \Delta C_{n_{FINS}} (SP) - \Delta C_{n_{FINS}} (S)$

Suffix (S) denotes store loads in presence of pylon, designated "store plus pylon induced loads", store on port wing pylon attached to wing.

Suffix (SP) denotes total loads measured on the store/pylon assembly, designated "total store plus pylon loads", store on starboard wing; pylon attached to store

Suffix (SW) denotes store loads in the presence of the wing with no pylon

Suffix (ISOL) denotes isolated store loads with no wing or pylon

3. MODEL DETAILS

3.1 Wing-fuselage Combination

The principal dimensions of the wing-fuselage combination used in the tests are given in Fig.1(a).

/The wing has an aspect ratio....

The wing has an aspect ratio of 2.82, a taper ratio of 0.33, 45° sweepback on the 0.5c line and a 6% thick, R.A.E 102 section throughout. It has no warp and is mounted symmetrically on a fuselage of relatively large diameter. This wing-fuselage design has been tested in various transonic tunnels in order to investigate model interference effects[2]; the flow over the wing at Mach number from M = 0.6 to M = 1.6 is described in detail in Ref.3.

The wing planform ("Warren 12") and thickness/chord ratio are typical of the aircraft design for which external store load estimates are likely to be required but the design does not include the features which are needed to maintain subcritical-type flow at transonic speeds, or even to obtain the best possible performance at high subsonic speeds with a wing of this sweepback and thickness/chord ratio. Ref.3 shows that the flow pattern over the wing at Mach numbers near M = 1.0 is very complex. At positive incidences, however, most of the serious flow separation effects are likely to occur above the wing upper surface and hence should not be too significant in the context of the loads on under-wing stores. It was felt therefore that the choice of model should be satisfactory for tine present programme. Some support for this view is afforded by the nature of the results actually obtained in the tests: as will be seen later, no really erratic changes in store loads were observed near M = 1.0. It should be possible to extrapolate the present results to those that might have been obtained on a good transonic aircraft design by considering how the changes in design philosophy are likely to affect the local flow field and particularly, the local sidewash beneath the wing.

No fin or tailplane was fitted to the model. This should have no significant effect on the measured store loads but it detracts from the usefulness of the overall results as measured on the six-component balance inside the fuselage. These overall results are not presented in this note.

Slots were machined in the lower surface of the wing at 0.30, 0.50 and 0.75 semispan, on both port and starboard sides, to provide locations for the stores and space for the balance wiring. The slots were filled with removable-make-up pieces smoothed to the wing contour.

3.2 Store-Pylon Assembly

The store-pylon configurations used on either wing panel were identical, apart from clearance gaps as shown on Fig.1(b). The position of the pylon relative to the store was the same for all chordwise and spanwise positions tested (see Fig.1(c)). As a result, the pylon position relative to the wing varied with store chordwise position, the pylon-wing junction being over the forward half of the wing lower surface when the store centre was below the wing leading edge, and being over the rear half of the wing lower surface when the store mid-point was at x_s = 0.50. The pylon was swept forward (relative to the wing) at an angle of 53.5 (defining this angle such that a vertical pylon would be unwept) and as shown in Fig.1(c), this results in a quite representative arrangement when x_s = 0 but not when x_s = 0.50. In practice, for the position such as $x_s \approx 0.50$, the store would probably be supported by a pylon that was swept back relative to the wing and which was attached to the forward part of the wing lower surface. The swept forward pylon was used in the present tests irrespective of store position mainly in the interests of simplifying the manufacture and rigging; there is however some merit in maintaining the same pylon-store intersection in a systematic test series because then, the pylon-induced effects on the store at a given test condition (M, α, β,) are merely a function of the local wing-induced sidewash field. Even so, the fact that the x_s = 0.50 store position was not combined with the sort of pylon that would probably be used in practice may be important

/The store with....

The store with its tail fins was tested at $x_s = 0$, 0.15 and 0.50 at the wing mid semispan station and also at $x_s = 0$, $y_s = 0.75$ and $x_s = 0.50$, $y_s = 0.30$, (see Fig.1(a)). Also, the store without the tail fins was tested at the same three positions at mid semispan.

For all test locations, the store centreline was at 1.40 store diameters below the wing chordal plane and the appropriate values of z/c are 0.140, 0.168 and 0.226 for $y_s = 0.30$, 0.50 and 0.75 respectively. The issue as to whether to vary y_s at constant z as in the present tests or at constant (z/c) is somewhat difficult to resolve. (z/c) may appear a sensible parameter at first sight but this is not necessarily the case; for example, it will be seen later when considering the local sidewash fields that at supersonic speeds, z may be the more appropriate parameter. Even at subsonic speeds, it could be argued that a spanwise traverse at constant (z/c) below a tapered wing will not give the effects of y_s alone unless the store size were also varied with spanwise position so as to maintain a constant value for the ratio of store diameter/local wing chord. In essence, this means that for a tapered wing, changes in y usually imply changes in quite a number of other variables, and hence, the &averse at constant z as in the present tests is probably Just as suitable as any other proposal, provided due allowance is made for this when analysing the results.

3.2.1 Store

The streamlined store, length 13.176", max.diameter 1.586", fineness ratio 8.32, was constructed to the following ordinates, (see Fig.1(b));

X"	0.25	0.50	0.75	1.00	1.25	1.50	1.75	2.0	2.5	3.0
R"	0.150	0.240	0.313	0.372	0.427	0.478	0.526	0.567	0.637	0.687
X"	3.50	4.00	4.50	5.00	5.50	6.00	6.50	7.00	7.50	0.00
R"	0.728	0.757	0 777	0.790	0.793	0.787	0.780	0.760	0.730	0.693
X"	9.00	9.50	10.00	10.50	11 00	11.50	12.00	12.50	13.00	13.176
R"	0.620	0.577	0.527	0.474	0.4221	0.367	0.313	0.2501	0.181	0.176

The store was tested with and without small cruciform tail fins. The dimensions of the fins are given in Fig.1(b). The fins were positioned at 45° to the vertical. The quarter-chord point of the mean aerodynamic chord of the fins is $0.414 l_s$ aft of the store mid-point.

Pylon

The pylon was untapered and swept forward relative to the wing at an angle of 53.5' (this angle being defined such that a vertical pylon would be unswept). The pylon chord was equal to half the store length. The aerofoil section was basically R.A.E.102, 5% thick based on a chord of 7.900" but was truncated at 6.588" to give a thick trailing edge. The thickness/chord ratio based on the actual pylon chord was 6% (see Fig.1(b)).

3.2.3 Mechanical Details

The stores on either wing panel were attached to the undersurface of the wing by means of a six-component strain gauge balance and a strut which as shown in Fig.1(b), passed through the hollow pylon with a small clearance gap on all sides. On the port wing, the pylon was attached to the wing and not to the store and thus, the balance measured the loads on the store in the presence of the pylon and the wing (these are referred to subsequently as the STORE PLUS PYLON-INDUCED (S) LOADS.) On the starboard wing, the pylon was attached to the store but not to the wing so that the balance on this side measured the loads acting on the full store/pylon assembly in

/the presence of... .

the presence of the wing (these are referred to as the TOTAL STORE PLUS PYLON (SP) LOADS). A clearance gap of about 1/16" was provided between the store and the bottom of the pylon for the (S) case, and between the top of the pylon and the wing for the (SP) case. It was felt that these gaps would not be large enough to have any substantial effect on the measured loads. Analysis of the results show that the fin contribution to the loads is as much as 20% higher from the (SP) results as compared with the (S) results. The major part of this difference is probably due to the forward effect of the fins on the pylon load and without further tests it is impossible to separate this from any effects due to the gap in the pylon-store junction which might have caused disturbed flow over the fins in the (S) case. In any case of doubt the results for the (SP) case should be the most reliable.

4. DETAILS OF TESTS

As noted above, tests on the store with its tail fins were made at five alternative locations as shown in Fig.1(a): at $x_s = 0$, 0.15 and 0.50 for $y_s = 0.50$, and at $x_s = 0.50$, $y_s = 0.30$ and at $x_s = 0$, $y_s = 0.75$. Also, the store without fins was tested at the three locations at mid semispan.

For most of these configurations, tests were tide at nominal Mach numbers of 0.60, 0.90, 0.96, 1.02, 1.20 and 1.41. A few tests were also made at $M_{nom} = 0.80$, 0.99 and 1.10 to confirm that the Mach-number values chosen for the main test programme were adequate to define the transonic trends in the variation of store loads with Mach number. The tests were made at a stagnation pressure of 1 atmosphere and the Reynolds number based on the wing mean chord varied from about 4.0×10^6 at $M = 0.60$ to about 5.0×10^6 at $M = 0.90$ and above. An incidence range from -3° to $+12^\circ$ at $\beta = 0^\circ$ and a sideslip range of $\pm 5^\circ$ at $\alpha = 0^\circ, 6^\circ$ and 12° was covered at each Mach number for each store configuration.,

Transition was fixed with bends of 0.004" - 0.005" Ballotini in Araldite as follows :

(a) On the wing: round the leading edge and back to 0.10c on both surfaces,

(b) On the fuselage: a band round the nose, 1½" wide, centred 5" from the apex,

(c) On the pylons: from 0.05c to 0.100 on both surfaces,

(d) On the stores: a band round the nose, ⅛" wide, centred ½" from apex,

(e) On the store fins: from 0.05c to 0.10c on both surfaces of all fins.

In addition to the test configurations quoted above, an additional test was made on the clean wing-fuselage with no stores or pylons. This was to determine the incremental effect of the stores on the overall aerodynamic characteristics of the complete configuration. These data are however not included in the present note.

5. ACCURACY & REDUCTION OF RESULTS

Appropriate tunnel constraint corrections to model incidence were applied but no corrections were made for the effects of model blockage on Mach number and dynamic pressure. Near $M = 1.0$, the nominal Mach numbers should be corrected for model blockage: earlier tests on various models of this particular wing-fuselage configuration showed that $M_{nom} = 0.96$ should correspond to about $M_{corrected} = 0.945$, $M_{nom} = 0.99$ to about $M_{corr} = 0.97$ and $M_{nom} = 1.02$ to about $M_{corr} = 0.99$, with the other Mach numbers of the

/present tests.....

present tests being unaffected. Corresponding corrections should really have been applied to the dynamic pressure but this omission should not have any marked effect on the conclusions drawn from the present test data.

The angles of incidence and sideslip have been corrected for the deflection of the main sting and balance under load. No allowance has been made for the small deflections of the store/pylon assemblies under load, or for the interference effects caused by the gaps at the store-pylon and pylon-wing junctions. As noted earlier, the gaps at the store-pylon junctions may have some effect on the flow over the aft part of the store. Hence it would be better to determine the fin contributions from the (SP) loads, remembering that these will then include any forward effects of the fins on the load on the pylon.

The accuracy of the results in coefficient form varies with Mach number owing to the associated changes in dynamic pressure. Based on the repeatability of results and a component instrument resolution of ±2 digitizer counts, the balance sensitivities are such that the general accuracy of the present results is believed to be as follows for both (S) and (SP) loads:

M	0.60	1.02	1.41
C_Y	±0.027	±0.014	±0.012
C_n	±0.0022	±0.0012	±0.0010

More scatter than this was observed for the (SP) loads for the test on the unfinned store at $x_s = 0.50$, $y_s = 0.50$; however, it was found after this test that the pylon mounting was somewhat loose. Despite the increased scatter, the mean curves drawn through the results of this particular test should still be reasonable.

6. PRESENTATION OF MEASURED LOAD DATA

The basic store and store/pylon sideforce and yawing moment data plotted against incidence and sideslip for the various store locations are presented in Figs.2 - 9. The variation of C_{Y_S} and $C_{Y_{SP}}$ (fins on and off) with incidence is given in Fig.2 for the three chordwise locations at mid semispan and the results for the three spanwise positions are compared in Fig.4. Figs.6 and 8 show the variation with sideslip for various incidences and store locations. The corresponding yawing moment data are given in Figs.3, 5, 7 and 9 for the same range of variables.

It should be noted that the (S) balance is located on the port and the (SP) balance on the starboard wing. This is immaterial when considering the variation of sideforce with incidence at zero sideslip; but it is important when considering sideslip effects. For instance, positive sideslip (nose to port) at zero incidence produces negative (outward) sideforce on a store located on the rearward (port) wing panel, and positive (inward) sideforce on a store located on the forward (starboard) wing panel. This is a function of the chosen sign convention because the sideforce on either store is actually acting in the same direction (i.e. to port for positive sideslip). It is convenient therefore when presenting the variation of sideforce with sideslip to plot the (S) and (SP) results together on one sheet but it must be remembered that the results are obtained from stores on different wing panels. The loads measured on a port store at positive sideslip are equivalent to those measured on a starboard store at negative sideslip.

/It will be seen:.....

It will be seen from Figs.2, 4, 6 and 8 that except at negative incidence, for both the (S) and (SP) loads, the sideforce varies in an approximately linear manner with both incidence and sideslip for all the configurations tested and over the full Mach number range of the tests. The data can therefore be analysed in terms of three quantities, C_{Y_o} (i.e. the sideforce at $\alpha = \beta = 0^o$), $dC_Y/d\alpha$, and $dC_Y/d\beta$. The variation of these quantities with Mach number and store location are plotted in Figs.10, 11 and 12 respectively. $dC_Y/d\beta$ has to be treated as a function of incidence and so values are shown in Fig.12 for $\alpha = 0^o$, 6.5^o and 12.9^o.

In contrast to the sideforce data, the variation of C_n with incidence can be very non-linear, particularly when the store has tail fins. The variation with sideslip is still reasonably linear, or to be more precise, the values for negative sideslip are similar to those for positive sideslip. Values of C_{n_o}, $dC_n/d\alpha$ and $dC_n/d\beta$ are presented in Figs.13, 14 and 15 respectively. Since $dC_n/d\alpha$ varies with α, two sets of values are plotted in Fig.14 corresponding respectively to $\alpha = 0^o$ and to high positive incidences.

The values of Cn as presented here are referred to the store mid-point. This is clearly a suitable choice when considering the moment of the (S) loads about the pylon-store fixation but it is not necessarily relevant when considering the moment of the (SP) loads about the pylon-wing fixation. As it happens, however, for the present configurations, the store mid-point lies immediately below the leading edge of the pylon at its junction with the wing and so this is still quite a reasonable choice as the x - coordinate reference centre. If this is indeed the case for a practical installation, Figs.3, 5, 7 and 9 show that the maximum values of C_n for a given store configuration can be estimated if one knows C_{n_o}, $(dC_n/d\alpha)_{\alpha = 0^o}$ and $dC_n/d\beta$. This is certainly true for the finned stores for which increasing positive incidence nearly always tends to reduce the values of C_n. This is therefore the justification for presenting the data in the form of Figs.13, 14 and 15.

It is arguable that a more appropriate moment reference centre for the (SP) loads might be the quarter-chord point of the pylon at its junction with the wing. Examination of the data shows that this would tend to increase the chance that critical (positive) yawing moments might be encountered at large positive incidences. On the whole, however, it would appear unlikely that this change of moment centre would materially alter the conclusions derived directly from the yawing moment data as plotted in this note.

Nevertheless it is clear that the fact that the variation of C_n with incidence can be markedly non-linear and the possibility that more than one moment reference centre may be significant for a given practical installation complicates the analysis of the yawing moment data. Instead of just considering the values of C_n about a particular moment centre, it may be better to think in terms of the following three quantities : C_{n_o}, the derived positions for the centre of load and finally, the maximum values of C_Y. Fig.16 shows how the fore-and-aft centre of load typically varies with incidence at a given Mach number; data derived from the (SP) loads, fins off or on, are given for the three store chordwise positions at mid semispan at three test Mach numbers. It will be seen that the position of the centre of load becomes somewhat indeterminate at a small positive incidence; this condition corresponds to where $C_Y = 0$, i.e., the incidence contribution to C_Y is just sufficient to cancel the C_{Y_o} term. At higher positive incidences, the general tendency is for the axial position of the centre of load to approach the store mid-point. If this is the appropriate moment centre from a stressing point of view, it follows that the critical stressing case could well correspond to a moderate positive incidence rather than a maximum positive incidence. For this reason, it was decided to choose $\alpha = 6.5°$ as as typical incidence for which to show how the position of the centre of load varies with Mach number. This variation is plotted in Fig.17 for both the, (S) and (SP) loads, fins on or off., This figure should not be used too indiscriminately. It should be remembered that as noted earlier, the maximum values of C_n for a given installation are likely to depend principally on the values of C_{n_0} and $dC_n/d\beta$; at positive incidences, the contribution due to incidence will generally tend to reduce the mom&t.*, it is only at negative incidence that this-term will have to be added to the other two and then, as shown in Fig.16, the position of the centre of load may be quite different from the-results plotted for $\alpha = 6.5°$ in Fig.17.

The product of the sideforce on the store/pylon and the depth of the centre of load below the pylon-wing fixation gives the root bending moment about this fixation and so to complete the picture, Figs.18 and 19 provide. some typical data for the depthwise position of the centre of load on the full store/pylon assembly, These positions are obtained by dividing the measured rolling moments on the store/pylon by the measured sideforce values. In Fig.18, the depth of the store load centre, non-dimensionalised with respect to z_{max}, the distance between the store centre-line and the wing chord plane, is plotted against incidence for three test Mach numbers while in Fig.19, the variation with Mach number is shown for the maximum test incidence, 12.9°. A comparison is provided between the results for the three store chordwise positions at mid semispan.. Figs.18 and 19 are effectively the s-equivalents of the x-pictures of Figs.16 and 17. The only distinction is that when considering the s-load centre and hence the bending moment about the pylon-wing fixation, it seems reasonable to assume that the critical stressing case will correspond to an extreme incidence condition; this contrasts sith the argument put forward earlier for considering an intermediate incidence when dealing with the yawing moment data.. This is the reason for choosing $\alpha = 12.9°$ as a suitable incidence in Fig.19 rather than $\alpha = 6.5°$ as in Fig.17.*

The centre of the (S) load on the stores with tail fins can-lie below the mean plane of the store whereas with the unfinned stores, the opposite tendency is apparent. The effect of the fins is similar when one considers the (SP) load centres: The effect is presumably due to interference between the pylon wake and the upper fins resulting in the load on the upper fins being less than the load on the lower fins. This result is important because it tends to increase the bending moments for the finned store about both the pylon-wing and the pylon-store fixations.

7. SUPPLEMENTARY DATA TO HELP IN THE ANALYSIS OF RESULTS

7.1 Local Flow Field Data

No actual measurements were made of the local flow fields beneath the wing-fuselage configuration of the present tests. Fortunately, however, data were available from N.A.S.A. sources for a fairly similar wing-fuselage layout. The two designs are compared in Fig.20; for convenience, the wing-fuselage of the present tests is referred to in the subsequent discussion as the "A.R.A. wing-fuselage". It will be seen that there are differences between the two designs in the wing aspect ratio, taper ratio, leading-edge sweep and in the ratio of fuselage diameter to wing span, These differences will have some effect on the absolute values of the local sidewash and dynamic pressure below the wing but the flow fields should still be similar qualitatively - at least for the Mach-number range for which the wing leading edge remains subsonic.

---

* One should not rule out the possibility that for the operational envelope of an actual aircraft, the negative-g case could possibly produce the more serious stressing condition, but this would not be true of the incidence range of the present tests which did not extend below $\alpha = -3°$.

/Local flow field data...

Local flow field data for the N.A.S.A. wing are available for both subsonic and supersonic speeds. Ref.4 gives data obtained at 100 m.p.h. in the Langley 7ft x 10ft tunnel while Ref.5 gives data obtained at M = 1.61 and 2.01 for the same wing but with a slightly different fuselage (see Fig.20). The important question is whether the results obtained for the N.A.S.B. wing at M = 1.61, when according to linear theory; its leading edge should be supersonic, are really relevant to the analysis of the present test data bearing in mind that throughout the test Mach-number range up to M = 1.41, there is no doubt that the leading edge of the A.R.A. wing would be subsonic; However, the Schliezen photographs in Ref.6 show that the leading-edge shock of the N.A S.A. wing is still detached at M = 1.61. This is confirmed by the local flow field data reproduced in the present note, e.g. the contours of local Mach number as plotted in Fig.21. It is explained in Ref.6 that the leading-edge shock is still detached at M = 1.61 because of the effects of the finite wing thickness. It is shown that for wings of the present thickness/chord ratio and sweepback, one can assume that the flow field that actually exists at say, M = 1.60 roughly corresponds with what would be predicted by linear theory for II = 1.40. It follows that the flow field data obtained at M = 1.61 can be used as a general guide to the local flow conditions under the A.R.A. wing at the supersonic Mach numbers in the present tests. The only point to remember is that whereas at subsonic speeds, one would make the comparison at a given x/c, 2y/b and z/c, the comparison at supersonic speeds should be made for points which are in about the same position relative to the wing leading-edge and trailing-edge shock fronts. This has several implications: one should consider the nett wing rather than the gross wing; the coordinates z and y should strictly be measured from the Mach-line through the wing root leading edge and finally, z is more significant than z/c. This last point is particularly significant for a tapered wing; in Fig.21, lines at a constant z of 2.1" are included on the three pictures to illustrate how z/c for a given z varies across the span.

Since the flow field data from the N.A.S.A. tests are only being used as a general guide, the actual accuracy of the basic data is not too important but for the record, it should perhaps be quoted hers. Ref.4 states that the measured sidewash values obtained in the tests at low speeds should be reliable to an accuracy of better than $\pm 1.5^{\circ}$, and the local dynamic pressure ratios should be within ± 0.025. Ref.5 quotes the accuracy of the supersonic tests in the form that the total local flow angularity (which can be taken as approximately $\sqrt{2}$ x the local sidewash) should be given to about ±10% with an added uncertainty in the region of the leading-edge and trailing-edge shock waves. The sidewash contours etc. included in the present note should be accurate to a better standard than just quoted because of the effective smoothing of the data implicit in the drawing of these contours.

Information derived from the N.A.S.A. flow-field data is given in Figs. 21-27. It should be emphasized that these particular figures, e.g., the sidewash contours were not presented in the original references; they have been derived by suitable cross-plotting and interpolation. Also, the results are analysed in greater detail than in the original references.

An alternative to using the N.A.S.A. experimental data would have been to calculate directly, e.g., by Refs. 4, 7 and 8, the local flow field beneath the A.R.A. wing-fuselage. As explained in Ref.1, however, this can be very laborious and the end-product is often still only accurate enough for a qualitative estimate of the store loads. Hence it was not attempted in the present case except that some estimates were made of the sidewash due to incidence at supersonic speeds using the charts of Ref.7. These are given in Fig.26 and discussed below in section 7.1.2. Several reasons can be put forward as to why even when one knows the local flow field accurately, one can still only obtain moderate estimates of the loads on stores placed in these flow fields. For example, no allowance is usually made for the effect of a pylon on the flow field; also, as shorn in Figs.22, 24, there can be very rapid changes in the local sidewash over

/a very short distance....

a very short distance particularly in the x-direction and hence it is difficult to obtain sensible mean values; again, the direction of flow over the rear of a store and its tail fins my depend significantly not merely on the local sidewash induced by the wing-fuselage at the position of the fins but also on the local sidewash acting over the nose of the store. To help in understanding how a typical local flow field can induce a load distribution along the length of a store, an example has been extracted from Ref. 9, plotted in Fig.28 and discussed below in section 7.2.

The main features of the local flow field data presented in Figs. 21 - 27 are considered under three headings : the sidewash at zero incidence (7.1.1), the sidewash due to incidence (7.1.2) and the local dynamic pressure (7.1.3).

7.1.1 Local Sidewash At Zero Incidence

Fig.22 illustrates how the local sidewash near mid semispan varies with depth below tne wing at both subsonic and supersonic speeds. It is clear that, as would be expected, a close correlation exists between the contours of constant sidewash and what one might expect to find as the contours of local Mach number. Important distinctions can be drawn as follows between the local sidewash at subsonic and at supersonic speeds, viz,

(1) At subsonic speeds, ring-induced sidewash is present well ahead of the wing leading edge (and also, although this is less important in the present context, well downstream of the trailing edge). At supersonic speeds, wing-induced sidewash is confined to the region between the wing leading- and trailing-edge shocks,

(2) At subsonic speeds, the local flow field dies out below tine wing in a direction normal to the wing chord but at supersonic speeds, the flow field is propagated rearward and downward in the directions of the local Mach-lines. This can be seen by comparing the contours of constant sidewash in Fig.22(b) with those of local Mach number in Fig.21(b),

(3) The rate of decay of the local flow field with depth below the wing is more rapid at subsonic than at supersonic speeds. For example, in Fig.22, at say, $z/c = 0.6$, the local sidewash induced by the wing at low speeds would not be greater than about $\pm 0.5^{\circ}$ at any chordwise positions whereas at $M = 1.61$, values ranging from -3.5° to -1.3° are observed,

(4) Except possibly very close to the wing surface, the local angles of sidewash are much greater at $M = 1.61$ than at low subsonic saeeds. Positive sidewash, i.e. flow out towards the wing tip, is observed ahead of either the leading edge (subsonic speeds) or the Mach-line originating from near the leading edge (supersonic speeds), i.e. between the leading-edge shock, and the Mach line from the leading edge. Aft of this, the local sidewash is negative with the maximum values being observed roughly below the wing maximum thickness at subsonic speeds but just ahead of the wing trailing-edge shock at supersonic speeds. For a typical store depth of say $z/c = 0.2$, the maximum positive and negative values of local sidewash are near $\pm 1.5^{\circ}$ at low speeds but are as high as $+6^{\circ}$ and -3° at $M = 1.61$. On the other hand, the variation of local sidewash with chordwise position is much greater at supersonic speeds and therefore it is likely that for many stores, the effective mean values of sidewash would not show the same order of increase between subsonic and supersonic speeds.

It is evident that not only is the sidewash distribution over a store likely to vary significantly with Mach number but also such variations are closely dependent on the store depth and chordwise position. To take just one illustration of this point, let us consider the effect of increasing the depth of a store having its nose just ahead of the wing leading edge and its

/tail fins below....

tailfins below the wing maximum thickness. At subsonic speeds, the sidewash over the store nose would decrease monotonically with increasing store depth but at supersonic speeds, the sidewash would first decrease and then suddenly vanish altogether as the store nose protruded ahead of the leading-edge shock. The sidewash over the tail fins would also decrease monotonically with increasing store depth at subsonic speeds but at supersonic speeds, it would not only decrease but would ultimately change sign becoming positive rather than negative.

Fig.23 shows how the local sidewash is likely to vary with spanwise position. The contours of constant sidewash at subsonic speeds are plotted for a constant z/c (0.15) while for M = 1.61, they are plotted for a constant value of z which corresponds to z/c = 0.276 at 0.25 x semispan or 0.56 at 0.85 x semispan (owing to the wing taper). It will be seen that at low subsonic speeds, the local sidewash tends to decrease with movement out from the mid semispan position. This is in striking contrast with the results for M = 1.61 which show that both the maximum positive sidewash downstream of the wing leading-edge shock and the maximum negative sidewash upstream of the wing trailing-edge shock increase greatly as one moves out across the span. Comparing the values for y_s = 0.25 and 0.85, these increase from 3° to 8° and from $-\frac{1}{2}$° to $-2\frac{1}{2}$° respectively. It should be noted that the chordwise distribution of local sidewash at supersonic speeds depends on the position of the wing leading-edge and trailing-edge shock waves. This means that at low supersonic speeds, when the leading-edge shock is lying well ahead of the wing leading edge, the maximum positive sidewash will occur further ahead of the leading edge at the outer spanwise positions. This would have been even more apparent if the contours had been plotted for a given z/c rather than a given z. It does not necessarily follow therefore that the mean effective sidewash over the store at a certain depth and chordwise position would increase as the store was moved outward but it is clear that this is likely to happen in many cases.

7.1.2 Sidewash Due To Incidence

Figs.24 and 25 present data for $\alpha = 8°$ corresponding to the results in Figs.22 and 23 respectively for $\alpha = 0°$. Unfortunately, the tests at M = 1.61 and $\alpha = 8°$ only provided data for one particular depth below the wing (z/c = 0.37 at y_s = 0.55). The contours in Fig.24(b) can therefore only be drawn locally near this particular depth and even then, only by analogy with Fig.22 (b). To supplement these sparse supersonic data, therefore, estimates were made of the sidewash due to incidence at M = 1.41 under the A.R.A. wing, using the charts of Ref.7 The results are shown in Fig.26. These charts are based on linear theory and hence as noted earlier, these values derived for M = 1.41 should be reasonably consistent with the experimental data for M = 1.61 now being discussed. To obtain data corresponding to the loads on stores underneath the A.R.A. wing at M = 1.41, the calculations should have been made for a lower Mach number. These extra calculations have not been carried out but it is easy to see that the main difference from the results presented here would arise from the lower sweep of the leading-edge and trailing-edge shock fronts.

Many of the differences between the flow patterns at subsonic and supersonic speeds already noted for $\alpha = 0°$ continue to apply in the results for $\alpha = 8°$. For example, at subsonic speeds, the wing-induced sidewash still amounts to about 3° at 0.5c ahead of the wing leading edge - the forward limit of the present test data - and it is unlikely to be insignificant until 1.5c ahead of the leading edge whereas at supersonic speeds, it is confined to the region downstream of the wing leading-edge shock. *

* Strictly, the test results for M = 1.61 indicated a local sidewash of about -2° ahead of the wing leading-edge shock and downstream of the wing trailing-edge shock but this is presumably the sidewash induced by the incidence of the fuselage.

/The later analysis.....

The later analysis of the store load data will be based on quantities such as C_{Y_0} and $dC_Y/d\alpha$ rather than the values of C_Y at say, $\alpha = 8^o$. It is appropriate therefore to refer primarily to the values of (c/a) rather than to the values of σ at $\alpha = 8^o$. First, the values of (σ/α) are everywhere positive, i.e. flow outward towards the wing tip. The maximum values of (U/a) occur below the wing leading edge at subsonic speeds and near the Mach-line originating from the wing leading edge at supersonic speeds. It is in these regions that the values are most sensitive to the depth below the wing. For example, Fig.26(b) shows that at ys = 0.50, a change from z/c = 0.140 to z/c = 0.226 can reduce the maximum value of (σ/α) derived for M = 1.41 by about 30%; the effects aft of about mid-chord are fairly small. At subsonic speeds, the variation in (c/a) with depth would tend to be rather greater than at supersonic speeds.

Within the range of the available data, the values of (σ/α) tend to increase with distance out along the span. This trend is more pronounced at supersonic speeds. For example, Fig.26 shows that in a traverse at the constant depth selected for the store positions of the present test investigation, the maximum values of (c/a) increased from about 0.32 at $y_s = 0.30$ to about 0.84 at $y_s = 0.75$. If the traverse had been made at constant z/c, the increase would have been even greater, i.e. from about 0.32 to about 1.00.

These effects of spanwise position do not merely apply near the wing leading edge; they persist over the whole range of chordwise positions for which there is any wing-induced sidewash. For example, they would affect the loads on the tail fins of the store. Fig.26(a,c) includes lines showing the locus of the quarter-chord point of the store fins when the store is moved spanwise at $x_s = 0$. Due to the wing taper, this point moves from 0.35c at $y_s = 0.30$ through 0.410 at $y_s = 0.50$ to 0.55c at $y_s = 0.75$. Despite this rearward movement, Fig.26 shows that (c/a) still increases considerably with movement out along this locus.

The contours of constant sidewash at a = 8^o as plotted in Figs.24, 25 depend on the relative contributions from the sidewash at zero incidence and the sidewash due to incidence. The relative proportion of these two contributions is not the same at supersonic as at subsonic speeds and this leads to certain differences in the final results. For example, the maximum sidewash at a = 8^o occurs below the wing leading edge at subsonic speeds in sympathy with the variation in the values of σ/α); at M = 1.61, however, the maximum values still tend to appear just downstream of the wing leading-edge shock because of the high values already present in this region at zero incidence. The effects of spanwise position could be analysed in a similar manner e.g., at subsonic speeds, the changes between the results for $y_s = 0.50$ and $y_s = 0.75$ at a = 0^o, tend to oppose the changes due to incidence whereas at supersonic speeds, the effects tend to be additive.

7.1.3 Local Dynamic Pressure

Typical results for low subsonic speeds extracted from Ref.4 are presented in Fig.27. The top figure shows the variation in dynamic pressure ratio with chordwise position and incidence at z/c = 0.15, $y_s = 0.50$, while the bottom figure gives the variation with (z/c) at a = 0^o.

At zero incidence, over most of the chord, the local dynamic pressure is higher than the freestream value, reaching a maximum below the wing maximum thickness; for z/c = 0.15, this maximum amounts to about 1.10. With increasing positive incidence, the local dynamic pressure below the wing is reduced with the minimum values occurring below the wing leading edge. By a = 8^o, the minimum for z/c = 0.15 is about 0.82. Similarly, at negative incidence, the opposite trend is observed and by a = -8^o, values

/ for (q/q_o) greater than..

for (q/q_o) greater than 1.25 are obtained over all the forward part of the chord at $z/c = 0.15$ with a local maximum as high as 1.50.

It follows that the variation of the local dynamic pressure ratio with incidence will tend to reduce the store side loads at positive incidence but increase them at negative incidence. This is one of the reasons why the negative-g condition should not be forgotten when assessing what might be the critical stressing cases for a given store installation.

No figure is presented for the local dynamic pressure ratios at super-, sonic speeds. Analysis of the data in Ref.5 suggests however that except possibly in the regions of the leading-edge and trailing-edge shockwaves, the dynamic pressure ratios are then much closer to 1.0 than those shown in Fig.27 for subsonic speeds. At supersonic speeds, therefore, it is reasonable to relate the store side loads with just the local sidewash distributions.

7.2 Typical Side Load Distributions On Underwing Stores

The discussion above has shown that the local wing-induced sidewash and the dynamic pressure is likely to vary considerably along the length of a store mounted underneath a sweptback wing. Hence, even when the sidewash distribution is known, it may be difficult to estimate the side load distribution and hence the overall sideforce and yawing moment on a store/pylon assembly. This is the correlation that is attempted later in section 8 when analysing the store load measurements of the present tests. Since these did not actually include any pressure plotting on the store and hence any side load distributions, it seemed worthwhile reproducing some results from Ref. 9 to serve as a background for some of the remarks in section 8. These side load distributions were obtained at low subsonic speeds and typical results are presented in Fig.28. A streamlined store of fineness ratio 6.5 without tail fins was first tested in isolation at $\alpha = 0^\circ$, $\beta = -5^\circ$. It was then positioned at 0.25c beneath the mid semispan section of an 8.5% thick, 40° swept port wing panel with the store mid-point at 0.112c behind the local wing leading edge, and sideforce distributions were obtained at $\alpha = \beta = 0^\circ$; $\alpha = 0^\circ, \beta = -5^\circ$; and $\alpha = 8^\circ$, $\beta = 0^\circ$. Finally, the store was attached to the wing by means of an unswept pylon of chord 0.295c with the pylon leading edge coincident with the wing leading edge, (see sketch on Fig.28).

The distribution of side load on a store in isolation at an angle of sideslip β will depend on the store shape. For a store with an ogival nose and tail, with a cylindrical centre section, potential flow theory for bodies of revolution predicts that the nose and tail carry loads of equal magnitude but in opposite directions whilst the cylindrical section carries no load. Hence according to potential flow theory, the side load on such a store would be zero but there would be a large yawing moment. Viscous flow effects modify this theoretical loading over the tail of the store and as shown by the curve for the isolated store at $\beta = -5^\circ$ in Fig.28(b) the loading over the rear is then insufficient to compensate for the loading over the nose of the store.* Integration of this distribution for the isolated store gives $C_{Y_{ISOL}} = 0.064$ and $C_{n_{ISOL}} = 0.085$ (relative to the store mid-point as the moment reference centre) and the centre of pressure at about 0.83 store lengths ahead of the nose of the store.

When the store is positioned beneath the 40° swept wing, Fig.28(a) shows that at $\alpha = 0^\circ$, $\beta = 0^\circ$, the wing-induced store side load is already of considerable magnitude. Over the nose of the store, the load is negative because of the positive sidewash (Fig.22(a)). Over the mid-part of the store where the side load is greatest, the load is positive partly because the sidewash aft of the wing leading edge is negative (Fig.22(a)) and partly as a consequence of the positive sidewash over the nose of the store -

* A method for the estimation of the loads on isolated stores of similar shape is given in Ref.10.

/ - this interrelation is deduced...

- this interrelation is deduced from the load distribution on the isolated store. Towards the rear of the store, the load decreases and ultimately again changes sign; these trends are partly due to the decrease in local sidewash towards the wing trailing edge and partly because of boundary-layer effects related to the pressure gradients over the mid-part of the store.- Integration of this load distribution given in Fig.23(a) gives $C_{Y_{SW}}$ = 0.11 and $C_{n_{SW}}$ = 0 -for $\alpha = \beta = 0^o$. Most of the side load in this example is induced near the store mid-point giving zero resultant yawing moment but this is a function of the particular position of the store relative to the wing. A change in this position would modify the side load distribution. The addition of the pylon to the store at $\alpha = \beta = 0^o$ gives a pylon-induced load over the store downstream of a point just ahead of the pylon leading edge. The sign of this pylon-induced load is positive as would be expected since the local sidewash over the pylon is negative (Fig.22(a)) and the magnitude of the pylon-induced load should be a direct function of the magnitude of the local sidewash near the pylon-store junction.

The wing- and pylon-induced effects are almost independent of sideslip as can be seen by comparing the wing- and pylon-induced load distributions in Fig.28(b) for $\alpha = 0^o$, $\beta = -5^o$ with those for $\alpha = \beta = 0^o$ given above.

Fig.28(c) shows how the wing-induced effects increase as the incidence is increased to 8^o. For the store in isolation, there would of course be no side load at $\alpha = 8^o$, $\beta = 0^o$ and therefore the curve marked "no pylon" shows the wing-induced effects. The form of this curve is opposite to that shown above for $\alpha = 0^o$, $\beta = -5^o$ and this is because the local sidewash over the store is positive (Fig.24(a)). Its shape is different in detail however with much larger local load values near x = 0.3 - 0.4l_s followed by a more rapid change to a load of the opposite sign. These detailed differences correlate with the fact that the local sidewash will reach a maximum near x = 0.4l_s because this point is below the wing leading-edge; Similarly, it is the decrease in the local angles of sidewash towards the rear of the store that accounts for the more pronounced reduction in the loads in this region as compared with the distribution for the isolated store. The load distribution as shown in Fig.28(c) is therefore clearly a function of the store chordwise position and would be modified if this position were changed. Despite the non-uniform nature of the flow field, it should be possible to derive a qualitative idea of the load distribution from the local sidewash distribution together with the side load distribution on the isolated store. It is important to realise however that except near the nose of the store, there is not just a simple correlation between the local sidewash and the local side load at a given point; the load over the rear of the store depends not merely on the local flow conditions but also on conditions over the nose.

The pylon-induced load distribution changes sign between $\alpha = 0^o$ and $\alpha = 8^o$; the negative load at $\alpha = 8^o$ is associated with the large positive sidewash in the region of the pylon-store junction (Fig.24(b)). Comparison of Fig.28(a) and (c) show that the pylon is likely to give a large increase in the absolute value of $dC_{Y_S}/d\alpha$ but since the main effects are confined to the region of the pylon-wing junction which is fairly symmetrical relative to the store mid-point, the pylon effects on C_n will be less pronounced.

For the three test conditions of Fig.28, the following sideforce and yawing moment coefficients are obtained by integration of the "with pylon" and "no pylon" distributions (S and SW values respectively):

$\alpha = \beta = 0^o$: C_{Y_S} = 0.26, C_{n_S} = 0.009 ; $C_{Y_{SW}}$ = 0.11, $C_{n_{SW}}$ = 0

$\alpha = 0^o$, $\beta = -5^o$: C_{Y_S} = 0.60, C_{n_S} = 0.082 ; $C_{Y_{SW}}$ = 0.20, $C_{n_{SW}}$ = 0.087

$\alpha = 8^o$, $\beta = 0^o$: C_{Y_S} = -0.46, C_{n_S} = -0.102 ; $C_{Y_{SW}}$ = -0.11, $C_{n_{SW}}$ = -0.11

/The unfinned store-swept.....

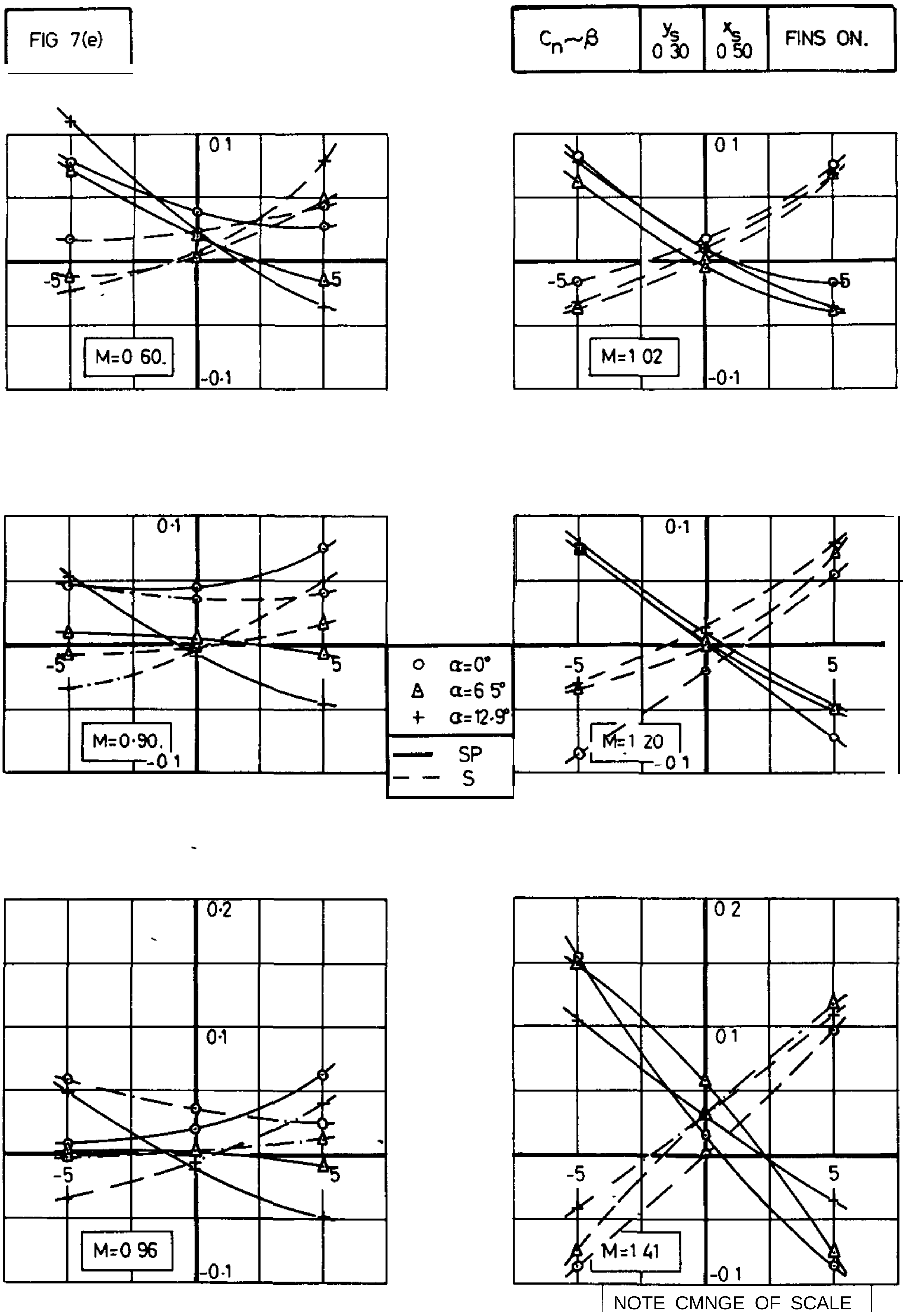

FIG. 7 (e). y_s=0·30, x_s=0·50, FINS ON.

It is probable that too much attention should not be paid to the reduction in $|dC_Y/d\alpha|$, et small negative incidences. It is quite possible that at larger negative incidences, $|dC_Y/d\alpha|$ increases again: for example, it was noted earlier that at subsonic speeds, et least, an increase might be expected due to the higher local dynamic pressure ratios over the store at negative incidence (Fig.27). For the rest of the discussion, therefore, it seems sufficient to consider the three quantities, C_{Y_0} ; $dC_Y/d\alpha$ and $dC_Y/d\beta$ as deduced from the results et positive incidence and to note how these vary with store position and Mach number. There is a significant incidence-sidelip cross-coupling effect and so $dC_Y/d\beta$ must be treated as'a function of incidence.

8.1.1 . C_Y, The Sideforce at $\alpha = \beta = 0^O$

The variation of C_{Y_0} with Mach number for the three store chordwise positions et mid semispan is shown in Fig.10(a) and for the other spanwise positions in Fig.lO(b). The trends for the further forward store positions, x_s =0 and 0.15, are much as predicted in Ref.1, but the variation in C_{Y_0} with store chordwise position and to a lesser extent, spanwise position is much greater than suggested in Ref.1.

With x_s = 0 and 0.15, C_{Y_0} is positive at subsonic speeds tending to rise to a maximum near ii = 1.0; et supersonic speeds. C_{Y_0} decreases with-increasing Mach number, becoming-negative beyond a Mach number that is near M = 1.3 - 1.4 for x_s = 0 but is beyond the test range for x_s = 0.15. With x_s = 0.50, at subsonic speeds below about M = 0.90, C_{Y_0} is'much smeller than for the further forward store positions; between M = 0.90 and 1.00 however, C_{Y_0} increases considerably and so at low supersonic-speeds, there is less variation with store chordwise position; the decrease in C_{Y_0} with Mach number is now delayed to Mach numbers beyond the test range and so by M = 1.41, C_{Y_0} is greeter for x_s = 0.50 than for x_s = 0 or 0.15.

The fin contribution to C_{Y_C} also depends on the store chordwise position; it varies from about +0.15 for x_s = 0 to 0.05 for x_s = 0.15 and to -0.20 for x_s = 0.50.

The effects of store spanwise position are difficult to summarise because they clearly depend both on Mach number and on the store chordwise position. Subsonically, for x_s = 0, C_{Y_0} decreases as the store is moved out from ys = 0.50 to y_s = 0.75 but supersonically, the decrease in C_{Y_0} with Mach number is delayed by moving the store out and hence C_{Y_0} can be greater for y_s = 0.75.

At first sight, the changes in C_{Y_0} with Aiaoh number and store position may appear difficult to explain and this may well be true in a quantitative sense. Qualitatively, however a detailed correlation can be established with the local sidewash characteristics discussed earlier in section 7. For example,

(a) The positive values of C_{Y_0} for the further forward stores et subsonic. speeds are consistent with the side load

/distributions for....

distributions for $\alpha = \beta = 0^o$ shown in Fig.28. The negative sidewash over the pylon and the middle part of the store exercises the dominant effect; in addition, while it is true that the positive sidewash over the nose of the store gives a small negative loading over the nose, this is at least partly offset by the fact that negative loading over the nose induces a positive contribution over the rest of the store.

(b) The decrease in C_{Y_0} at subsonic speeds as the store (and pylon) is moved aft can be explained by the reduction in the mean negative sidewash over the pylon and the mid-part of the store; also, when $x_s = 0.50$, the nose of the store is not yet sufficiently far aft to experience any significant negative sidewash. Two interesting comments can be made here. First, if the pylon had not been moved aft with the store and if the rearward store had been mounted on a sweptback pylon (relative to the wing) from the forward part of the wing lower surface, the decrease in C_{Y_0} might not have been as great. Secondly, if the store were moved even further aft than $x_s = 0.50$, it is possible that the reduction in C_{Y_0} might be arrested since then, a significant positive loading would be induced over the nose of the store,

(c) The reduction in C_{Y_0} at subsonic speeds as the store is moved aft is even more pronounced for the finned store because the fin contribution changes from being positive for $x_s = 0$ to being negative for $x_s = 0.50$. This implies that the mean sidewash over the fins is negative for $x_s = 0$ and positive for $x_s = 0.50$. A trend in this direction can be expected from the wing-induced sidewash as shown in Fig. 22(a) but not necessarily a change of sign. This point could be resolved by considering the effect of the flow over the nose of the store: for $x_s = 0$, this could accentuate the negative sidewash over the fins while for $x_s = 0.50$, it could be inducing some positive sidewash. This is an illustration therefore of where a point-by-point correlation of the side load and wing-induced sidewash may indicate the first order effects but not necessarily the whole story. Also, it is an illustration of how the measured load data can be explained qualitatively but where the quantitative correlation is not entirely satisfactory: on the basis of the sidewash data in Fig.22, one would not really have expected such a large negative fin contribution to C_{Y_0} at subsonic speeds at $x_s = 0.50$,

(d) The rapid increase in C_{Y_0} for $x_s = 0.50$ between about $M = 0.90$ and $M = 1.00$ is clearly associated with the change in velocity and hence sidewash distribution below the wing from the subsonic symmetrical-type of Fig.22(a) to the supersonic asymmetrical type of Fig.22(b) for which the negative sidewash increases back to just ahead of the wing trailing-edge shock. This change increases the negative sidewash over the pylon and it is noticeable in Fig.10(a) that the increase in C_{Y_0} between $M = 0.90$ and $M = 1.00$ is much more pronounced in the (SP) than in the (S) data. It is rather more surprising to find that the fin contribution to C_{Y_0} does not change much in this range,

/ (e) The marked.....

(e) The marked decrease in C_{Y_0} with Mach number above abut $M = 1.0$ for the forward stores at $x_s = 0$ and $x_s = 0.15$ can be explained with reference to the sidewash contours in Fig.22. As the Mach number increases, the wing leading-edge shock will approach the wing leading-edge and will become more swept back; when it passes downstream of the nose of the store, the wing-induced sidewash over the nose will fall to zero; also, as the sidewash field becomes more swept, the mean sidewash over the pylon and the middle part of the store will become less negative and ultimately will change sign. Both these factors could contribute to the decrease in C_{Y_0} with Mach number,

(f) It is also clear by reference to Fig.22(b) that this decrease in C_{Y_0} with M above $M = 1.0$ will be postponed to higher Mach numbers for stores mounted further aft. Indeed, one can deduce that there are store positions for which the opposite trend might be present at low supersonic speeds. Such a case could arise for stores mounted such that the nose still lay downstream - but not too far downstream of the wing leading-edge shock. In such a position, the positive wing-induced sidewash over the nose of the store could be materially greater than at subsonic speeds and also, if as in the present tests the length of the store were comparable to the wing chord, the negative wing-induced sidewash over the rear of the store could also be greater. Hence, for such a case, C_{Y_0} could initially increase with Mach number at low supersonic speeds before starting to decrease and such a trend is observed for the finned store at $x_s = 0.50$, $y_s = 0.50$. Another important variable in this context is likely to be the depth of the store; if this ware increased, the decrease in C_{Y_0} with M would be observed at lower Mach numbers,

(g) The reduction in C_{Y_0} at subsonic speeds as the store at $x_s = 0$ is moved out from $y_s = 0.50$ to $y_s = 0.75$ is consistent with the reduction in the local angles of sidewash as shown in Fig.23(a). Similarly, the opposite trend at Mach numbers above $M = 1.0$ is consistent with the opposite trend in the sidewash values as shown in Fig. 23 (b). Perhaps the better way of looking at the supersonic comparison is however to say that the decrease in C_{Y_0} with Mach number is postponed to higher Mach numbers by an increase in y_s. This is as would be predicted because the parameter that matters is the distance of the store aft of the wing leading-edge shock (this is clear by reference to Fig.23(b)),

(h) Moving the store at $x_s = 0.50$ in from $y_s = 0.50$ to $y_s = 0.30$ reduces C_{Y_0} particularly at the higher Mach numbers and leads to values that are very small throughout the Mach-number range. This is again quite plausible in terms of the local sidewash values for the present model: Fig.23 shows for example that at supersonio speeds, the sidewash for $y_s = 0.30$ is very small except in a local region just downstream of the wing leading-edge shock and it follows that the mean values over the length of the store would certainly be small. It should be emphasised here that these results for $y_s = 0.30$ would not necessarily be obtained for a real aircraft configuration; they apply in the

/present instance because...

present instance because the fuselage- induced sidewash over the store at zero incidence is zero or at least very small. This would not necessarily be true for a real aircraft layout - see section 10 below.

To sum up the effects of store position on C_{Y_0}, it seems that at subsonic speeds, the largest positive values are likely to be obtained for stores mounted below the wing leading edge at near mid.semispan, i.e. near $x_s = 0$, $y_s = 0.50$ and that moving the store either inboard or outboard or more particularly, moving it aft should reduce C_{Y_0}. It should perhaps be remembered that sny comments on the effects of spanwise position have to be based on the results for a finned store. At supersonic speeds, the conclusion is less clear but as the Mach number increases above $M = 1.0$, there will be a growing tendency for C_{Y_0} to increase with both y_s and x_s. Before leaving these conclusions, one should emphasise that a positive value for C_{Y_0} probably implies some relief in the maximum side load under the critical stressing condition which is almost certainly associated with the maximum positive incidence for any given application: Hence large positive values of C_{Y_0} can be beneficial (although it should always be checked that these do not lead to a more serious stressing case at negative-g). It is indeed the decrease in C_{Y_0} with Mach number above $M = 1.0$ for the further forward store locations that is a primary factor in giving an increase in the maximum side load at supersonic speeds as compared with low subsonic speeds. In many cases, this decrease in C_{Y_0} can be a more powerful term than any increase in $|dC_Y/d\alpha|$.

8.1.2 $dC_Y/d\alpha$, Sideforce Due To Incidence

The variation of $dC_Y/d\alpha$ with Mach number and store position is shown in Fig.11. It will be seen that the changes with store position can be very much greater than the changes with Mach number for a given position.

On the basis of Ref.1, an increase in $|dC_Y/d\alpha|$ with Mach number at subsonic speeds was expected followed by a decrease near $M = 1.0$ and then by a subsequent increase. These detailed changes are really only observed for the stores at $x_s = 0$ and even for this position, the changes in $|dC_Y/d\alpha|$ do not amount to more than about ±15% at the most. For $x_s = 0.15$, the changes with Mach number are trivial but for $x_s = 0.50$, a more definite trend is observed particularly when $y_s = 0.50$. In this last case, $|dC_{Y_{SP}}/d\alpha|$ for the finned store increases from about 0.11 at subsonic speeds to about 0.15 at $M = 1.2 - 1.4$.

If one combines the values of $dC_Y/d\alpha$ in Fig.11 with the values of C_{Y_0} in Fig.10, one finds that the values of C_Y at a given positive incidence tend to increase with Mach number for all the store configurations, the effects being least for the intermediate chordwise position, $x_s = 0.15$. For $x_s = 0$, the increase is primarily related to the decrease in C_{Y_0} while for $x_s = 0.50$, the increase is primarily related to the changes in $|dC_Y/d\alpha|$.

The largest absolute values of $dC_Y/d\alpha$ are obtained with the store at $x_s = 0$, $y_s = 0.75$. Moving the store in to $y_s = 0.50$ tends to reduce $|dC_Y/d\alpha|$ particularly near and just above $M = 1.0$. Moving the store aft at

$/y_s = 0.50$ gives . . .

y_s = 0.50 gives a very great reduction in $|dC_Y/d\alpha|$, the values for x_s = 0.50 being in general only about half those for x_s = 0.* Moving the store in to y_s = 0.30 at x_s = 0.50 gives a further reduction in $|dC_Y/d\alpha|$, particularly in the case of the (SP) data.

The changes in $dC_Y/d\alpha$ with store/pylon position and Mach number can be correlated qualitatively with the sidewash data presented in Figs.24 - 26. For example,

(a) The most striking effect is the reduction in $|dC_Y/d\alpha|$ as the store is moved aft at a given spanwise position and this can be explained in term of the decrease in the mean effective sidewash over the pylon and middle part of the store. The reduction in $|dC_Y/d\alpha|$ is greater at subsonic than at supersonic speeds and this can be related to the fact that significant values of $|\sigma/\alpha|$ are maintained back to the wing trailing edge at supersonic speeds (Fig.26). Quantitatively, however, the correlation is not quite so good. On the basis of the sidewash data, one might have expected something like a 25% reduction in $|dC_Y/d\alpha|$ as the store was moved back from x_s = 0 to x_s = 0.50, but in fact, a reduction of about 50% is observed.

(b) As the store is moved out at a given chordwise position, $|dC_Y/d\alpha|$ increases particularly at supersonic speeds and this trend is also consistent with predictions based on the local sidewash data. For example, subtraction of the values of σ for $\alpha = 0^o$ and 8^o at subsonic speeds in Figs.22(a) and 24(a) shows that σ/α only increases slightly between y_s = 0.50 and y_s = 0.50 and y_s = 0.75; at supersonic speeds, on the other hand, the increase in σ/α with y_s is much more pronounced as shown in Fig.26.

(c) As an illustration of how the changes in $|dC_Y/d\alpha|$ with Mach number for a given store position can be explained in terms of the sidewash data, let us consider the results for the store at x_s = 0, y_s = 0.50. $|dC_Y/d\alpha|$ first increases with Mach number at subsonic speeds; this trend would be expected in the sub-critical range because then, the flow under the wing at high speeds can be related to the incompressible flow around an analogous wing. This correlation would suggest an increase with Mach number in the maximum values of σ/α below the wing leading edge and hence over the pylon and the mid-part of the store. Second, near M = 1.0, $|dC_Y/d\alpha|$ decreases with Mach number and this change corresponds to when a mixed-flow régime is developing. If one constructed pictures similar to Fig.24(b) and 26 for a supersonic Mach number lower than M = 1.6, the wing leading-edge shock would lie much further ahead of the wing and so the pylon and the mid-part of the store and even the store nose would lie downstream of region of high local sidewash behind the wing leading-edge shock. It is plausible to suggest that under these conditions, the local sidewash over the pylon could be less than at high subsonic speeds and if so, the observed decrease in $|dC_Y/d\alpha|$ would follow.

---

* The (SP) data for the store without tail fins at x_s = 0.50, y_s = 0.50, are not included in Fig.11 because the $C_Y - \alpha$ curves in this particular case seem rather scattered: at the end of this test, it was found that the store was loose and this is the probable explanation of the scattered results.

/Finally, above:....

Finally, above about $M = 1.2$, $|dC_Y/d\alpha|$ increases again and it is reasonable to suggest that this is when the nose of the store is beginning to experience the high local values of $|\sigma/\alpha|$ downstream of the wing leading-edge shock. By the same token, this increase in $|dC_Y/d\alpha|$ between about $M = 1.2$ and 1.4 would be followed by a decrease at some higher Mach number outside the range of the present tests when the nose of the store and ultimately, part of the store-plyon intersection lay upstream of the bow shock and hence in a region where there is no wing-induced sidewash,

(d) As a second illustration of how the Mach-number effects can be explained, consider the results for the store at $x_s = 0.50$, $y_s = 0.50$. In this case, there is only a small change in $|dC_Y/d\alpha|$ until about $M = 0.9$ but then, as the Mach number is increased further to $M = 1.2$ there is quite a pronounced increase amounting to about 30% in the case of the (SP) values for the finned store. Cme is tempted to ascribe this increase to an increase in the values of $|\sigma/\alpha|$ below the rear half of the wing lower surface. It cannot however be quite as simple as this because there is hardly any change with Iiach number in the fin contribution to $|dC_Y/d\alpha|$. It is possible that the changes in σ/α are more pronounced over the mid-part of the store and the pylon than over the fins. Later tests may show that the variation of $|dC_Y/d\alpha|$ with M for a store in this position maybe somewhat different if the store is mounted on a sweptback rather than a swept forward pylon.

One final point should be made about the values of $|dC_Y/d\alpha|$. It has been seen that the changes with iiach number for most of the configurations tested are fairly small and in general, less than might have been predicted using the empirical method proposed in Ref.1 This conclusion should not however be generalised too far until the test programme has been extonded to include stores mounted at different depths below the wing. To judge from the sidewash data in Figs.22 - 26, it seems likely that larger increases in $dC_Y/d\alpha$ with Mach number will be observed for stores at greater depth.

8.1.3 $dC_Y/d\beta$, Sideforoe Due To Sideslip

The variation of. $dC_Y/d\beta$ with Mach number for the different store/pylon configurations at mid semispan are shown in Fig.12(a) and for the other spanwise positions in Fig.12(b). Values are presented for three incidenoes, $\alpha = 0^o$, 6.5^o and 12.9^o.

To the first order, one might have expected that $dC_Y/d\beta$ would be independent of Mach number, store position and incidence but in fact, all of these variables can have a significant effect. This is because the local sidewash over the store/pylon will change with β and it does not necessarily follow that the changes under the forward and rearward wing panels will always be in opposite directions. Hence, the changes in sidewash can in principle either give an increase or a decrease in $dC_Y/d\beta$ while under some conditions, coincidentally, the changes in sidewash under the two wing panels would be the same and this would not affect $dC_Y/d\beta$. As might be expeoted, the consequent effects of Mach number, store position and incidence are somewhat interrelated and in trying to sum up the effects of any one of these variables, the remarks have to be qualified with reference to the other two. Despite this, a summary of the more important trends is given below :

(a) The general tendency is for $|dC_Y/d\beta|$ to increase with Mach number. At low incidence, this increase occurs fairly suddenly near $M = 1.0$, but at higher incidences it is spread

/over a wider......

over a wider Mach-number range. The increase tends to be greatest for the finned stores mounted in the aft position at $x_s = 0.50$. The (S) and (SP) data indicate similar variations with Mach number.

The principal reason for a change in $dC_Y/d\beta$ with Mach number is that the loading over a store at a given angle to the flow will vary between subsonic and supersonic speeds, but the fact that the changes are somewhat dependent on the store chordwise position confirms that the effects of Mach number on the local sidewash field also play a part. Primarily, the effect of sideslip on the sidewash field must be similar to the effect of a change in sweepback but qualitatively, one can expect significant effects in regions where at zero sideslip, $d\sigma/dx$ is either large or changing sign. Conditions near $x_s = 0.50$ provide a good example. At $\alpha = 0^o$ at subsonic speeds, Fig.22(a) shows that $|\sigma|$ decreases both ahead of and to the rear of $x_s = 0.50$ and this characteristic helps to ensure that the changes in sidewash with β under the forward and rearward wing panels compensate for one another in their effect on $dC_Y/d\beta$ for a store at $x_s = 0.50$. At supersonic speeds, on the other hand, Fig.22(b) shows that $d\sigma/dx$ does not change sign near $x_s = 0.50$ and there will now be a tendency for the effects under the two wing panels under sideslip conditions to add up rather than to compensate. This analysis is far from complete because it ignores the variation in σ with wing sweep but it could help to explain why the increase in $|dC_Y/d\beta|$ with Mach number is particularly apparent for the stores at $x_s = 0.50$.

(b) The effects of store chordwise position on $dC_Y/d\beta$, are not very significant at subsonic speeds but at supersonic speeds, $|dC_Y/d\beta|$ tends to increase as the store is moved aft. This is certainly true comparing the results for $x_s = 0.15$ and $x_s = 0.5$; but at high incidences, it is not always true between $x_s = 0$ and $x_s = 0.15$. Primarily, one can take $dC_Y/d\beta$ to be independent of x_s at subsonic speeds and to vary at supersonic speeds according to the relation :

$$|dC_Y/d\beta| = |dC_Y/d\beta|_{x_s = 0}\, e^{-0.064 x_s}$$

This relation was deduced from the results for the stores at the mid semispan station * and appears to apply irrespective of whether the store has tail fins or not and irrespective of whether (S) or (SP) data is being considered,

(c) The variation in $dC_Y/d\beta$ with spanwise position is difficult to determine from the limited results of the present tests but for $x_s = 0.50$, $|dC_Y/d\beta|$ decreases as the store is moved in from $y_s = 0.50$ to $y_s = 0.30$, by about 0.05 for the (SP) values or 0.02 for the (S) values. There is also some suggestion that the values of $|dC_Y/d\beta|$ decrease as the store is moved out from $y_s = 0.50$ to

* Strictly, the mean values of $dC_Y/d\beta$ for either subsonic or supersonic speeds were used - i.e. Fig.33(a) rather than Fig.12(a).

/$y_s = 0.75$.....

$y_s = 0.75$ at $x_s = 0$ but this trend is less clearly established. To sum up, it seems that $|dC_Y/d\beta|$ is greater near mid semispan than elsewhere but it may be unwise to draw such a general conclusion.

(d) In nearly all the cases, $|dC_Y/d\beta|$ increases appreciably with incidence. In Ref.1 an increase of 25% was quoted as a typical change between $\alpha = \beta = 0^\circ$ and $\alpha = \beta = 10^\circ$ and the present results are fairly consistent with this prediction although they serve to emphasise that "a percentage increase" is not the most appropriate way in which to express the change. In extreme cases, the change in $dC_Y/d\beta$ between $\alpha = 0^\circ$ and $\alpha = 12.9'$ amounts to as as much as 60% but there is the odd case where $|dC_Y/d\beta|$ actually decreases slightly with incidence.

The results can be resolve&better by expressing the change in $dC_Y/d\beta$ with incidence as an increment rather than as an appreciable change. At subsonic speeds, the (S) and (SP) data for both the finned and unfinned stores can be reduced to a single relation, viz,

$$|dC_Y/d\beta| = |dC_Y/d\beta|_{\alpha=0} - 0.004\alpha$$

where a is expressed in degrees. Strictly, there is some tendency for the quantity "0.004" to decrease as the store is moved aft.

At supersonic speeds, the difference between $|dC_Y/d\beta|_S$ and $|dC_Y/d\beta|_{SP}$ tends to increase with incidence and therefore, two relations are needed, viz

$$|dC_Y/d\beta|_S = |dC_Y/d\beta|_{S\,\alpha=0} - 0.002\alpha$$

$$|dC_Y/d\beta|_{SP} = |dC_Y/d\beta|_{SP\,\alpha=0} - 0.005\alpha$$

Strictly, these relations apply only when $x_s = 0$; in both cases, the results suggest a definite trend for the variation with incidence to decrease as the store is moved aft; indeed, when $x_s = 0.50$ the (S) data indicate a decrease rather than an increase in $|dC_Y/d\beta|$ with α (Fig.12(a)).

The tendency for $dC_Y/d\beta$ to vary more with incidence when the store is below the wing leading edge is understandable since it is in this region, particularly at supersonic speeds, that the local sidewash over the pylon and the nose and mid-part of the store is likely to be most sensitive to small changes in either incidence or sideslip.

8.1.4 Effects of Mach Number and Store Position on Maximum Side Loads

The assessment of how the maximum side loads on the store/pylon for a given application are likely to vary with store position and Mach number depends on the incidence and sideslip range dictated by the aircraft flight envelope. This will determine the relative magnitudes of the contributions from C_{Y_0}, $dC_Y/d\alpha$ and $dC_Y/d\beta$. In general, however, the critical stressing case is likely to correspond with the maximum positive incidence combined with sideslip in the appropriate sense to give an additive contribution to C_Y. Under these conditions, the aerodynamic and inertia forces should be acting in the same direction. In general, the maximum side load under these conditions should decrease as the store is moved aft and also probably, as the store is moved inboard, i.e, of the configurations included in the present tests, the smallest values were obtained with the store at $x_s = 0.50$ / $y_s = 0.30$. Further, it is...

$y_s = 0.30$. Further, it is probable that when expressed in non-dimensional coefficient form, the values will be smaller at supersonic speeds than at subsonic speeds.

These are broad general conclusions and they need some qualification because they will not necessarily apply in all cases. Points worth noting include the following :

(i) The general tendency for the maximum side 'load to decrease as the store is moved aft will nearly always be true at low supersonic speeds because in the aft positions, $|dC_Y/d\alpha|$ should be-less and C_{Y_0} should be more positive. (It should be noted all through this discussion that a positive value for C_{Y_0} means that this is a relieving term when considering the side load at positive incidences). A factor working in the opposite sense is that the values of $|dC_Y/d\beta|$ at supersonic speeds will tend to be greater for the aft stores but normally, this should not be sufficient to offset the trend dictated by the behaviour of C_{Y_0} and $|dC_Y/d\alpha|$,

(ii) At subsonic speeds, the position is not quite so clear. Then $|dC_Y/d\alpha|$ will show a considerable reduction as the store is moved aft but this might be offset in certain cases by the reduction in the positive C_{Y_0}. Hence the general trend could be reversed if the maximum positive incidence mere not too large. Also, for some aircraft applications (as seen below in section IO), fuselage-induced sidewash can materially increase the negative sidewash at zero incidence and hence the positive values of C_{Y_0}; this would certainly reduce the maximum values of C_Y at positive incidence and could modify the trend nith chordwise-position,

(iii) The normal tendency for the maximum values of C_Y to increase, between subsonic and supersonic speeds may possibly not apply for certain aft-mounted storeconfigurations for which the increase in C_{Y_0} near $M = 1.0$ could reverse the normal trend. Also, for stores mounted well forward, the maximum values of C_Y may occur at transonic speeds because it is possible for $|dC_Y/d\alpha|$ to be still increasing with Mach number when C_{Y_0} has already started to decrease,

(iv) It is most important to remember that in'practice, the maximum side loads as distinct from the maximum values of C_Y may well occur at trsnsonic speeds for quite a range of configurations. This is because transonic Mach numbers are likely to be associated with higher values of $\frac{1}{2}\rho V^2$ than are the supersonic Mach numbers. It is just in the *transonic* region near $M = 1.0$ that the loads will be most difficult to predict to a good accuracy and hence experimental checks on specific installations are always likely to be required.

The above remarks have been based on the assumption that positive incidences will provide the critical stressing case. This may not always be true particularly if one is considering an example giving a large positive value of C_{Y_0}. The maximum negative-g condition should then be checked

/because in such cases......

because in such cases, the contributions from C_{Y_o}, $dC_Y/d\alpha$ and $dC_Y/d\beta$ can all be in the same sense. If this proves to be a more critical stressing case than the positive condition, it is even more likely that moving the stores aft would reduce the maximum values of C_Y.

8.2 Store/Pylon Yawing Moments

Figs.3 and 5 show that the variation of C_n with incidence is not as linear as the variation of C_Y, particularly when the store has tail fins. The changes in slope are more pronounced when the stores are in the forward positions; for $x_s = 0.50$, the changes are fairly trivial especially at supersonic speeds. Near and just above $M = 1.0$, the $C_n - \alpha$ curves can be non-linear because there is a significant change with Mach number in progress and this is occuring at slightly different Mach numbers according to incidence. Leaving aside this Mach-number range, the general tendency is for $|dC_n/d\alpha|$ to become more positive above some incidence (α_1) which depends on both Mach number and store position. This is particularly true for the finned store and it is therefore the fin contribution to $dC_n/d\alpha$ that is largely responsible for the change in slope at α_1. For $x_s = 0, \alpha_1 = 3^o$ at $M = 0.6$, 0^o at $M = 0.96$ and is negative at supersonic speeds. For $x_s = 0.15, \alpha_1$ is near 7^o at $M = 0.6$, 3^o at $M = 0.96$ and 0^o at supersonic speeds. If one uses Figs.22 and 24 to deduce the likely characteristics of the local sidewash fields at these values of α_1, it appears that they could correspond approximately with when the local wing-induced sidewash over the fins of the store is changing sign from negative to positive. It may be more appropriate to say that this is when the wing-induced sidewash over the fins becomes of the same sign as the sidewash over the nose of the store. To judge from the $C_n - \alpha$ curves, the fins then become more effective. This can only be advanced as a very tentative and incomplete correlation; measured load distributions or pressure distributions on the store would be needed to carry the explanation further. Without trying to be too precise, however, the fact that the $C_n - \alpha$ curves are less linear than the $C_Y - \alpha$ data is perhaps only to be expected since the yawing moments depend primarily on the flow over the nose and tail of the store whereas the sideforce values depend primarily on the local sidewash over the pylon and mid-part of the store : in other words, the yawing moments depend critically on the detailed non-uniformity of the flow field whereas the sideforce values, to the first order, depend more nearly on the sidewash at a certain point in the field.

Despite the non-linear $C_n - \alpha$ curves, it was still thought worthwhile analysing the data in terms of C_{n_o}, $dC_n/d\alpha$ and $dC_n/d\beta$ as in sections 8.2.1, 8.2.2 and 8.2.3 below. One reason for doing this is that as shown in Figs.3 and 5, the maximum absolute values of C_n for the finned stores are usually obtained near zero incidence i.e., if C_{n_o} is positive, $dC_n/d\alpha$ is usually negative and vice versa and so in practice C_{n_o} may be the most important term.

8.2.1 C_{n_o} Yawing Moment at $\alpha = \beta = 0^o$

The variation of C_{n_o} with Mach number for the different store positions at mid semispan is shown in Fig.13(a) and for the other spanwise positions in Fig.13(b).

/For the further......

Fur the further forward store positions, $x_s = 0$ and 0.15, the values of C_{n_0} are negative (i.e. a nose-outward moment) and the absolute values increase with Mach number considerably. For $x_s = 0$, this increase mostly appears in the subsonic range but for $x_s = 0.15$, it occurs later and persists up to M = 1.4. As the store is moved aft, the values, of C_{n_0} become less negative until for $x_s = 0.50$, the values are positive at all Mach numbers in the test range. Taking as an example the (SP) values for the finned store, at subsonic speeds these range from about -0.1 at $x_s = 0$, through -0.03 for $x_s = 0.15$ to +0.08 for $x_s = 0.5$; at M = 1.4, the corresponding values are -0.27, -0.19 and +0.04. Fig.13(b) shows that spanwise position does not have a marked effect on the values of C_{n_0} although there is a fairly consistent trend for C_{n_0} to become more negative as the store is moved inboard.

The fin contribution to C_{n_0} is negative (i.e. nose-out) for the forward store positions but is positive for $x_s = 0.50$. In contrast to the fin contribution to C_{Y_0} which is roughly independent of Mach number, the fin contribution to C_{n_0} is appreciably larger at supersonic speeds than at subsonic speeds.

Qualitatively, the C_{n_0} data can be related to the local sidewash fields in a similar manner to the values of C_{Y_0}. For example,

(a) The negative values of C_{n_0} obtained for the forward store locations are due to the positive sidewash over the nose of the store and the negative wing-induced sidewash over the tail of the store. Both these characteristics contribute to the nose-out moment and both would be expected to increase with Mach number. This is consistent with the increase in $|C_{n_0}|$ with M at subsonic speeds,

(b) At supersonic speeds, when $x_s = 0$, the nose of the store becomes subject to the large positive sidewash behind the wing leading-edge shock at a relatively low supersonic Mach number and hence, this explains the large negative values of C_{n_0}. Beyond M = 1.4, i.e., outside the range of the present tests, the store nose would lie ahead of the leading-edge shock and then, a decrease in $|C_{n_0}|$ might be expected. With $x_s = 0.15$, the mean sidewash over the nose of the store would still be increasing with Mach number between M = 1.0 and M = 1.4 and again, this is consistent with the fact that C_{n_0} is still becoming more negative with increasing Mach number in this range,

(o) With $x_s = 0.50$, the sidewash over the nose of the store would probably be negative rather than positive while the effective sidewash over the tail allowing for the angle induced by the flow over the nose might well be positive. This means that the

/sidewash ....

sidewash distribution from nose to tail for $x_s = 0.50$ is in the opposite direction to what it is for the forward store locations and this explains why Cn_o is positive rather than negative.

(d) The same considerations explain the change in sign of the fin contribution to C_{n_o} as the store is moved aft. There is also an increase in the fin contribution at supersonic speeds as compared with subsonic speeds; this could be partly due to larger sidewash over the fins at supersonic speeds and partly to the fact that there would then be no forward influence from the fins on the flow over the rest of the store.

(e) The effects of spanwise position on C_{n_o} can also be related with the sidewash characteristics. For example, with $x_s = 0$, moving out from $y_s = 0.50$ to $y_s = 0.75$ gives a decrease in $|C_{n_o}|$ at subsonic speeds but an increase at supersonic speeds and this is consistent with the changes in the wing-induced sidewash as shown in Fig.23. Similarly, moving the store in from $y_s = 0.50$ to $y_s = 0.30$, at $x_s = 0.50$ should reduce the wing-induced sidewash over the store at all Mach numbers and this is borne out by the reduction in the values of C_{n_o} (Fig.13(b)).

8.2.2 $dC_n/d\alpha$, Yawing Moment Due To Incidence

The variation of $dC_n/d\alpha$ with Mach number for the different store positions at mid semispan is shown in Fig.14(a) and for the other spanwise positions in Fig.14(b). Two sets of values of $dC_n/d\alpha$ are presented, described respectively as the "slope at zero incidence" and "slope at high incidence". Strictly, the values labelled "at high incidence" apply when $\alpha > \alpha_1$ and as noted earlier, α_1 is often quite small, e.g., for $x_s = 0$, $\alpha_1 = 3^o$ at M = 0.6 decreasing to some negative incidence at M = 1.4 while for $x_s = 0.15$, $\alpha_1 = 5^o - 7^o$ at subsonic speeds decreasing to about 0^o at M = 1.2 - 1.4. When α_1 is near 0^o, the values of $dC_n/d\alpha$ for $\alpha = 0^o$ may be somewhat uncertain and this accounts for some of the erratic variation in the values shown in Fig.14. Too much attention should not be paid to this; rather, one should concentrate on the main trends.

For the store without tail fins, the values of $dC_n/d\alpha$ at zero incidence do not vary greatly with store chordwise position but at higher incidences, there is a significant change, e.g, from about 0 to -0.01 as the store is moved aft from $x_s = 0$ to $x_s = 0.50$. Two factors probably contribute to this change. First, the nose of the store is nearer the region of maximum σ/α when $x_s = 0.50$ and second, at subsonic speeds at least, the nose of the store would then also be in a region of higher dynamic pressure (Fig. 27).

For the finned store, the effects of chordwise position are most pronounced. This is because particularly at high incidences, the fin contribution to $dC_n/d\alpha$ decreases greatly as the store is moved aft, e.g, it is about 0.02 when $x_s = 0$ but only about 0.005 when $x_s = 0.50$. The decrease in the fin contribution as the store is moved aft would be predicted since the fins are then further away from the region of high σ/α.

As regards the effect of store spanwise position it is difficult to establish any consistent trends.

/Mach-number effects.......

Mach-number effects on $dC_n/d\alpha$ are also difficult to summarise simply. For $x_s = 0$, $dC_n/d\alpha$ tends to become more positive with increasing Mach number, particularly at supersonic speeds. For $x_s = 0.15$, the trend is in the same direction but somewhat smaller. For $x_s = 0.50$ at subsonic speeds, the trend is in the opposite direction but this reverses again above $M = 1.0$. None of these changes with Mach number amount to more than about 0.01 in $|dC_n/d\alpha|$; in all cases, they appear to be related to changes in the flow over the nose of the store; the fin contribution to $dC_n/d\alpha$ never varies significantly with Mach number.

$dC_n/d\beta$, Yawing Moment Due to Sideslip

The C_n-β curves in Figs.7 - 9 are reasonably linear or to be more precise $dC_n/d\beta$ has much the same value irrespective of whether β is positive or negative. This does not always apply for forward positions of the finned store. &an values of $dC_n/d\beta$ for stores at the mid semispan station are shown in Fig.15(a), fins off, of.15(b), fins on. As with $dC_Y/d\beta$, values are presented for $\alpha = 0^o$, 6.5^o and 12.9^o.

It should be noted that although the (SJ?) and (S) values of $dC_n/d\beta$ were measured on stores on opposite wing panels, both have been plotted on Fig.15 as if they were both located on the starboard wing panel.

For the finned store, the values of $dC_n/d\beta$ are always negative, i.e, positive sideslip, nose to port, gives a nose-outward moment on a store beneath the starboard wing panel. Except at low incidences and subsonic speeds, the fin contribution is usually in the same sense.

For the store without fins, $dC_n/d\beta$ is negative at subsonic speeds but near and above $M = 1.0$, there is a variation towards a positive value, e.g, the (SP) values for $x_s = 0$ vary from about -0.013 at subsonic speeds to about +0.003 at supersonic speeds at $\alpha = 0^o$ or from about -0.002 to about +0.015 for $\alpha = 12.9^o$. The effect of store chordwise position is trivial at zero incidence but becomes significant as the incidence is increased, giving a variation towards a more negative value for $dC_n/d\beta$ as the store is moved aft.

For the finned store, Fig.15(b) shows that the principal difference is that the variation with Mach number near and above $M = 1.0$ is in the opposite sense to that observed for the unfinned store. The (SP) values for $x_s = 0$ vary from about -0.009 at subsonic speeds to about -0.024 at supersonic speeds at $\alpha = 0^o$ and from about -0.018 to about 4.035 at $\alpha = 12.9^o$. Cnoe again, store chordwise position has relatively little effect at $\alpha = 0^o$ but becomes more important as the incidence is increased with the variation again being in the opposite sense to that observed for the unfinned store.

8.3 Store/Pylon Side Load Centres

8.3.1 z-coordinate of Load Centre

In view of the non-linear nature of the C_n-α curves, it may be preferable for stressing purposes to think in terms of the values of C_{n_o}, $dC_n/d\beta$ and the x-coordinate of the centre of load due to incidence rather than the values of $dC_n/d\alpha$. Typical plots of the variation of the chordwise oentre of pressure (y/d) with incidence for the stores at the mid semispan station are presented in Fig.16 while the variation with Mach number at $\alpha = 6.5^o$ is given in Fig.17. men $C_Y = 0$, the position of the centre of pressure is

/indeterminate and so...

indeterminate and so the values near $\alpha = 3^o$ are not of great significance. Fig.16 shows that for the finned store, the centre of pressure tends to approach the store mid-point as the incidence is increased. Hence, assuming that the store mid-point is a representative moment centre when considering the store-pylon or pylon-wing fixations, the moments at the maximum positive incidence stressing condition should be fairly small. This is why $\alpha = 6.5^o$ rather than $\alpha = 12.9^o$ was selected for the cross-plots in Fig.17, but it should be noted that at $\alpha = 6.5^o$, the centres of pressure are still a fair distance sway from the asymptotic values they tend to approach at high incidence. Also, the values for $x_s = 0.50$ approach their limiting asymptote from the rear whereas the values for $x_s = 0$ and 0.15 approach from the forward end. This means that Fig.17 tends to present an exaggerated picture as regards the effects of store chordwise position; if it had been for $\alpha = 12.9^o$, the effects would still tend to be in the same sense but would be much smaller. One should therefore be careful about drawing quantitative conclusions from Fig.17; qualitative trends should however be indicated correctly.

Au the curves in Fig.17 show that at subsonic speeds, the centre of pressure tends to move forward slightly whereas above M = 1.0, the general tendency is for it to move rearward although for the finned stores this last trend is sometimes reversed above M = 1.2. The centres of pressure are further forward when $x_s = 0.15$ than when $x_s = 0$ or 0.50. This variation with store chordwise position is understandable since it is when $x_s = 0.15$ that the nose of the store is nearest the region of maximum (σ/α) and clearly, the flow over the nose plays a major part in determining the yawing moments on the store. The variations in centres of pressure with both Mach number and store chordwise position are less pronounced in the (SP) data than in the (S) data; this is because the loads on the pylon give an appreciable increment in C_Y but only a relatively small change in C_n.

At a = 6.5^o (Fig.17), the centre of load on the store itself can in an extreme case be as far forward as the store nose (fins off', $x_s = 0.15$, M = 1.0) while at the other extreme, it can be about 1 x store diameter aft of the store mid-point (fins on, $x_s = 0.5$, supersonic M). At higher incidences, the range of possible values around the store mid-point would be much less. The centres of load for the full store/pylon assembly at a = 6.5^o vary between about 2d ahead of the store mid-point and Id aft of the store mid-point; by $\alpha = 12.9^o$, they lie within ±0.2d of the store mid-point for the finned store and between 0.4d and 1.0d for the store without fins.

8.3.2 s-coordinate of Centres of Pressure

Some typical examples of how the depthwise centre of pressure varies with incidence for the stores at mid semispan are shown in Fig.18 while Fig, 19 presents a cross-plot against Mach number at the maximum positive *incidence*, $\alpha = 12.9^o$. These values are clearly relevant when assessing the bending moment of the side load about either the pylon-wing or pylon-store fixations. Once again, the positions are indeterminate when $C_Y = 0$ but unlike the chordwise centres of pressure, Fig.18 shows that the depthwise centres very quickly approach their asymptotic values as the incidence is either increased or decreased from the condition giving $C_Y = 0$. In fact, the evidence of Figs.18 and 19 is that neither incidence nor Mach number has much effect on the depthwise load centres.

This leaves the store chordwise position and the presence or absence of the tail fins as the only variables having any significant effect. The influence of the tail has already been noted. Both the (S) and (SP) data confirm that the addition of the fins tends to move the load centres downward, particularly when the stores are mounted at $x_s = 0.50$. The probable explanation is that the upper fins lose some effectiveness since they lie in or near the wake of the pylon.

/As would be expected....

As would be expected, the (S) load centres for the unfinned stores lie near the store mid-plane. When the fins are present, they vary from about the store mid-plane for $x_s = 0$ to about $0.12z_{max}$ or more appropriately 0.4d below this plane for $x_s = 0.50$.

The (SP) load centres, even before the fins are added, are slightly sensitive to the store chordwise position: they vary from about 0.17 - $0.20z_{max}$ above the store mid-plane for the forward store locations to about $0.30z_{max}$ above for $x_s = 0.50$. Marginally, the lowest positions - and hence, the largest bending moments about the pylon-wing fixation for a given side load - are obtained when $x_s = 0.15$. The (SP) load centres for the finned stores vary less with store chordwise position because the change in fin contribution with x_s is in the opposite sense to the change observed for the store without fins. It is still true however that the lowest load centres are obtained with $x_s = 0.15$ and the highest positions with $x_s = 0.50$.

9. COMPARISON OF SIDEFORCE RESULTS WITH PREDICTIONS BY EMPIRICAL METHOD

One of the primary objects of the present series of tests was to provide some data for comparison with the empirical method suggested in Ref.1 for the estimation of store/pylon sideforce. It is worth recalling here that the method of Ref.1 was intended to apply to the following store/pylon/aircraft wing combinations :

(a) Streamline stores of fineness ratio about 8:1, with or without small tail fins, of length approximately equal to the mean chord of the wing,

(b) Spanwise location of store between 0.25 and 0.80 x wing semispan. Chordwise location of store mid-point from about 0.25c in front of to about 0.50c behind the local wing leading edge. Depthwise location of store centre-line at about 1.5 store diameters below the wing chordal plane,

(c) Pylon 5% or 6% thick, chord equal to about half the local wing chord, attached to the wing in the region of the wing maximum thickness point and swept forward, unswept or swept back according to the chordwise position of the store,

(d) Store/pylon combinations located beneath aircraft wing designs ranging from 40° sweptback wings of moderate taper to 60° delta planforms.

The store/pylon configurations of the present tests satisfy all the above conditions with one exception. This is the point under (c) in which it was assumed that the pylon would be attached to the wing near the wing maximum thickness and would be swept forward, unswept or swept back according to the value of x_s. In the present tests, to ease the manufacture and rigging, the store was always supported on a swept forward pylon (i.e. swept forward relative to the wing) irrespective of its chordwise position and this meant that when $x_s = 0.50$, the pylon was attached to the rear of the wing lower surface.

The basis of the empirical method lay in the observation that C_Y for a given store/pylon arrangement and at a given Mach number would probably vary linearly with both incidence and sideslip. This assumption has been largely confirmed by the results of the present tests. As noted in section 8.1, it is only near zero incidence or at small negative incidences and when $x_s = 0.50$ that there is any significant departure from a linear

/variation. The general...

variation. The general linear trends are maintained even at transonic Mach numbers near M = 1.0 and so in this respect, the results provide definite reassurance that the basis for the empirical method was sound.

Fig.29 presents a typical comparison between the measured data and estimates by the empirical method using the various factors suggested in Ref.1. Comparisons are included for two Mach numbers, M = 0.90 and M = 1.41, for the store, fins off, at $x_s = 0$, $y_s = 0.5$. The empirical method as presented in Ref.1 did not provide for estimates of the (SP) loads at subsonic speeds.

Fig.29 shows that at the supersonic Mach number, M = 1.41, there is quite reasonable agreement between the predicted values and the measured data but that at M = 0.90, $|dC_Y/d\alpha|$ is seriously underestimated. This conclusion also applies for the other store positions of the present tests. At M = 1.41, $|dC_{Y_{SP}}/d\alpha|$ is still somewhat underestimated but the predicted value of $C_{Y_{o_{SP}}}$ is also too negative and these two effects tend to compensate for one another when considering the loads at positive incidence. $dC_Y/d\beta$ is predicted reasonably well at all incidences.

It is tempting to ascribe the comparative failure of the method to give an accurate estimate for $|dC_Y/d\alpha|$ at subsonic speeds to the fact that when the method was derived, more experimental results were available for supersonic Mach numbers such as M = 1.6 - 2.0 than for high subsonic speeds. It is likely however that this is too simple an explanation. The basic fault may lie in the assumption in Ref.1 that the factor expressing the variation of $|dC_Y/d\alpha|$ with store depth could be treated as being independent of Mach number. In view of the earlier discussion of the wing-induced sidewash fields, this assumption now seems unlikely to be true. It is probable that in fact, $|dC_Y/d\alpha|$ decreases with store depth more rapidly at subsonic than at supersonic speeds. In other words, if the depth of the store were increased, $|dC_Y/d\alpha|$ would show a larger variation with Mach number and this would imply better agreement between observed and predicted results. The test programme is to be extended to include store mounted at three different depths below the wing and until these results are available, it is premature to draw any final conclusions from the comparisons in Fig. 29. All that can be said at this stage is that the basic method appears to be sound but that some revision to the factors is undoubtedly needed.

No final revision of the method can be made until the results of the further tests are available but in the meantime, it may be useful to indicate what changes would be needed to provide better agreement with the results of the present tests. These tentative suggestions are given briefly below: for the present, they should be used with some reserve :

(1) $\underline{C_{Y_o}}$: The present results have indicated that the variation of C_{Y_o} with Mach number is much more dependent on the store chordwise position than was expected. The results for stores mounted in a forward position are fairly similar to the predictions by the empirical method but the results for $x_s = 0.50$ are undoubtedly different (Fig.10a)).

For stores located near mid semispan and at a depth near 1.4d (as for the present tests) it is suggested that the values of C_{Y_o} should be obtained from the carpet plots in Fig.30. This should take the place of Figs.48 and 51 in Ref.1 in which C_{Y_o} was assumed to be independent of store chordwise position.

/Fig.30 gives both....

Fig.30 gives both (S) and (SP) values for the store with or without tail fins and over the Mach-number range from M = 0.5 to M = 1.5.

Ref.1 did not propose any factor for the variation of C_{Y_o} with spanwise position and even with the present results, it is difficult to suggest any simple factor. Assuming that the stores are not mounted too far away from mid-semispan, it is suggested that intelligent use of Fig.10(b) coupled with a knowledge of the likely sidewash field under the wing at the appropriate Mach number should give some indication as to how the values of C_{Y_o} deduced from Fig.30 should be modified.

(2) $dC_Y/d\alpha$: As noted above, it now seems likely that the variation of $dC_Y/d\alpha$ with Mach number will be a function of the depth of the store. In Ref.1, values of $dC_Y/d\alpha$ computed for a given store chordwise and spanwise position and a given Mach number were then multiplied by a factor related to store depth and this last factor was taken as being independent of Mach number. It is this assumption that may prove to be invalid; if not, the factor K_{m_2} suggested in Fig.47 of Ref.1 to account for the variation of $dC_Y/d\alpha$ with Mach number will need revision.

Considering just the results of the present tests, if one is prepared to accept an accuracy at the worst of about ±15% in $dC_Y/d\alpha$, one could assume that the value for each store/pylon configuration was independent of Mach number. This accuracy is probably not good enough but plotting these mean values against either x_s or y_s as in Fig.31 does provide a quick indication of the effects of chordwise and spanwise position. These variations have been discussed in detail in section 8.1.2 above.

The bottom picture of Fig.31 shows the variation in $|dC_Y/d\alpha|_{mean}$ with x_s at $y_s = 0.50$. It will be seen that for both (S) and (SP) data, fins on or off $|dC_Y/d\alpha|_{mean}$ decreased linearly between $x_s = 0$ and $x_s = 0.50$. This is qualitatively as predicted in Ref.1 but quantitatively, the variation is somewhat larger than predicted. A suitable expression for the variation shown in Fig.31 is :

$$\left|dC_Y/d\alpha\right| = (1-x_s)\ \left|dC_Y/d\alpha\right|_{x_s = 0}$$

Strictly, this relation should only be used for $0 < x_s < 0.5$ and clearly, the relation would not apply far outside these limits. For example, when $x_s = 1.0$ (i.e, store mid-point below the trailing edge), the relation would suggest that $|dC_Y/d\alpha|$ would be zero at this point but this would certainly not be true since the store would still be influenced by the wing flow field. Also, when x_s is negative, (i.e, store mid-point in front of the wing leading edge), use of the above relation would imply that $dC_Y/d\alpha$ for such locations would be greater than for $x_s = 0$. Data in Ref.1 indicated however that the aerodynamic loads would probably decrease when the store was moved ahead of the leading edge and this was recognised in Fig.46 in Ref.1. As an interim measure, it is suggested that

/for stores ahead.....

for stores ahead of the leading edge, the sign of x_s should be changed before insertion in the relation for $dC_Y/d\alpha$, i.e. the relation should read :

$$\left|dC_Y/d\alpha\right| = (1-|x_s|)\ \left|dC_Y/d\alpha\right|_{x_s = 0}$$

In Ref.1 it was suggested that the variation of $dC_Y/d\alpha$ with y_s at a given x_s would be linear - at least, over the middle part of the span between about $y_s = 0.30$ and $y_s = 0.80$. For the empirical method, this linear variation was given in Fig.45 of Ref.1. In the present tests, results were only obtained for two spanwise positions at $x_s = 0$ and two positions at $x_s = 0.50$. If one assumes that the chordwise variation at $y_s = 0.30$ is similar to that observed at $y_s = 0.50$, a third point could be included on the graph of $\left|dC_Y/d\alpha\right|_{mean}$ with y_s for $x_s = 0$. Similarly, a third point could be included on the graphs for $x_s = 0.50$. Figs.31 and 32(a) show that the resulting variation with y_s is not linear; there is a considerable increase in $\left|dC_Y/d\alpha\right|_{mean}$ between $y_s = 0.30$ and $y_s = 0.50$ but little further change between $y_s = 0.50$ and $y_s = 0.75$. It is very difficult to decide whether one should accept these as general conclusions. As explained earlier, when the aircraft wing is tapered, changes in y_s imply changes in a number of other variables. For example, if a store of constant size is moved in the spanwise direction beneath a highly tapered wing, the size of the store relative to the local wing chord changes. Therefore, when it is near the tip, a smaller portion of the store experiences the high values of (σ/α) that apply below the wing leading edge and this could be one of the reasons that the increase in $\left|dC_Y/d\alpha\right|_{mean}$ with y_s is not maintained over the outer wing.

In practice, most stores will be mounted somewhere near the mid semispan station and on the evidence of Fig.31, it seems that for small changes in y_s around this position, one might as well assume that $dC_Y/d\alpha$ does not vary with y_s. For larger changes in y_s, the results from a generalised research series may not be applicable to an actual aircraft layout. For example, when the store is mounted near the wing root, it will be affected by the fuselage-induced sidewash (see section 10 below) while if it is mounted below the outer wing, the loads could be influenced by the specific tip shaping of the aircraft wing.

(3) $\underline{dC_Y/d\beta}$: From what was said earlier in section 8.1.3, it seems that for an empirical method of load prediction, it may be

/fair to assume.....

fair to assume that $dC_Y/d\beta$ has a constant value independent of Mach number at subsonic speeds and a different constant value, again independent of Mach number, at supersonic speeds. This is consistent with what was suggested in Ref.1, i.e, the factor K_{m_s} in Fig.53 of Ref.1.

On the other hand, certainly at supersonic speeds, the present test results do not support the contention of Ref.1 that $dC_Y/d\beta$ can be treated as independent of the store chordwise position. For example, the variation of $|dC_Y/d\beta|_{\alpha=0^o}$ with x_s as shown in Fig.33 At subsonic speeds, $dC_Y/d\beta$ can still be taken as independent of x_s but at supersonic speeds the results give the relation :

$$dC_Y/d\beta = |dC_Y/d\beta|_{x_s = 0} - 0.064 x_s$$

The negative sign in this relation implies that at positive α, β; $|dC_Y/d\beta|$ increases as the store is moved aft. This expression applies for both the (S) and (SP) data and irrespective of whether the store has tail fins or not. Strictly, it only applies at zero incidence but it is included here to give some idea of the effects of chordwise position.

As regards the effect of spanwise position, as with $dC_Y/d\alpha$, this can only be deduced from the present results by assuming that the effects of x_s are independent of y_s. The derived variation of $dC_Y/d\beta$ with y_s at either subsonic or supersonic speeds is shown in Fig.32(b). The curves for the store without fins were drawn on the assumption that the fin contributions to $dC_Y/d\beta$ did not vary with spanwise position. These curves in Fig.32(b) are similar qualitatively to the variation predicted in Fig.52 in Ref.1.

Relations for the variation of $dC_Y/d\beta$ with incidence have been given already in section 8.1.3. They are repeated here for convenience :

at subsonic speeds $|dC_Y/d\beta| = |dC_Y/d\beta|_{\alpha=0} - 0.004\alpha$

at supersonic speeds for the (SP) loads $|dC_Y/d\beta| = |dC_Y/d\beta|_{\alpha=0} - 0.005\alpha$

at supersonic speeds for the (S) loads $|dC_Y/d\beta| = |dC_Y/d\beta|_{\alpha=0} - 0.002\alpha$

In Ref.1 it was suggested that until further experimental evidence was available, the values of $dC_Y/d\beta$ should be increased by 25% to allow for the incidence-sideslip cross-coupling effect but it was not made clear that this 25% was intended to refer to a combination such as $\alpha = 10^o$, $\beta = 10^o$. As noted earlier, analysis of the present results suggest it is much better to use relations of the form quoted above rather than to treat the effects of incidence on $dC_Y/d\beta$ as a percentage increase.

Combining the various suggestions put forward above, a revised empirical method providing reasonable agreement with the present results would be as follows :-

/ (a), (b) etc.....

(a) Determine C_{Y_o} from Fig.30. No great loss of accuracy is anticipated if this figure is taken to apply to spanwise locations between about $y_s = 0.40$ and $y_s = 0.60$ for wings of small taper,

(b) Obtain $|dC_Y/d\alpha|$ at $x_s = 0$ from Fig.32(a) for the given spanwise location,

(c) Obtain $|dC_Y/d\beta|$ at $x_s = 0$ from Fig.32(b) for the given spanwise location and Mach number,

(d) Insert the values of the above 3 sideforce terms into the appropriate equations below to obtain expressions

$$C_Y = A + B\alpha + C\beta + D\alpha\beta$$

e.g.

(1) For (SP) (S) (ON) (OFF) at SUBSONIC speeds,

$$C_{Y_{\alpha\beta}} = C_{Y_o} + |dC_Y/d\alpha|\left(1-|x_s|\right)\alpha + \left[|dC_Y/d\beta| - 0.004\alpha\right]\beta$$

(2) For (SP) (ON) (OFF) at SUPERSONIC speeds,

$$C_{Y_{\alpha\beta}} = C_{Y_o} + |dC_Y/d\alpha|\left(1-|x_s|\right)\alpha + \left[|dC_Y/d\beta| - 0.064|x_s| - 0.005\alpha\right]\beta$$

(3) For (S) (ON) (OFF) at SUPERSONIC speeds,

$$C_{Y_{\alpha\beta}} = C_{Y_o} + |dC_Y/d\alpha|\left(1-|x_s|\right)\alpha + \left[|dC_Y/d\beta| - 0.064|x_s| - 0.002\alpha\right]\beta$$

(e) Finally, the desired values of α and β are inserted into the appropriate equations to derive $C_{Y_{SP}}$ or C_{Y_S} for fins on or off.

The signs of the various sideforce terms are applicable to stores mounted on the port wing panel where the effects of positive incidence and positive sideslip are additive. They combine to give an outwardly directed (negative) sideforce. For a store on the starboard wing panel, positive incidence produces an outwardly directed sideforce whilst positive sideslip produces an inwardly directed sideforce. Hence for this case it is necessary to reverse the signs of $|dC_Y/d\beta|$ whilst retaining the sign for $|dC_Y/d\alpha|$.

It must again be emphasised that the procedure set out above should only be regarded as an interim revision of the empirical method and it only applies for stores mounted at a depth of about 1.4 x store diameters below the wing chordal plane. A final revision of the method including an appropriate allowance for the effects of store depth will be included when the results of the later tests are available.

10. STORE SIDEFORCE FOR VARIOUS AD HOC STORE/AIRCRAFT CONFIGURATIONS

The proposed empirical method for estimating store/pylon sideforce either as presented in Ref.1 or in its tentative revised form in section 9 above is only intended to be used when the store/pylon/aircraft geometry satisfies the broad specification set out at the start of section 9. So far in this note, we have merely discussed the results from a series of general research tests in which these conditions were satisfied. Recently, however, store load measurements have been obtained in the A.R.A. transonic tunnel for a variety of ad hoc store configurations mounted beneath the wings of several different specific aircraft models. Some of these results have emphasised the dangers of applying the empirical method outside its proper range of validity and so for completeness, it was thought worth including a few typical examples in this note. In particular, these examples illustrate how the store sideforce values can be modified :

(a) If the store is no longer a simple body of revolution with or without small tail fins but instead, is fitted with significant wing-type lifting surfaces,

/ (b).....

(b) If the store length is no longer comparable with the local wing chord but is for example, much smaller than this,

and

(c) If the flow field beneath the wing-fuselage configuration is markedly affected by sidewash induced by the fuselage.

Fig.34 compares the values of C_{Y_o}, $dC_Y/d\alpha$ and $dC_Y/d\beta$ obtained for three different stores mounted at the same spanwise position ($y_s = 0.54$) beneath a 60° delta wing. Store A is similar to the store used in the research programme discussed earlier in this note; it is a body of revolution with some tail fins; it is mounted on an unswept pylon at a depth of 0.127c below the wing chordal plane and with the store mid-point at $\bar{x}_s = 0.28$. Store B is mounted in about the same position ($z_s = 0.121$ and $x_s = 0.30$) but it is a much smaller store than store A with a length, $l_s = 0.42c$ rather than $l_s = 0.80c$; also, store B has a much lower fineness ratio than Store A. Store C is unlike stores A and B in that it is a winged missile; it is mounted at a slightly greater depth ($z_s = 0.144$) and at a further forward position, $x_s = 0.02$.

Strictly, the empirical method for estimating the store/pylon side-force is only applicable in the case of store A. If one had nevertheless applied it to store B, despite its small size relative to the local wing chord, one would have obtained values virtually the same as those for store A. Fig.34 shows however that the measured values of C_Y for store A and B differ significantly. For example, C_{Y_o} for store B is less than for store A by about 0.1 at subsonic speeds, and by as much as 0.2 - 0.25 at supersonic speeds; as a result, even though there is a qualitative similarity between the variation of C_{Y_o} with Mach number for the two stores, the actual values differ greatly and C_{Y_o} for store B becomes negative above $M = 1.1$ whereas for store A, it remains positive throughout the test range up to $M = 1.4$. Also, $|dC_Y/d\alpha|$ is less for store B than for store A by some 20-40% according to the Mach number and there is a further small difference in the values of $|dC_Y/d\beta|$. All these changes can probably be traced to one major factor. This is that although the store mid-points are at much the same chordwise position, the nose of the smaller store B is still well behind the local wing leading edge whereas the nose of store A lies ahead of the leading edge. This means that the nose of store B is too far aft to experience the large sidewash just downstream of the wing leading-edge shock at low supersonic speeds and also, it is too far aft to experience the maximum values of (σ/α) which occur below the wing leading edge at subsonic speeds.

The differences between the results for stores A and B could therefore probably be explained in terms of the local sidewash field beneath the wing. They demonstrate however that further refinement to the empirical method would be necessary to make it apply to stores of such widely differing lengths. In passing, it may be noted that errors in estimating the values of C_Y for a typical stressing condition such as $\alpha = \beta = 10°$ may be less serious than the errors in estimating the individual terms, C_{Y_o}, $dC_Y/d\alpha$ and $dC_Y/d\beta$. This is because the errors in estimating these terms to some extent compensate for one another when considering a positive incidence condition. For example, for $\alpha = \beta = 10°$, $M = 1.40$, C_{Y_S} for stores A and B are respectively -2.6 and -2.3 and hence for such a

/condition, ...

condition, C_{Y_S} for the two stores is almost the same.

As might be expected, the results for store C, the winged missile, indicate much larger values for $|dC_Y/d\alpha|$ and $|dC_Y/d\beta|$ than for the two stores without wings. If the empirical method had been applied to predict the loads on store C, i.e. if the fact that it has wings had been ignored, the estimated values of C_{Y_o} would have been more positive than for store A at subsonic speeds (by about 0.05), and more negative at supersonic speeds (e.g. by about 0.15 at M = 1.4). $|dC_Y/d\alpha|$ for store C would have been estimated as being about 30% greater than for store A, due to the difference in the value of x_s. In fact, the measured results shown in Fig.34 indicate a reduction in C_{Y_o} varying from about 0.1 at subsonic speeds to about 0.35 at supersonic speeds and an increase by a factor of about 2.0 - 2.2 rather than 1.3 in $|dC_Y/d\alpha|$. Hence, as compared with predictions by the empirical method, one can say that the wings on store C have given a reduction of about 0.15 in C_{Y_o}, an increase of about 60% in $|dC_Y/d\alpha|$ and an increase of about 100% in $|dC_Y/d\beta|$.

One should be careful at this point to differentiate between changes in non-dimensional coefficients and changes in actual loads. The effects of the wings on store C appear particularly large when expressed in terms of C_Y but this is partly because the coefficients are always based on the frontal area of the stores which is considerably less for store C than for store A (0.73 sq.ins. model scale as compared with 1.54 sq.ins.). Quoting again values for $\alpha = \beta = 10^o$, M = 1.4, C_{Y_S} for store C is about -5.0 as compared with -2.6 for store A or -3.0 as predicted by the empirical method for a streamline store at the appropriate chordwise position. In actual loads, the measured value for store C is -23 lbs, the measured value for store A is -25 lbs and the predicted value for store C is -14 lbs. The fact that the actual loads for stores A and C are comparable is of course an important conclusion for the design of the store-pylon and pylon-wing fixations but it is clearly somewhat coincidental.

Some further results at transonic speeds are given in Fig.35 for store C mounted on a different pylon beneath a 40^o swept wing at a relatively inboard location. Again, the values of the three sideforce terms, ((S) values) are given and these may be compared with those for store C under the 60^o delta wing in Fig.34. It will be seen that there is virtually no correlation whatsoever between the two sets of results.

The geometry of the store C installations under the two wings differs in many respects. For the 40^o swept wing in Fig.35, the store is mounted further inboard, (y_s = 0.41 rather than y_s = 0.54), further to the rear (x_s = 0.16 rather than x_s = 0.02) and further below the wing (z_s = 0.22 rather than z_s = 0.144). All these changes and also the fact that it is a 40^o swept rather than a 60^o delta wing will tend under most conditions to reduce the wing-induced sidewash. On this basis, therefore, one might have expected smaller values for $|dC_Y/d\alpha|$ in Fig.35 than in Fig.34; as regards C_{Y_o}, the values might have been more negative at subsonic speeds and more positive at supersonic speeds. $|dC_Y/d\beta|$ might have tended to be greater at supersonic speeds. These conclusions bear no relation to the observed measured values which indicate a much more positive C_{Y_o} (e.g. at M = 0.6, 2.0 rather than 0.10), a much larger $|dC_Y/d\alpha|$ (at M = 0.6, -0.50 rather than -0.12) and a much greater $|dC_Y/d\beta|$ (M = 0.6, -0.50 rather than -0.10).

/Two factors remain....

Two factors remain to explain the discrepancy. Of these, much the more important is probably the fact that for the configuration in Fig.35, the store lies much closer to the fuselage, the distance between the edge of the fuselage and the inboard edge of the store (plan view) being only 0.075b/2 instead of 0.250b/2 as in Fig.34. It is not only the relative distance from the fuselage that matters; the shape of the fuselage and the cross-flow that it induces is equally significant. Oil flow photographs taken during tests on the model in Fig.35 confirmed that a very large fuselage-induced sidewash was present at the store station even at zero incidence and this is presumably responsible for the exceptionally large values of C_{Y_o}. Under sideslip conditions, this fuselage-induced sidewash would be expected to be considerably different under the port and starboard wings and this could account for the relatively large values of $|dC_Y/d\beta|$.

The second factor affecting the store loads in Fig.35 is the presence of the launcher. In this case, the (S) loads refer to the store and launcher, rather than just the store, but the maximum cross-sectional area of the store was still used when deriving the non-dimensional coefficients. In effect, this means that the so-called (S) loads are really a mean of what might be estimated as the (S) and (SP) loads and this could materially increase all three sideforce terms. This could account for an increase of possibly 0.3 in C_{Y_o} and possibly 0.15 in both $dC_Y/d\alpha$ and $dC_Y/d\beta$. Even so, this still leaves about 1.6 in C_{Y_o}, 0.25 in $dC_Y/d\alpha$ and 0.42 in $dC_Y/d\beta$ to be explained in terms of the extremely large fuselage-induced sidewash. It follows that the present simplified empirical method fails completely if one tries to apply it to a winged missile mounted fairly far inboard and near a fuselage inducing strong cross flow.

11. CONCLUDING REMARKS

This note has given the store/pylon sideforce and yawing moment results for a simple store, with or without tail fins mounted on a swept forward pylon at various positions beneath a 45° sweptback wing. The results have been analysed and related to the likely flow fields beneath the wing to indicate the effects of Mach number, and store chordwise and and spanwise position. Some indication has been included of the variation with incidence and Mach number of both the depthwise and chordwise centres of pressure due to incidence on both the store and the store/pylon.

Over most of the test range and for most of the configurations, C_Y is found to vary linearly with both incidence and sideslip and thus, the basis of the empirical method proposed in Ref.1 for estimating store/pylon sideforce is confirmed by the present results. Certain detailed changes to the factors in the method are however required.

/Many of the trends.....

Many of the trends in the sideforce and yawing moment data have been correlated successfully with the likely flow field characteristics and in particular, the wing-induced sidewash. Some of the main trends are as follows :

(i) For the forward mounted stores, C_{Y_o} is positive at subsonic speeds and decreases with Mach number above about M = 1.0, ultimately becoming negative. This is as predicted in Ref.1 but there is a much greater variation with chordwise position than was suggested earlier. For the aft-mounted stores, C_{Y_o} is relatively small at subsonic speeds but tends to increase near M = 1.0 so that at supersonic speeds, C_{Y_o} is greater than for the forward mounted stores.

(ii) For the store configurations of these tests, $|dC_Y/d\alpha|$ does not vary much with Mach number more than about ±15% about a mean value which depends greatly on the store position, decreasing as the store is moved aft or inboard. It is suspected that the variation of $|dC_Y/d\alpha|$ with Mach number is likely to depend significantly on the depth of the store but this has not so far been investigated. As compared with predictions by the method of Ref.1, $|dC_Y/d\alpha|$ was in reasonable agreement at supersonic speeds but was larger than predicted at subsonic speeds,

(iii) $|dC_Y/d\beta|$ increases with Mach number near M = 1.0 and this increase is particularly pronounced for stores mounted in an aft position. Thus, at supersonic speeds, $|dC_Y/d\beta|$ increases as the store is moved aft. A significant incidence-sideslip cross-coupling effect is confirmed in that in nearly all cases, $|dC_Y/d\beta|$ increases significantly with incidence. This increase is best expressed as an increment rather than as a percentage,

(iv) For the stores with tail fins, the largest values of C_n are obtained near zero incidence. Increasing incidence tends to reduce C_n and tends to move the centre of load nearer to the store mid-point. The values of C_{n_o} increase with Mach number up to near M = 1.0 and then decrease; they decrease considerably as the store is moved aft, the fin contributions to C_{n_o} change sign as the store is moved aft,

(v) The C_n-α curves are much less linear than the C_Y-α data. The incidence at which the change in slope occurs tends to decrease with Mach number and to increase as the store is moved aft; the actual change in slope becomes less as the store is moved aft.

The maximum values of C_Y and C_n for a particular store/pylon installation will clearly depend on the flight envelope and it is difficult to draw general conclusions. For a typical store location below the wing leading edge at mid semispan, it seems that in general, assuming the critical stressing case to correspond to maximum positive incidence, the maximum loads would decrease if the store were moved aft or if it were moved inboard. The maximum values of C_Y will almost always be greater at low supersonic speeds than at subsonic speeds; for forward mounted stores, this will be mainly because of the decrease in C_{Y_o} with Mach number coupled with some increase in $|dC_Y/d\alpha|$; for stores mounted further aft, this will be because the increase in $|dC_Y/d\alpha|$ and $|dC_Y/d\beta|$ more than offsets any

/relief due to an......

relief due to an increase in C_{Y_o}. In practice, however, transonic speeds may pose more critical loads than supersonic speeds because it is near $M = 1.0$ that the maximum values of $|dC_Y/d\alpha|$ can be recorded and more particularly, because in practice, transonic speeds are likely to be associated with low altitude and hence high-q conditions.

The depthwise centre of pressure tends to be independent of incidence and Mach number but to be sensitive to store chordwise position and to whether the store has fins or not. In the present tests, the centre of pressure was furthest from the wing and hence, the bending moments about the pylon-wing fixation greatest, when $x_s = 0.15$ and when the fins were present.

Finally, the note includes some illustrations taken from the results of ad hoc store-load measurements showing that the empirical method as at present formulated should not be used for :

(a) Stores that are small in relation to the local wing chord,

(b) Winged missiles,

(c) Configurations mounted well inboard and near a fuselage inducing a strong cross-flow.

LIST OF REFERENCES

1. MARSDEN, P. HAINES, A. B. — Aerodynamic loads on external stores : A review of experimental data and methods of prediction. A.R.C. R. & M. 3505, November, 1962.

2. O'HARA, F. SQUIRE, L. C. HAINES, A. B. — An investigation of interference effects on similar models of different size in various transonic tunnels in the U.K. A.R.A. WIND TUNNEL NOTE NO. 27. R.A.E. TECHNICAL NOTE NO. AERO 2606. February, 1959.

3. HALL, I. M. ROGERS, E. W. E. — Experiments with a tapered sweptback wing of Warren 12 planform at Mach numbers between 0.6 and 1.6. A.R.C. R. & M. 3271, July, 1960.

4. ALFORD, W. J. Jr. — Theoretical and experimental investigation of the subsonic-flow fields beneath swept and unswept wings with tables of vortex-induced velocities. NACA REPORT 1327 (Supersedes NACA TN 3738) 1957.

5. CARLSON, H. W. — Measurements of flow properties in the vicinity of three wing-fuselage combinations at Mach numbers of 1.61 and 2.01. NASA TM X-64, October, 1959.

6. MORRIS, O. A. CARLSON, H. W. GRIER, D. J. — Experimental and theoretical determination of forces and moments on a store and on a store-pylon combination mounted on a 45° swept-wing-fuselage configuration at a Mach number of 1.61. NACA RM L57K18, TIL/5822 January, 1958.

7. BOBBIT, P. J. MALVESTUTO, F. S. Jr. MARGOLIS, K. — Theoretical prediction of the side force on stores attached to configurations travelling at supersonic speeds. NACA RM L55L30b, TIL/5038, March, 1956.

8. BOBBITT, P. J. MAXIE, P. J. — Sidewash in the vicinity of lifting swept wings at supersonic speeds. NACA TN 3938, February, 1957.

9. TREBBLE, W. J. G. HOLFORD, J. F. — Low speed wind tunnel measurements and estimations of the pitching and yawing moments of tanks mounted on struts under 40° swept and straight wings. R.A.E. TECHNICAL NOTE AERO.2394, October, 1955.

10. SPENCE, A. HOLFORD, J. F. — The low speed effects of wing tip stores. R.A.E. TECHNICAL NOTE AERO 2279, November, 1953.

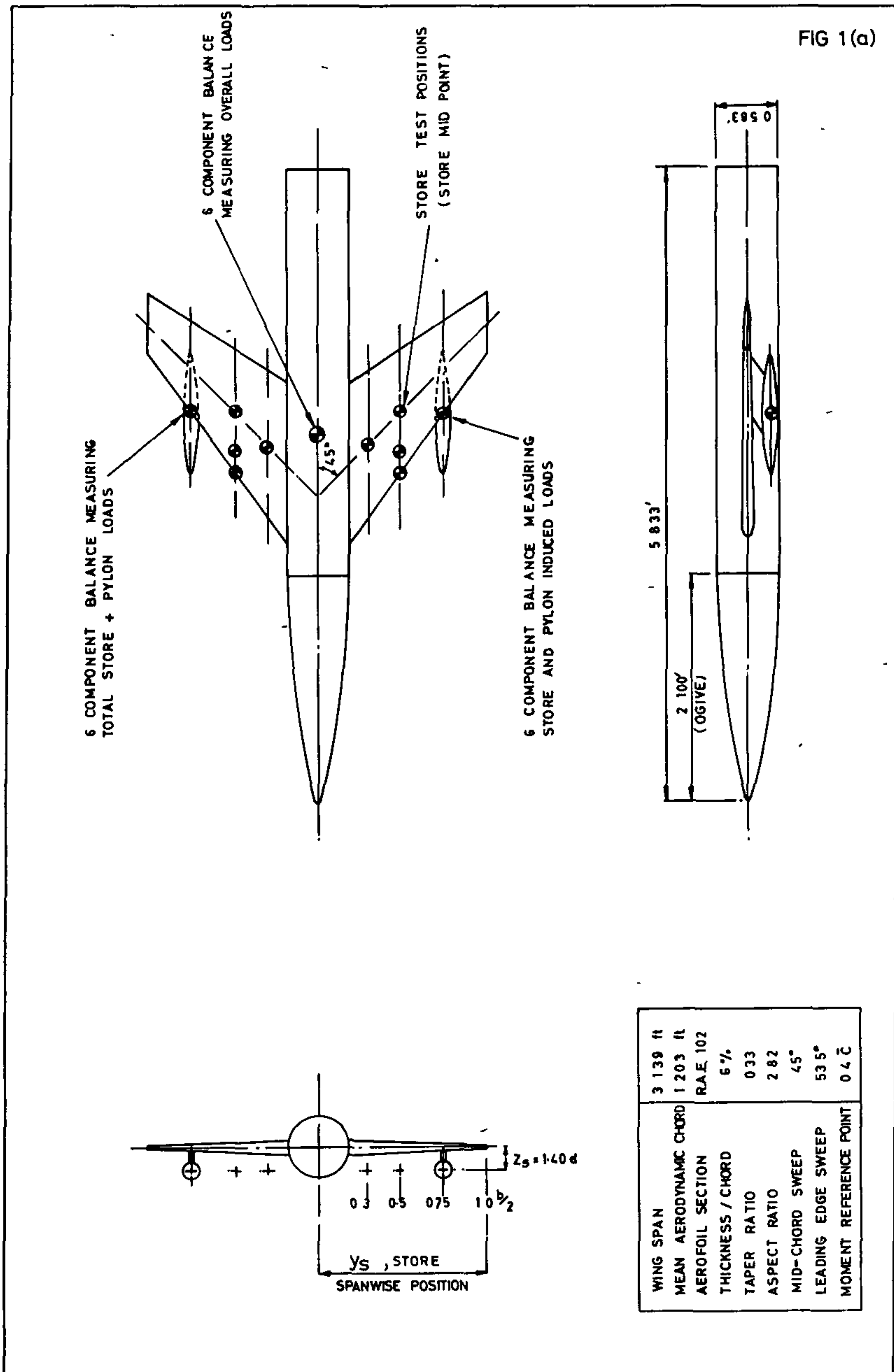

FIG. 1.(a). DETAILS OF MODEL AND STORES. DIMENSIONS OF WING-FUSELAGE COMBINATION AND STORE LOCATIONS.

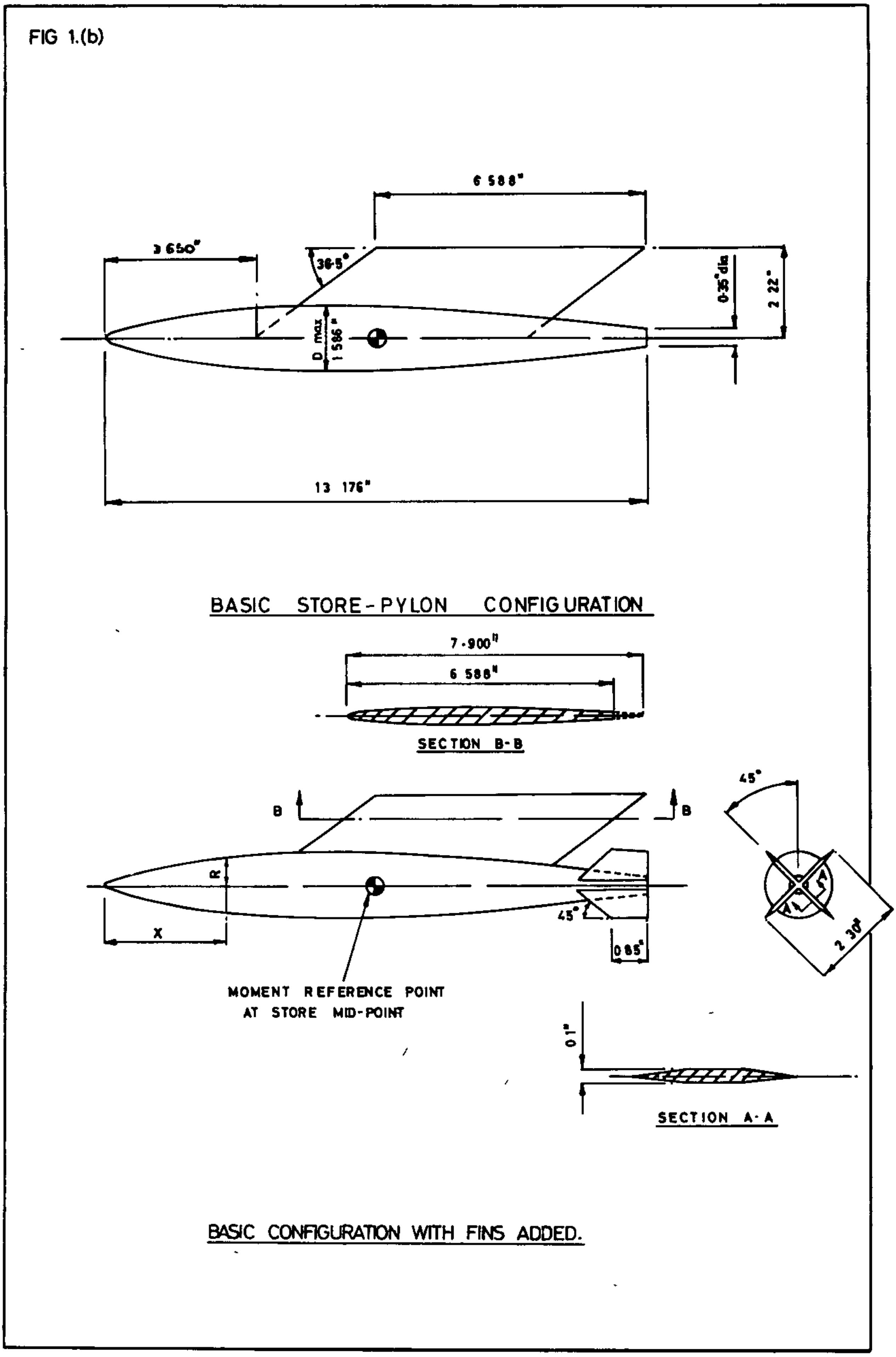

FIG. 1.(b). STORE-PYLON CONFIGURATIONS.

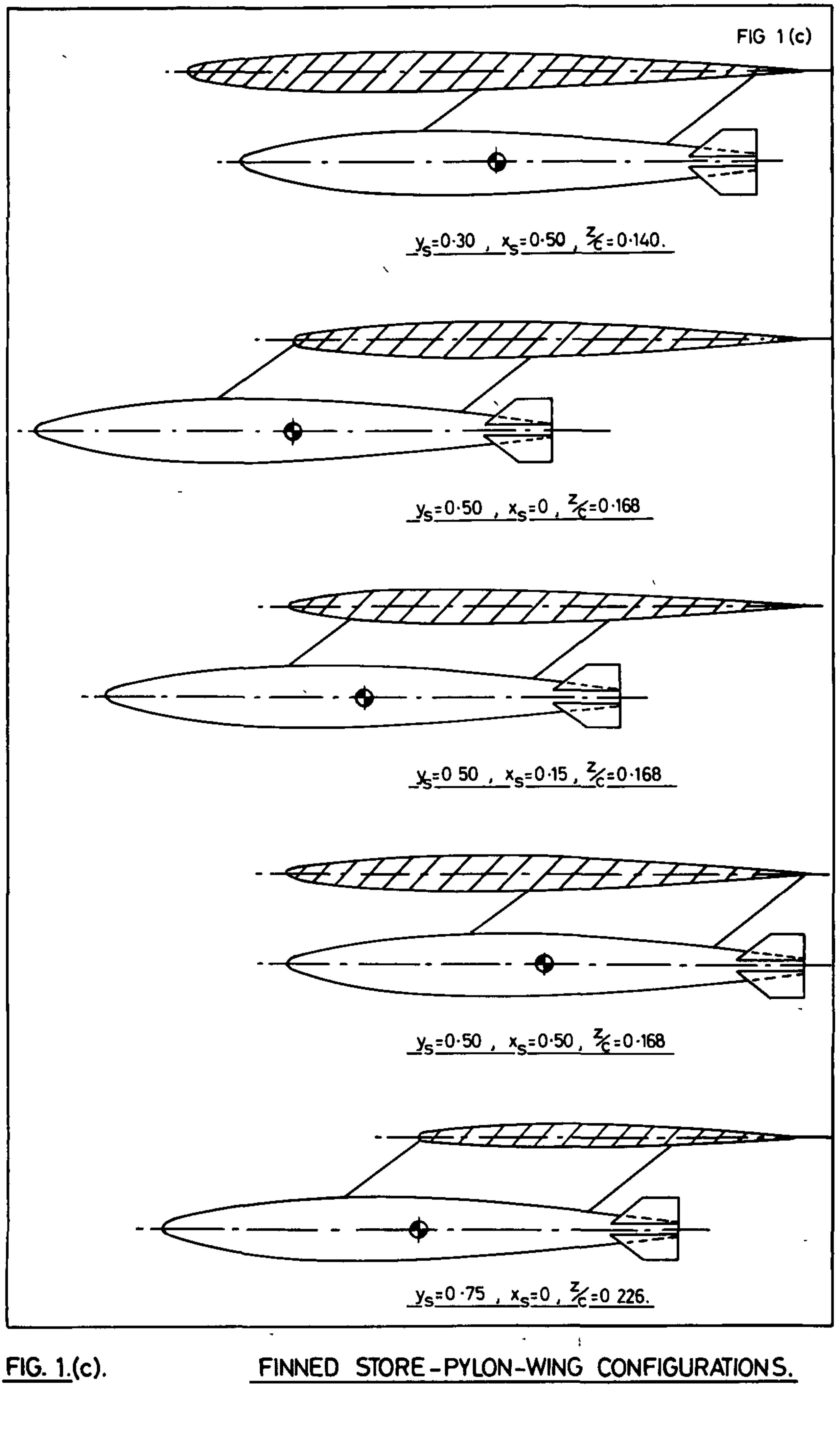

FIG. 1.(c). FINNED STORE-PYLON-WING CONFIGURATIONS.

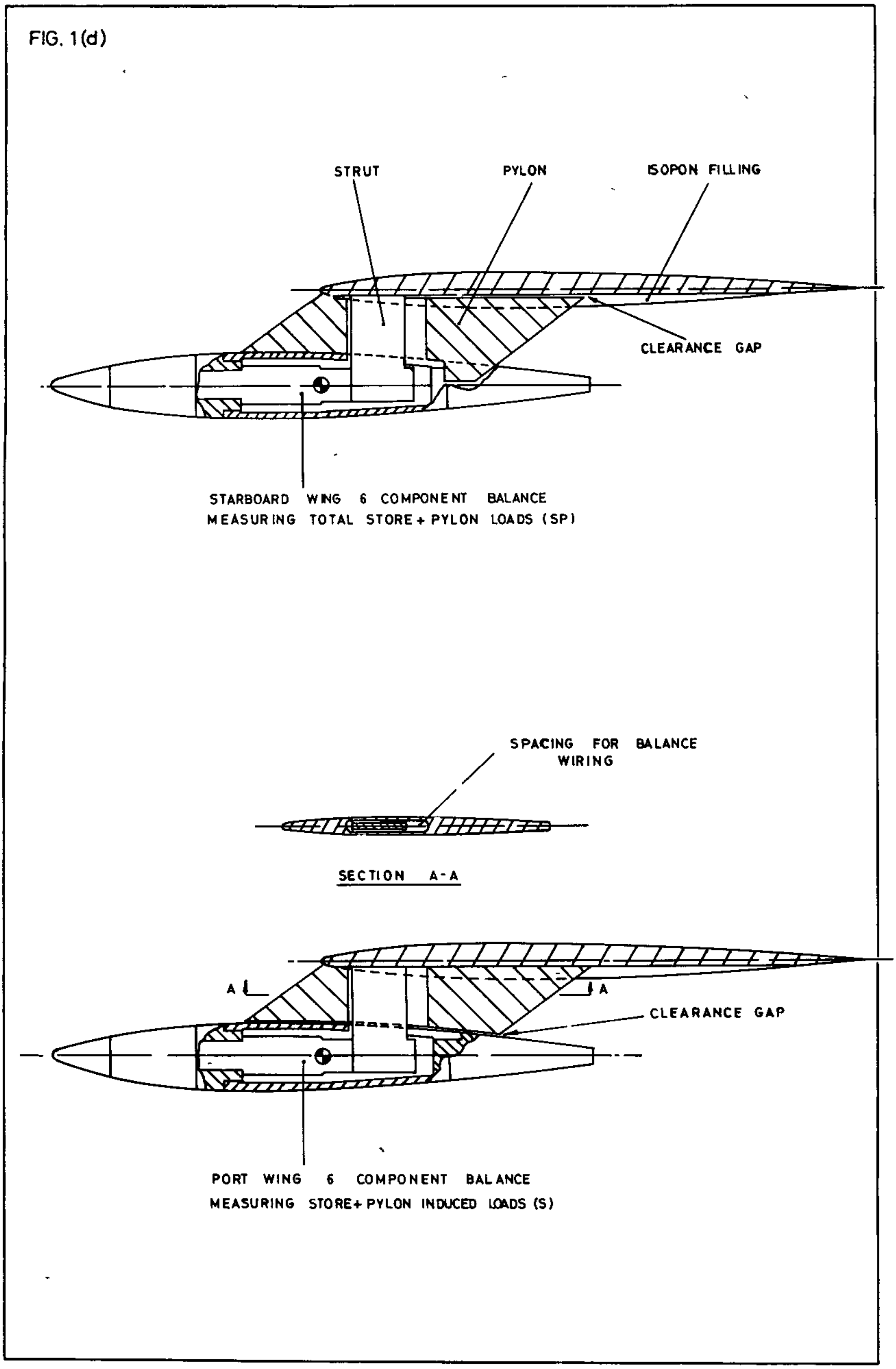

FIG. 1.(d). DETAILS OF STORE-PYLON-STRUT ASSEMBLY SHOWING CLEARANCE GAPS.

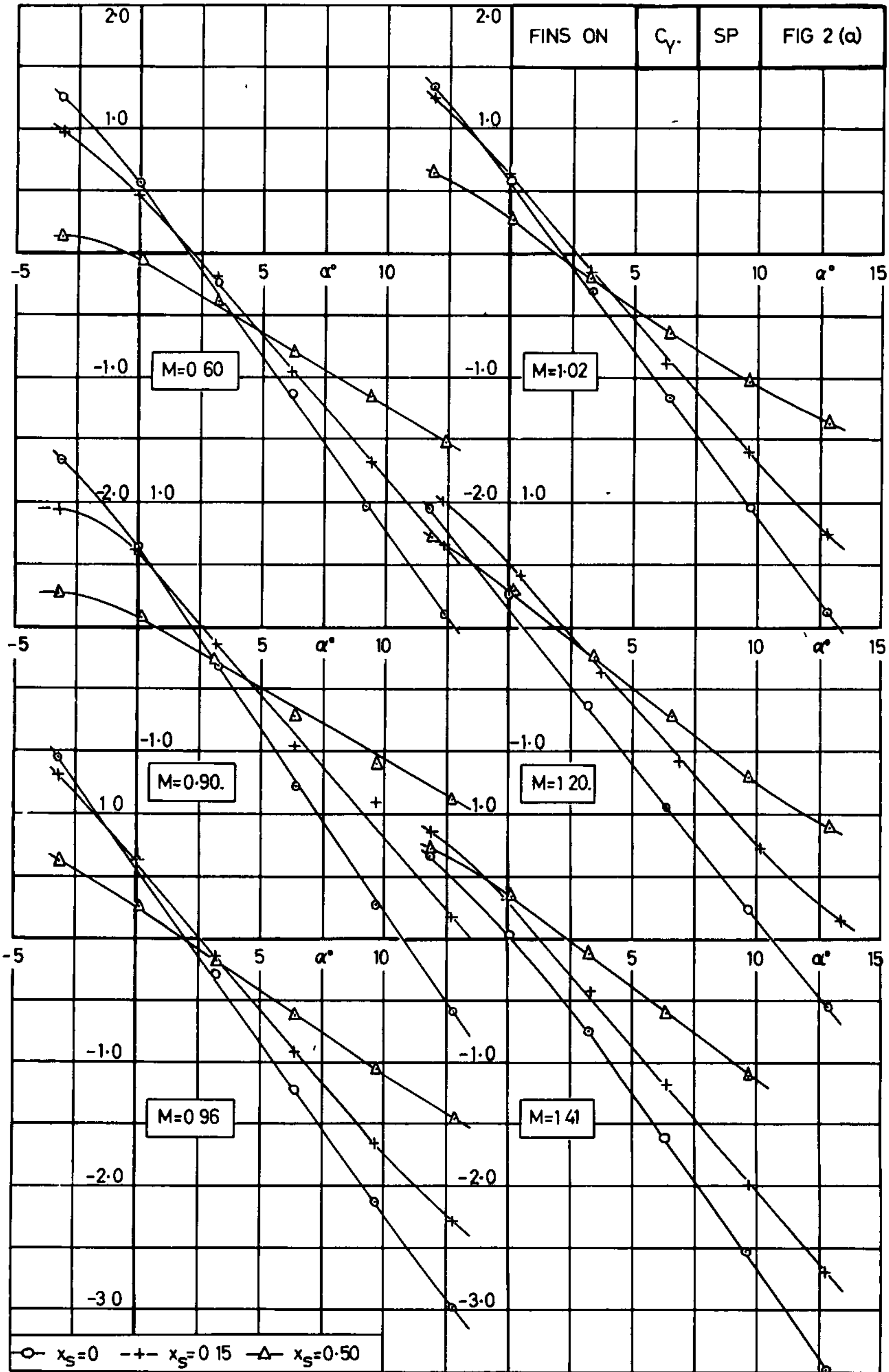

FIG. 2.(a). VARIATION OF STORE / PYLON SIDE FORCE WITH INCIDENCE FOR 3 CHORDWISE LOCATIONS. y_s=0·50, (SP) FINS ON.

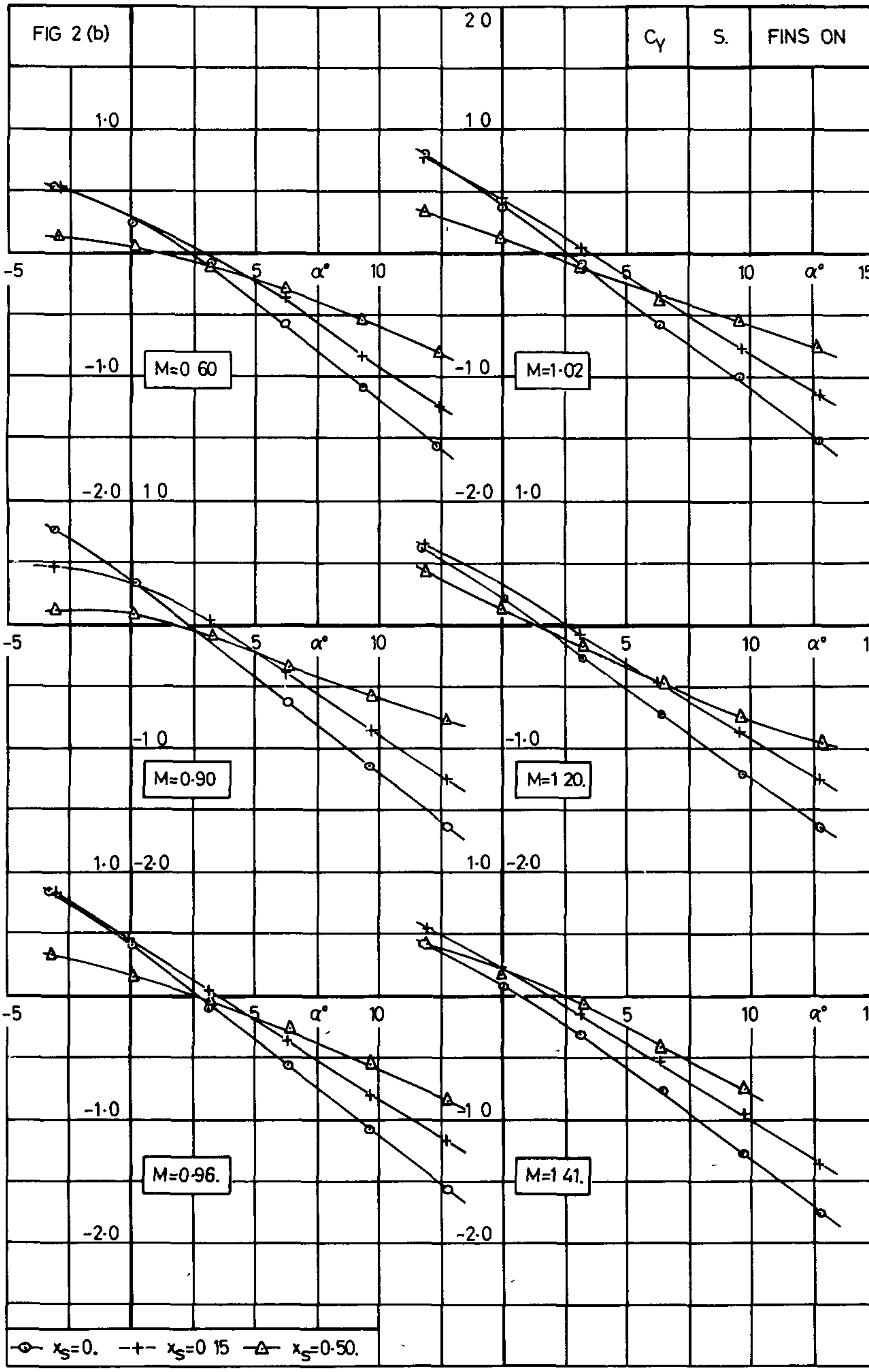

FIG. 2.(b). y_s=0·50, (S) FINS ON.

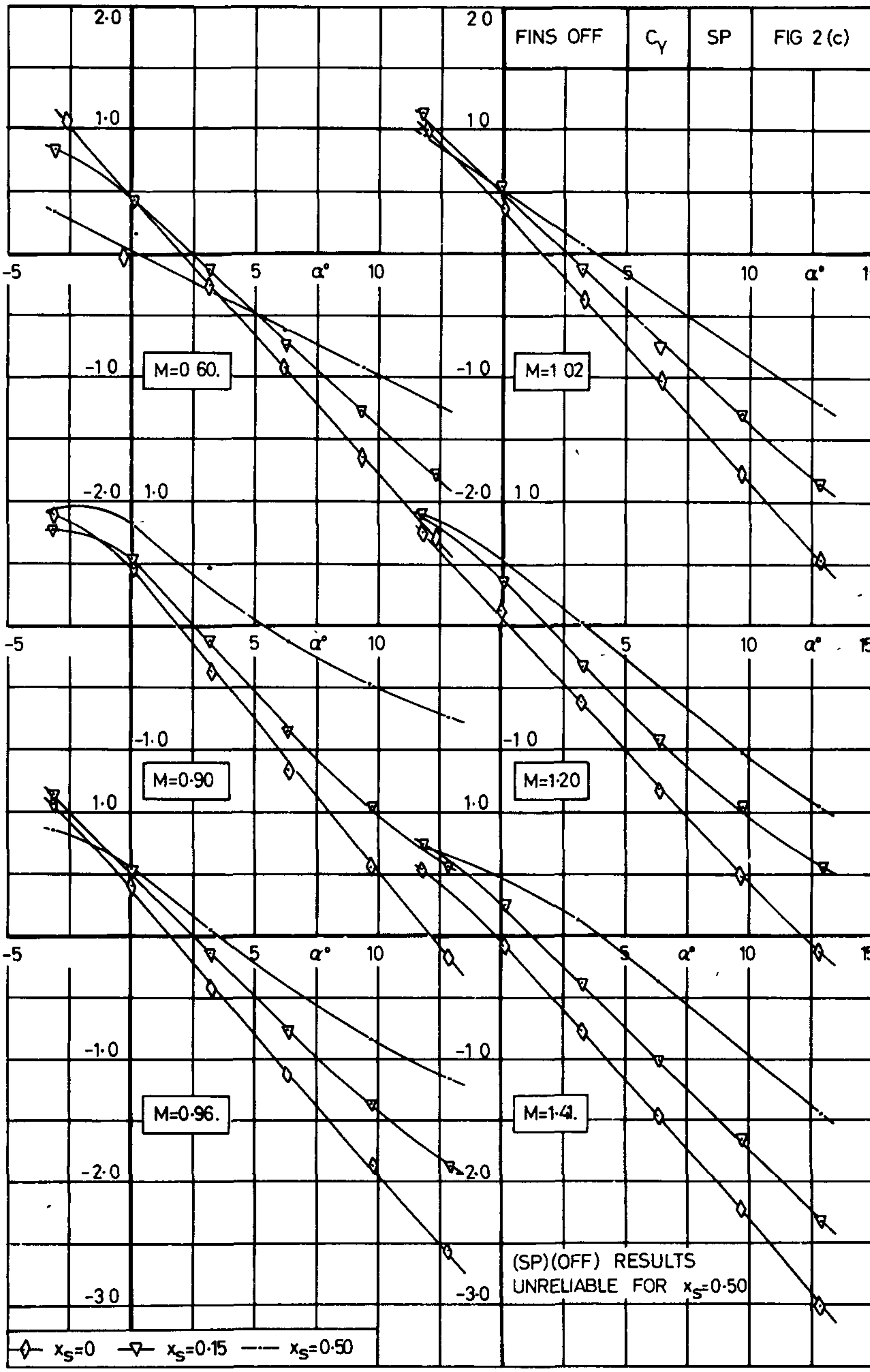

FIG. 2.(c). y_s=0·50, (SP) FINS OFF.

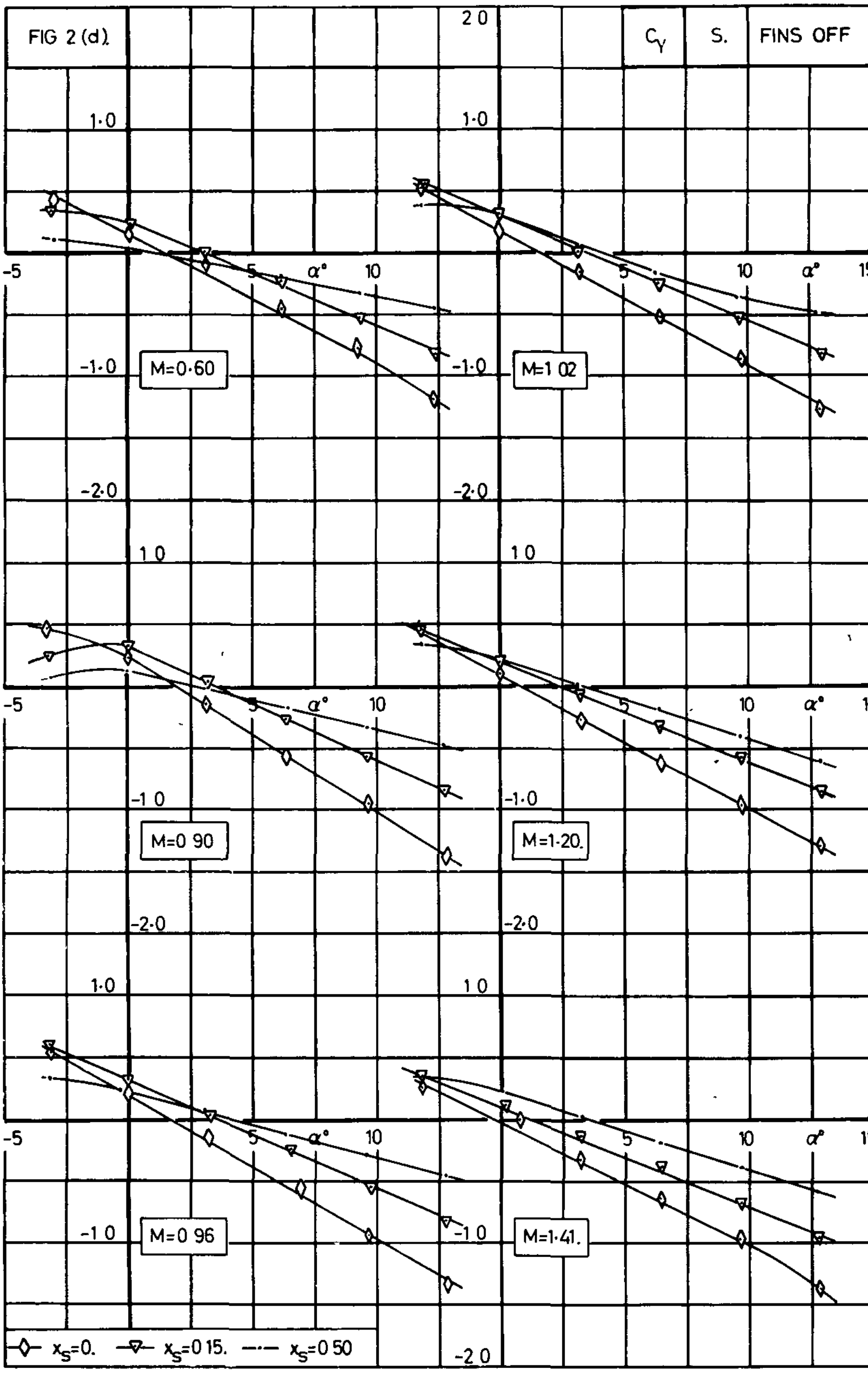

FIG. 2.(d). y_S=0·50, (S) FINS OFF.

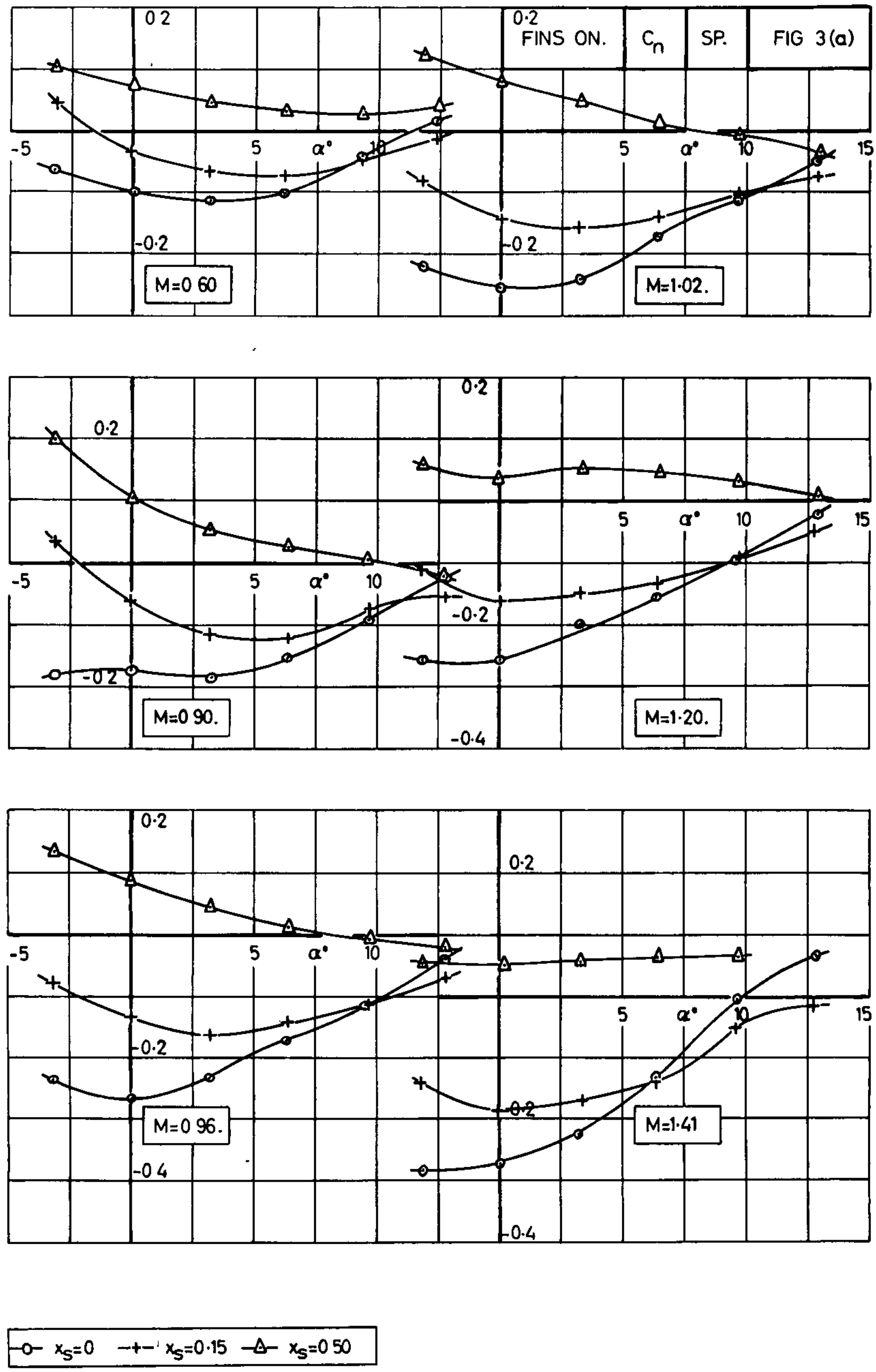

FIG. 3.(a). VARIATION OF STORE/PYLON YAWING MOMENT WITH INCIDENCE FOR 3 CHORDWISE LOCATIONS. y_s=0·50, (SP) FINS ON.

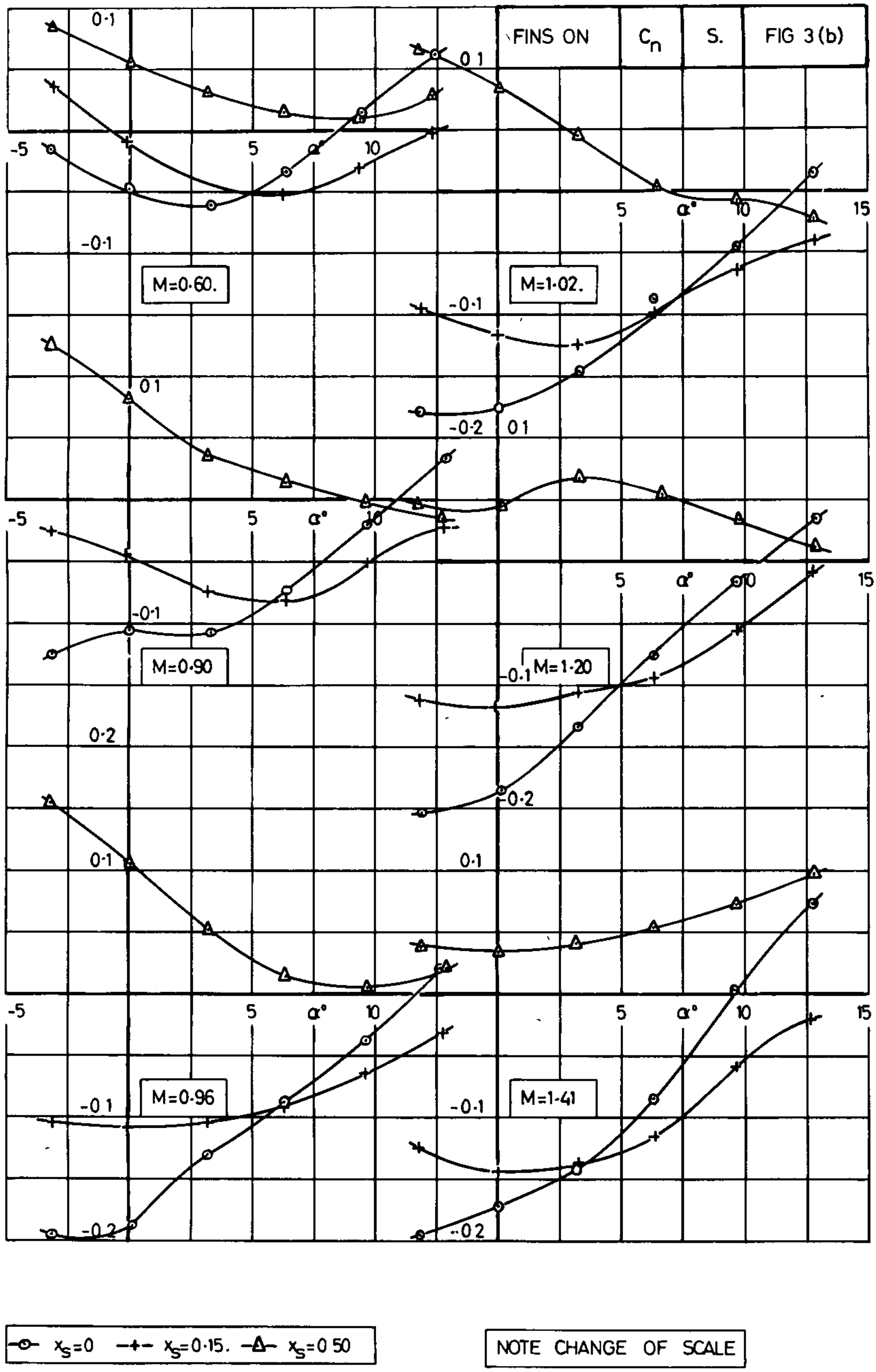

FIG. 3.(b). $y_s=0{\cdot}50$, (S) FINS ON.

FINS OFF	C_n	SP	FIG 3 (c)

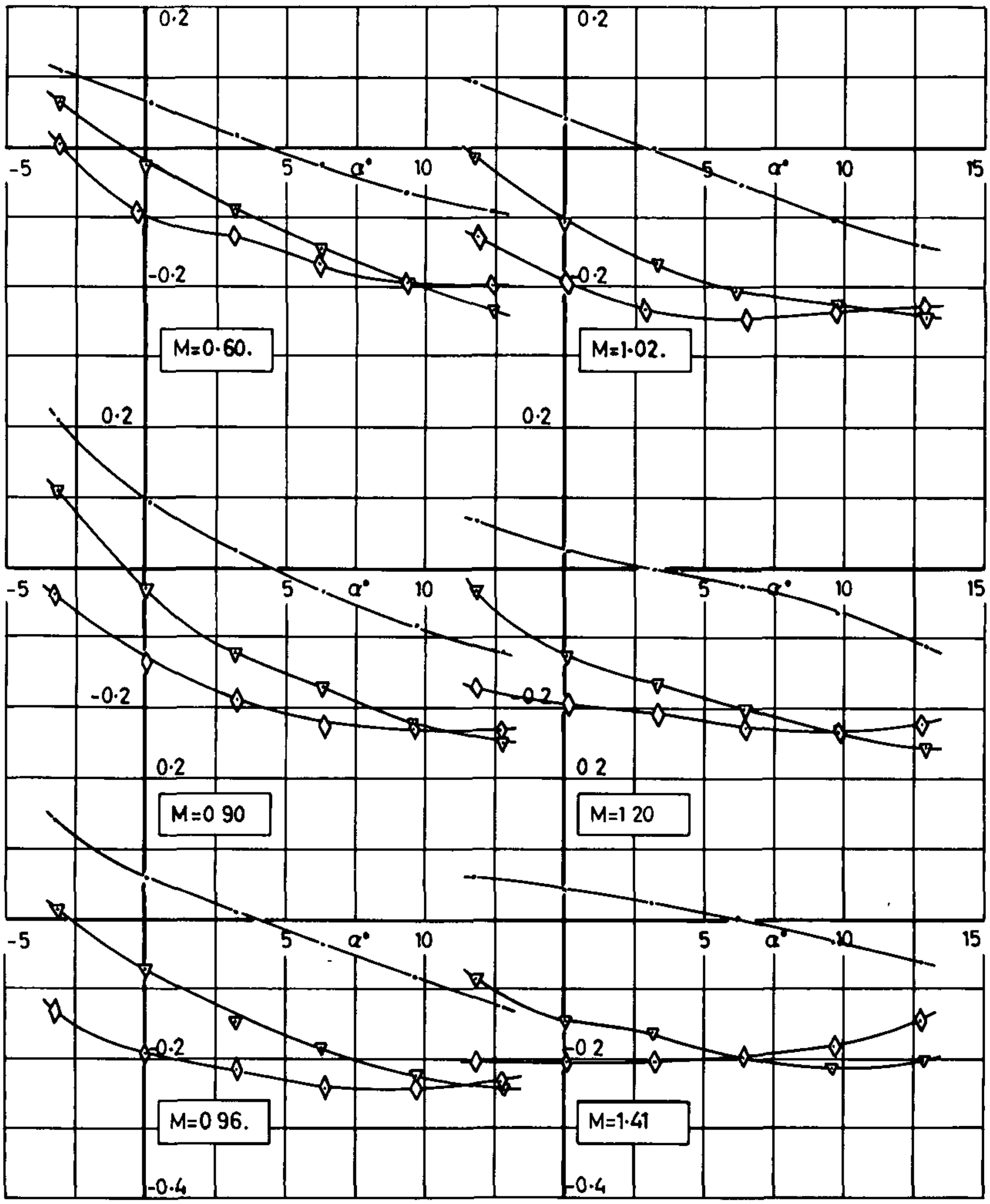

(SP)(OFF) RESULTS UNRELIABLE FOR x_s=0 50

—◇— x_s=0 —▽— x_s=0 15. —·— x_s=0·50.

FIG. 3.(c). y_s=0·50, (SP) FINS OFF.

FIG 3(d)

C_n	S.	FINS OFF

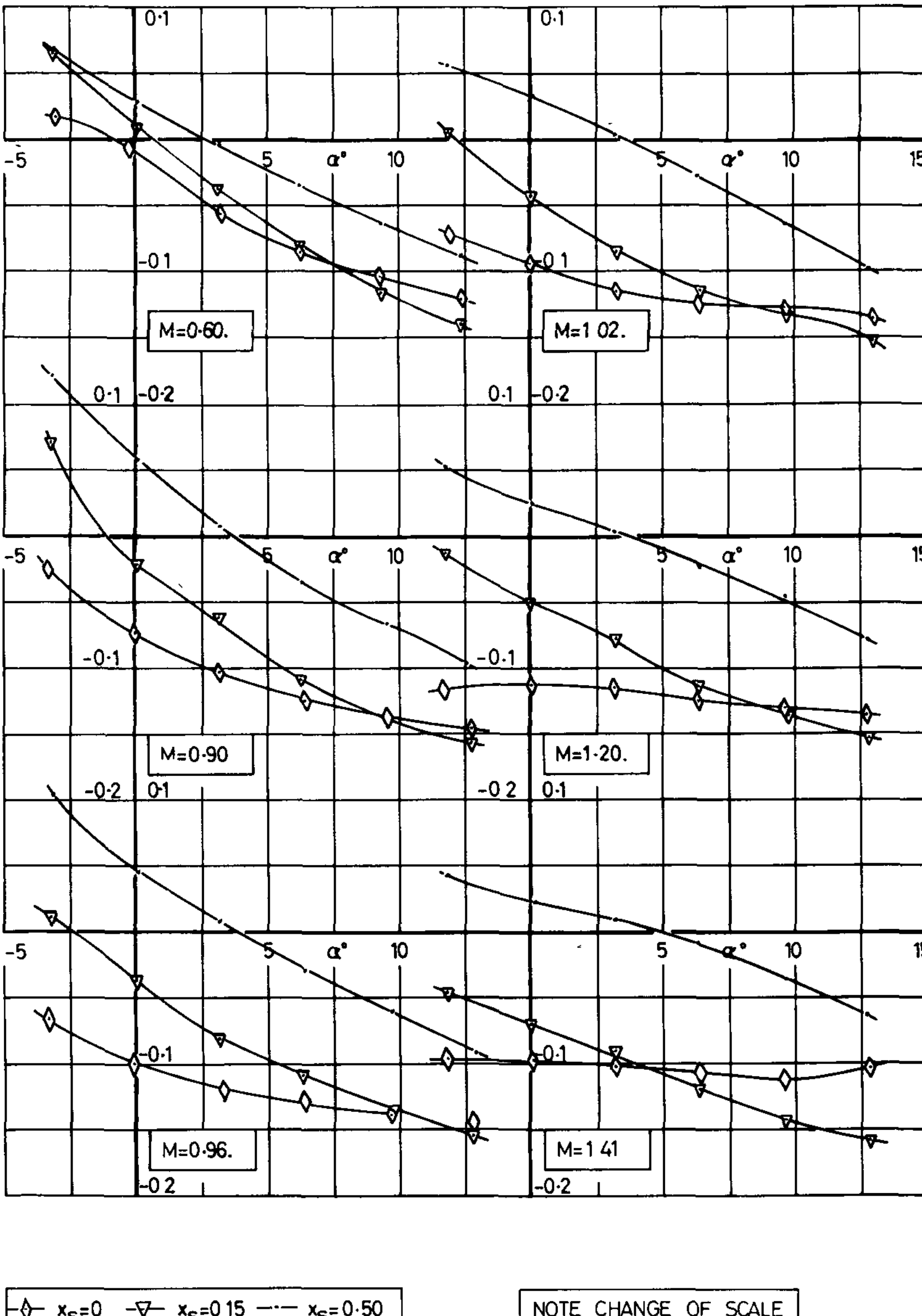

NOTE CHANGE OF SCALE

FIG. 3 (d). y_s=0·50, (S) FINS OFF.

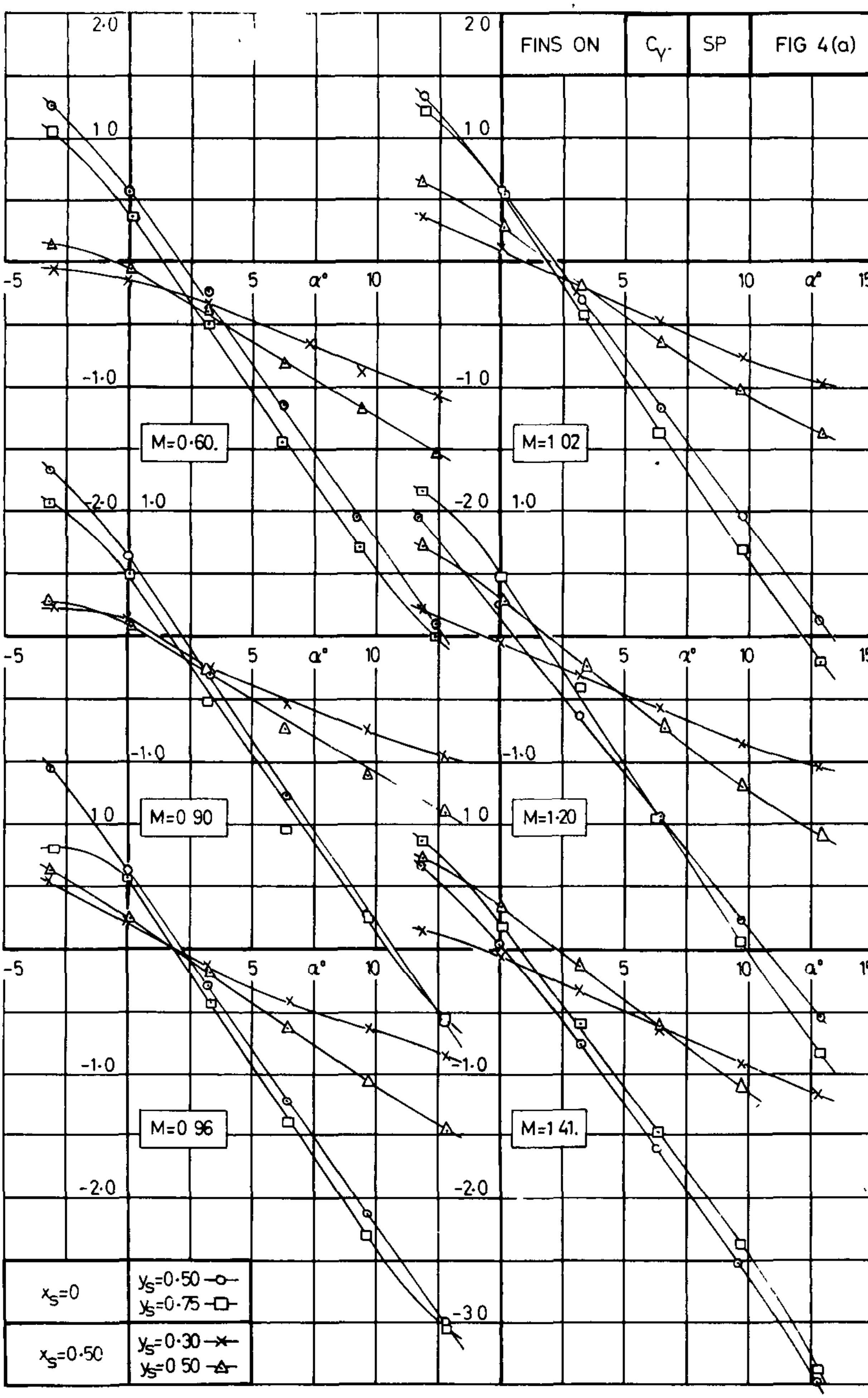

FIG 4.(a). VARIATION OF FINNED STORE / PYLON SIDE FORCE WITH INCIDENCE AT 3 SPANWISE LOCATIONS. (SP) FINS ON.

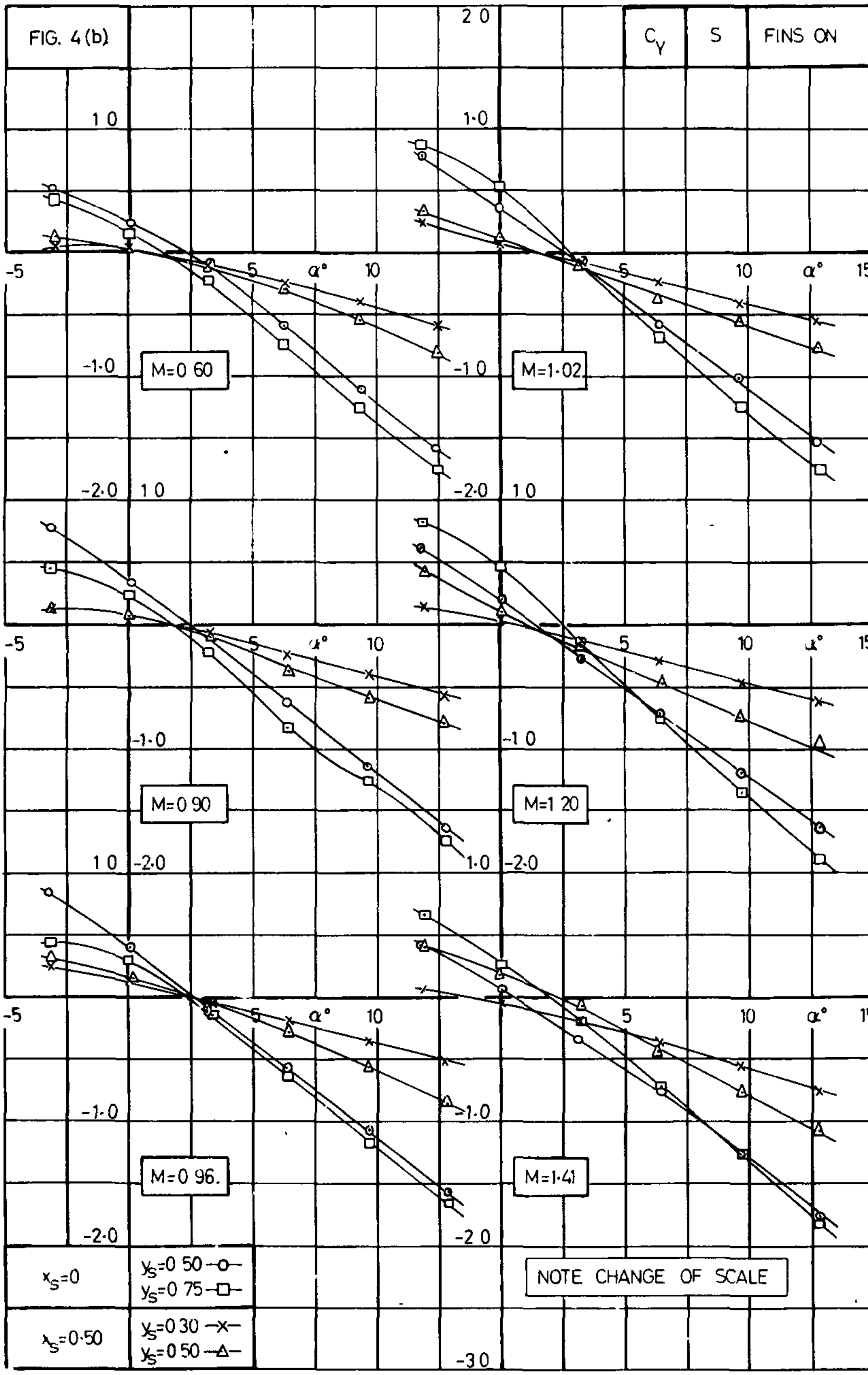

FIG. 4 (b). (S) FINS ON.

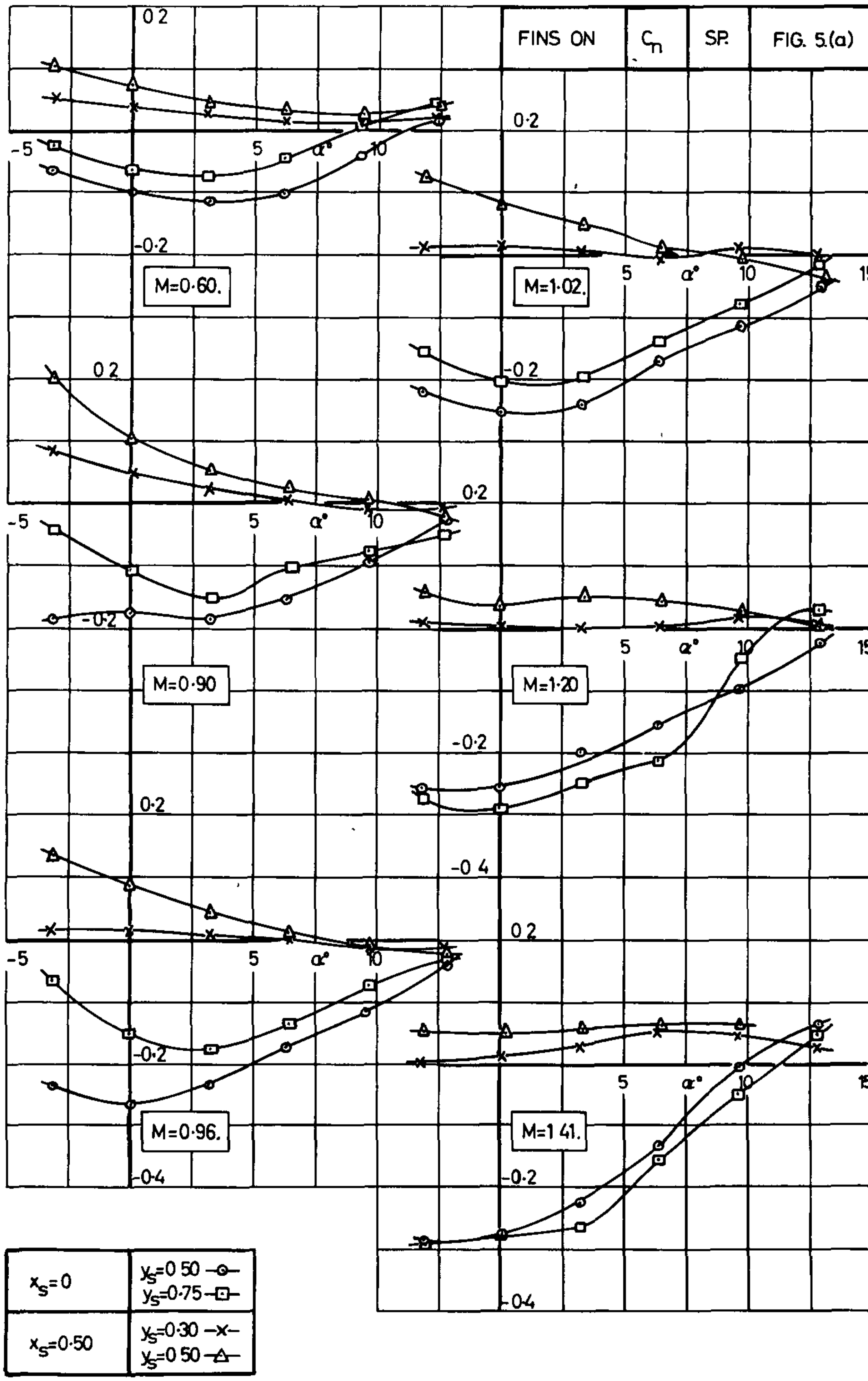

FIG. 5.(a). VARIATION OF FINNED STORE / PYLON YAWING MOMENT WITH INCIDENCE AT 3 SPANWISE LOCATIONS. (SP) FINS ON.

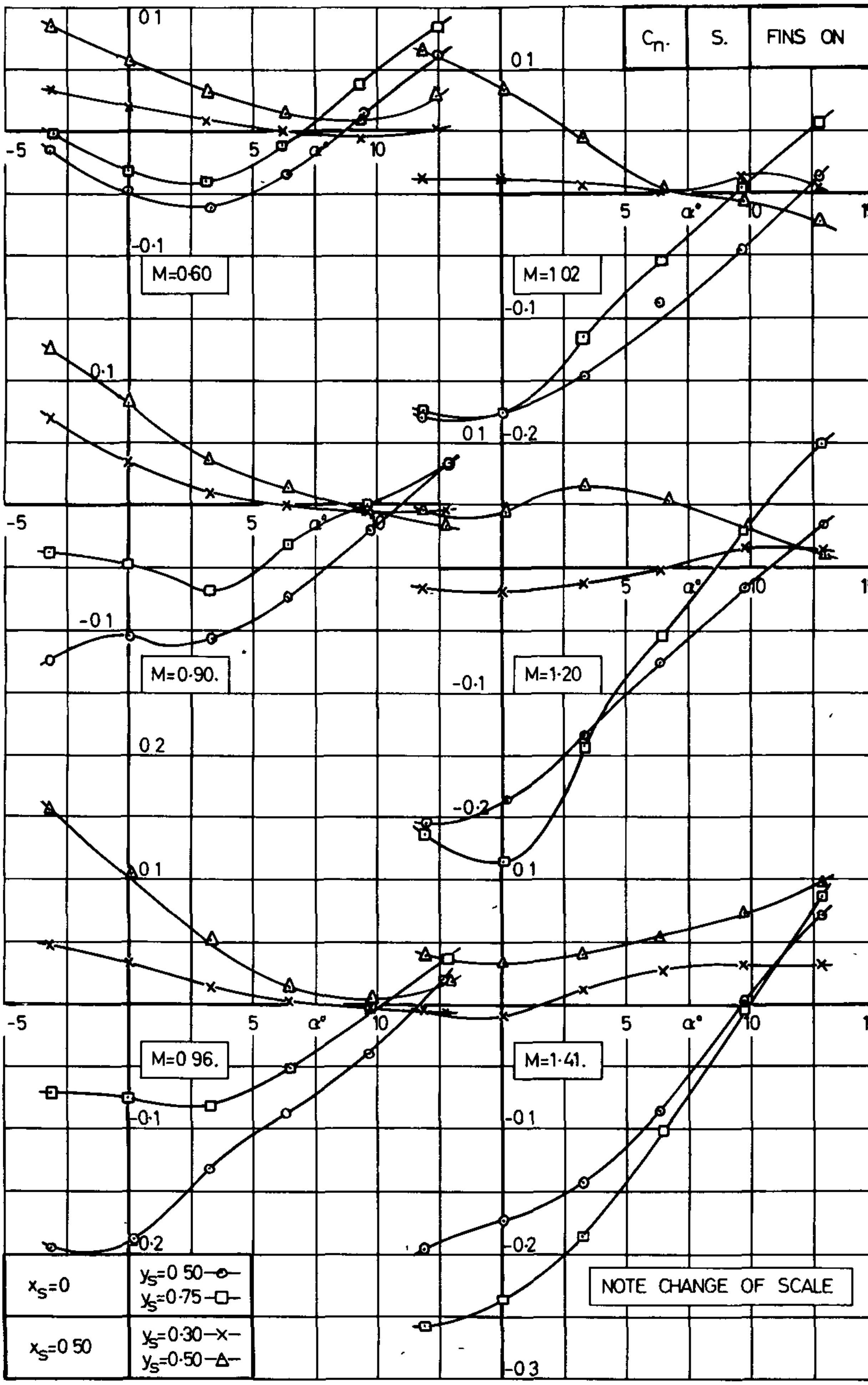

FIG. 5.(b). (S) FINS ON.

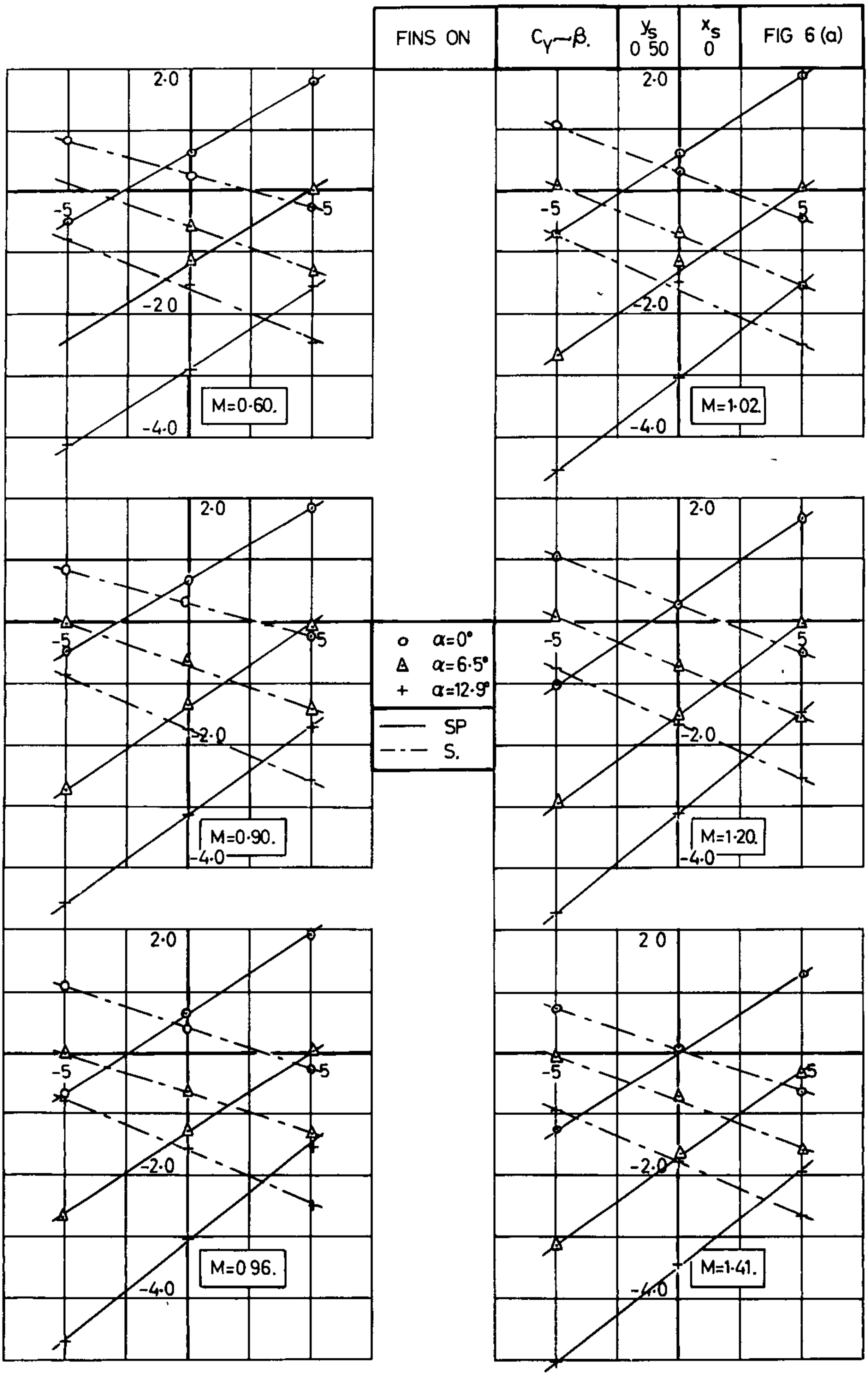

FIG. 6.(a). VARIATION OF FINNED STORE/PYLON SIDE FORCE WITH SIDESLIP.

y_S=0·50, x_S=0, FINS ON.

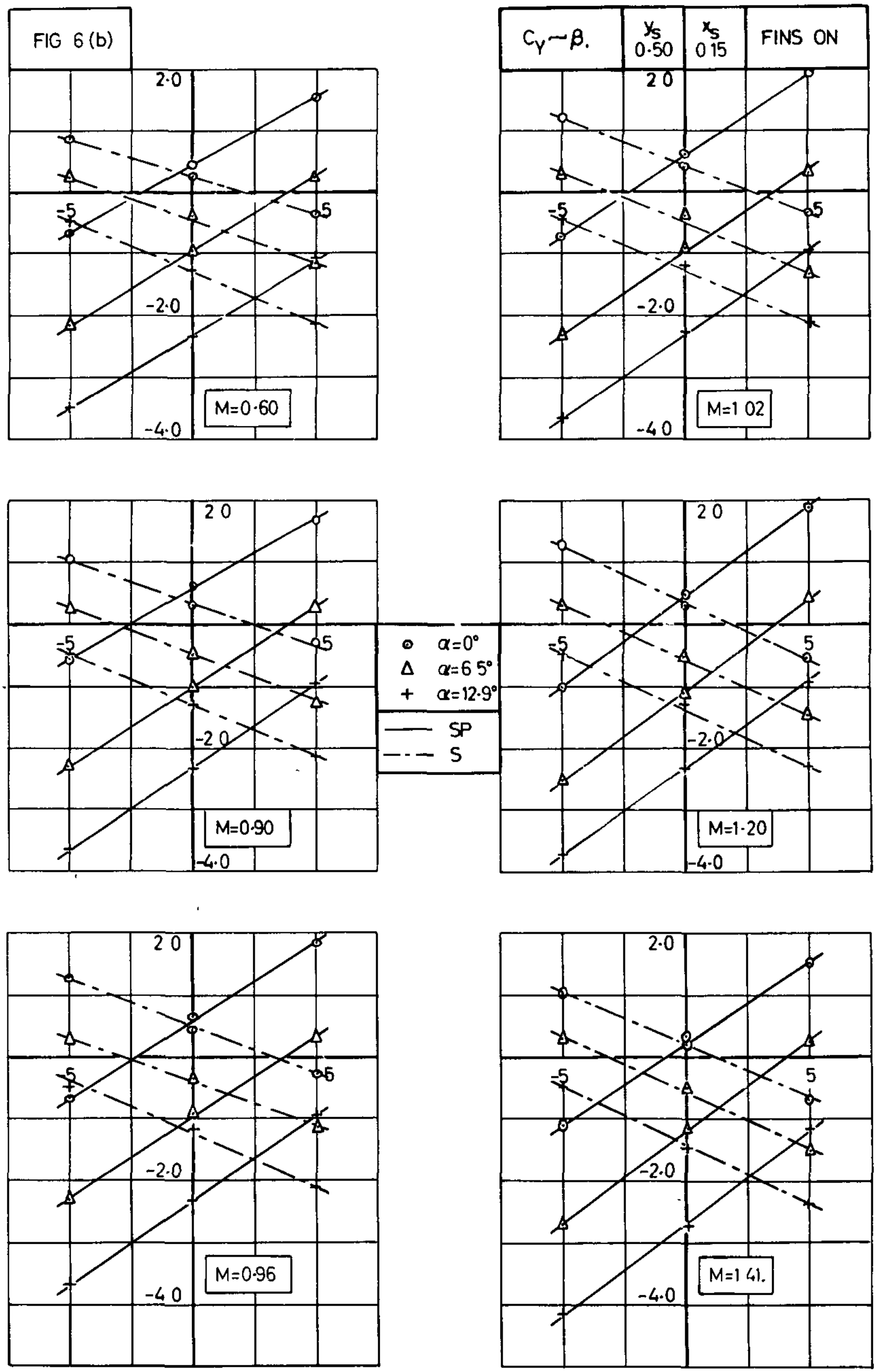

FIG. 6.(b). y_S=0·50, x_S=0·15, FINS ON.

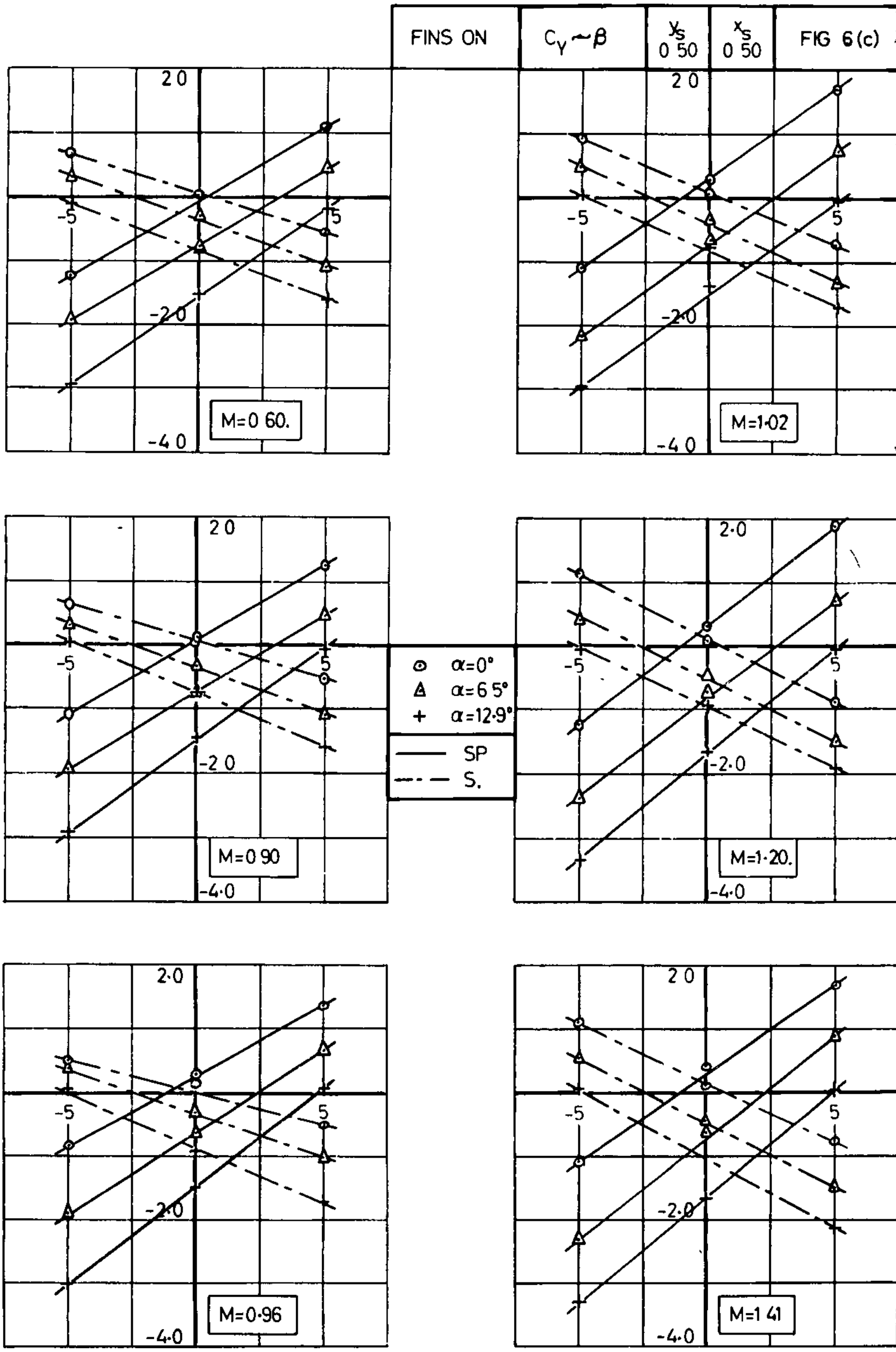

FIG. 6.(c). y_S=0·50, x_S=0·50, FINS ON.

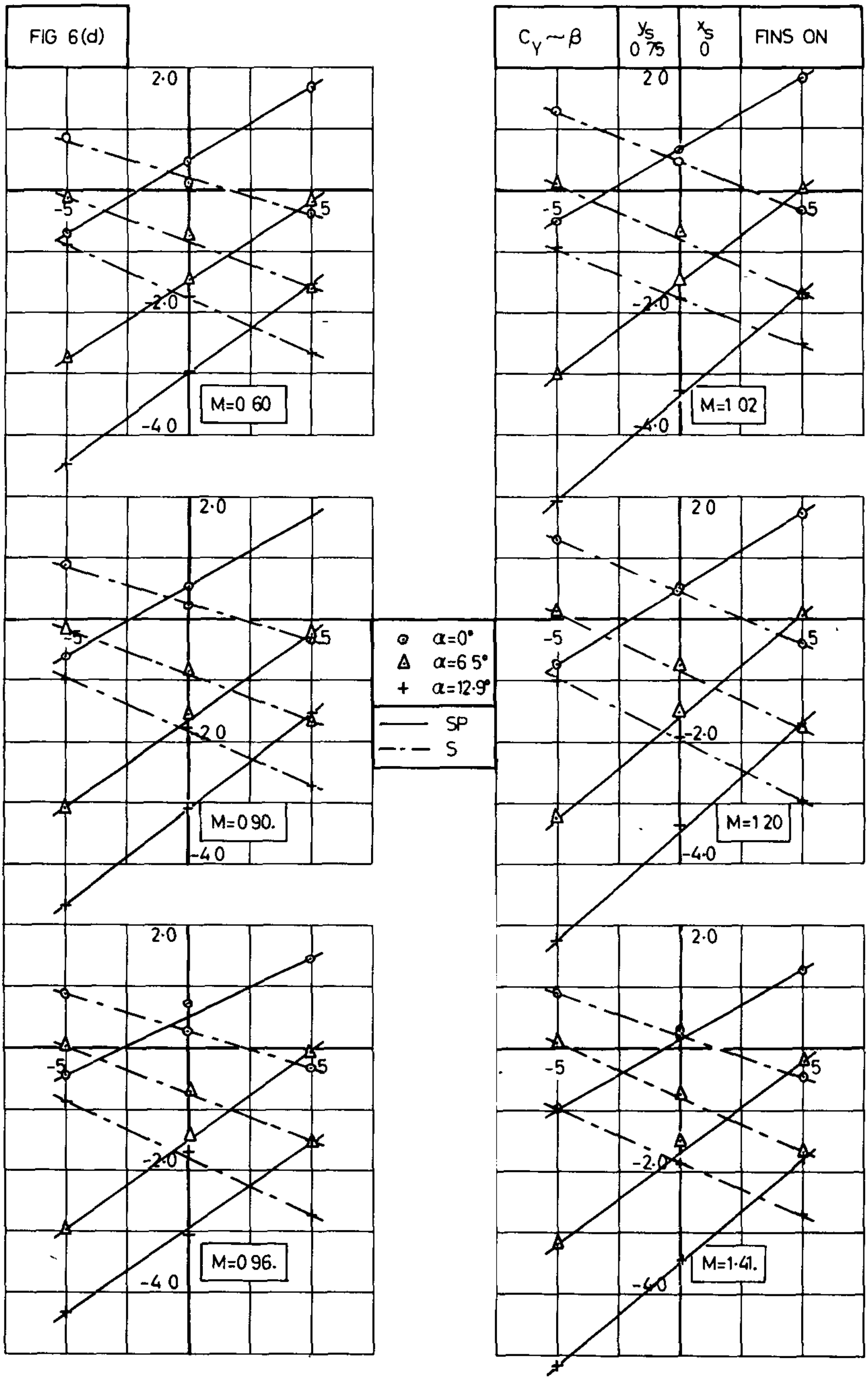

FIG. 6.(d). $y_S=0{\cdot}75$, $x_S=0$, FINS ON.

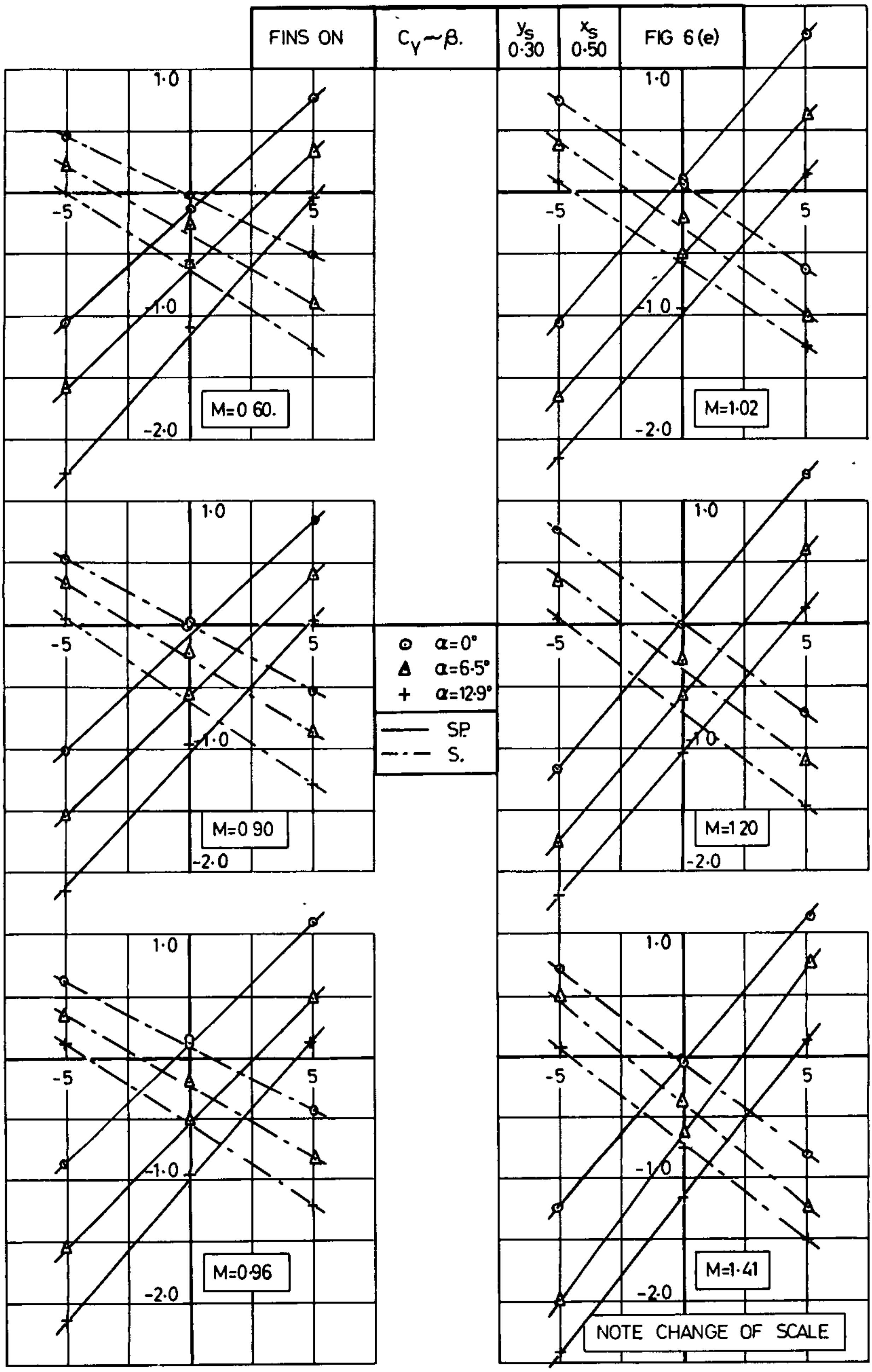

FIG. 6.(e). y_S=0·30, x_S=0·50, FINS ON.

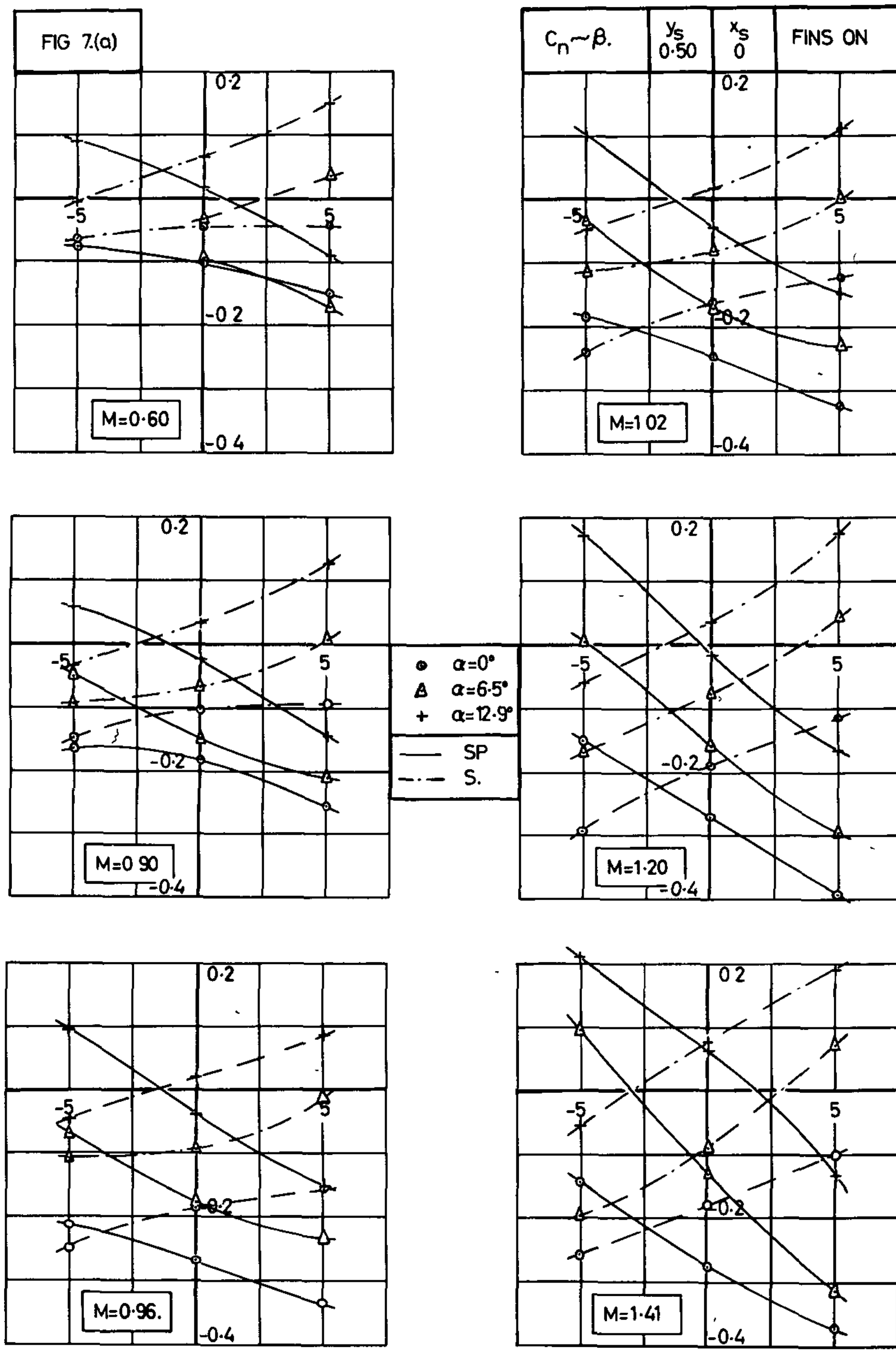

FIG. 7(a). VARIATION OF FINNED STORE/PYLON YAWING MOMENT WITH SIDESLIP.

$y_s=0{\cdot}50$, $x_s=0$, FINS ON.

FINS ON	$C_n - \beta$	y_s 0.50	x_s 0.15	FIG 7(b)

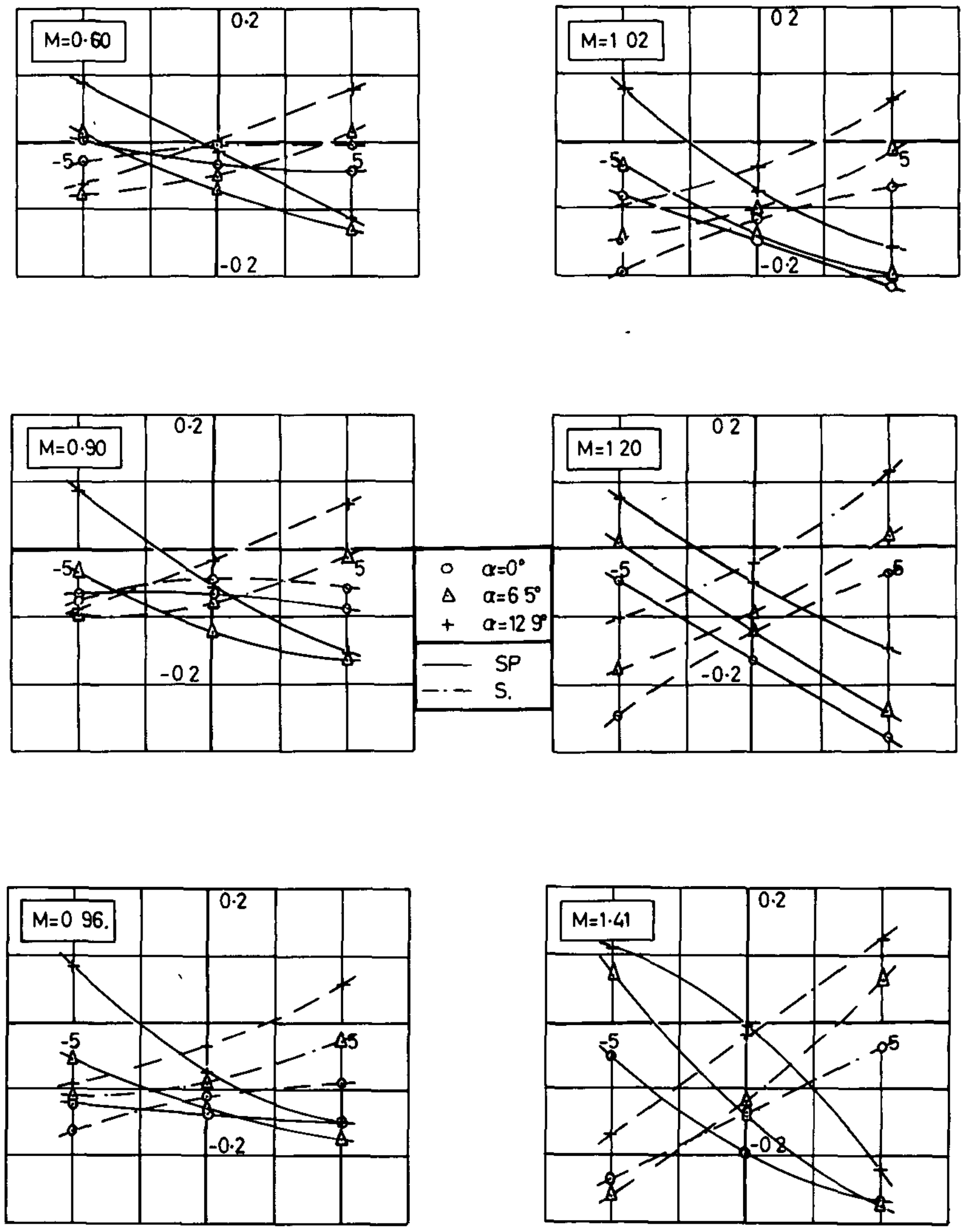

FIG. 7.(b). y_s=0·50, x_s=0·15, FINS ON.

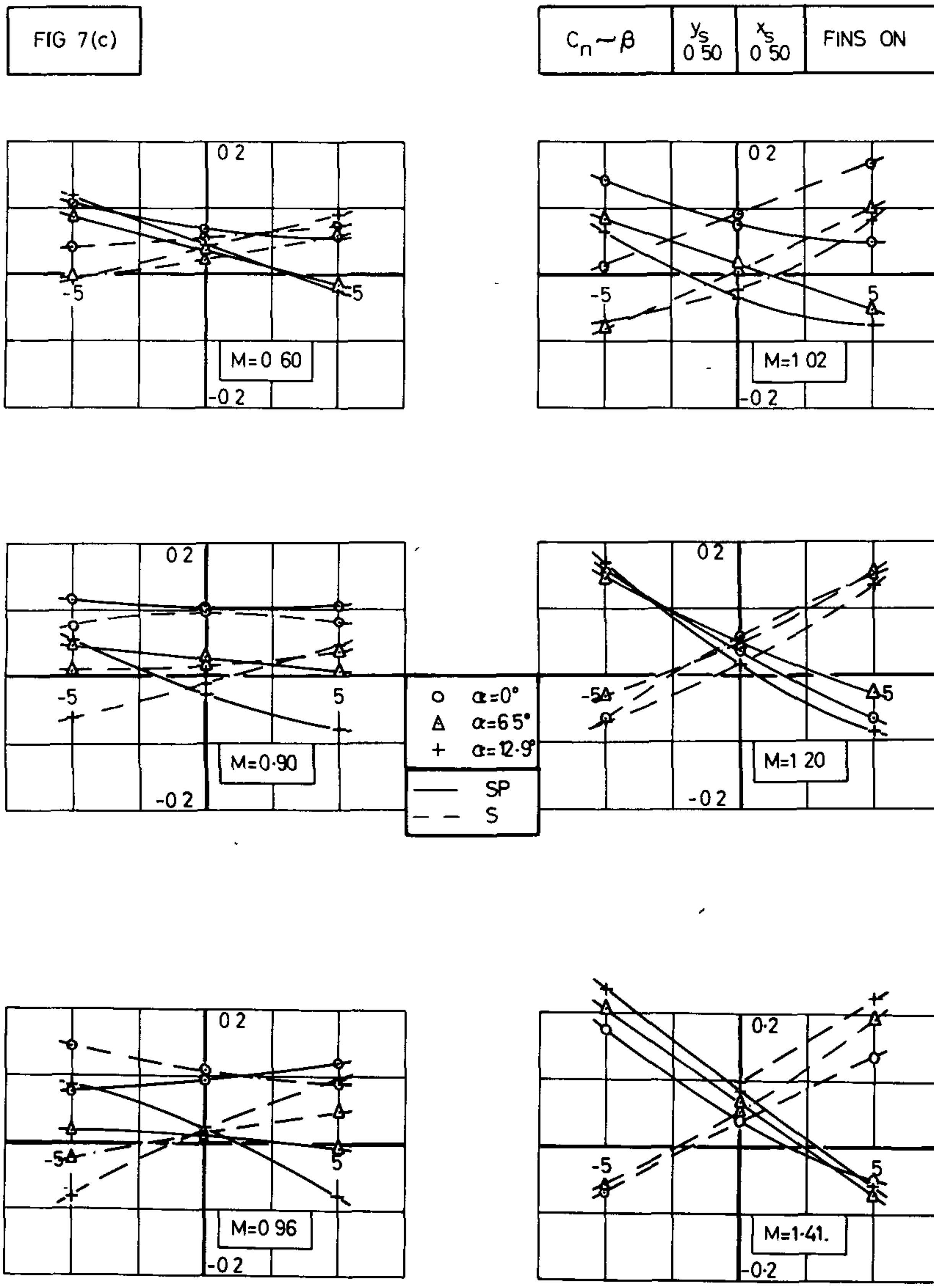

FIG. 7(c) y_s=0·50, x_s=0·50, FINS ON.

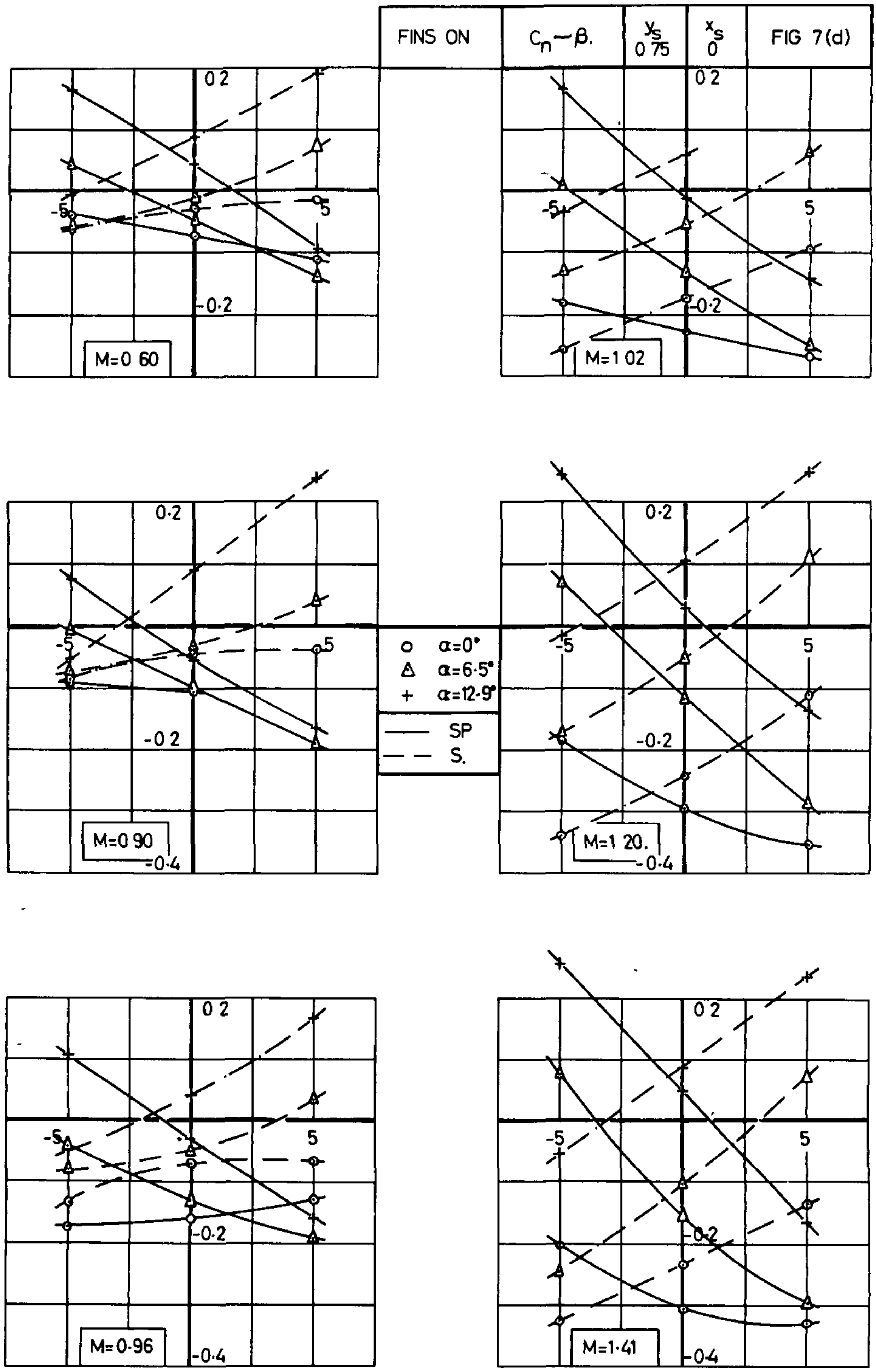

FIG. 7(d). y_s=0·75, x_s=0, FINS ON.

FIG 7(e)

$C_n \sim \beta$	y_s 0 30	x_s 0 50	FINS ON.

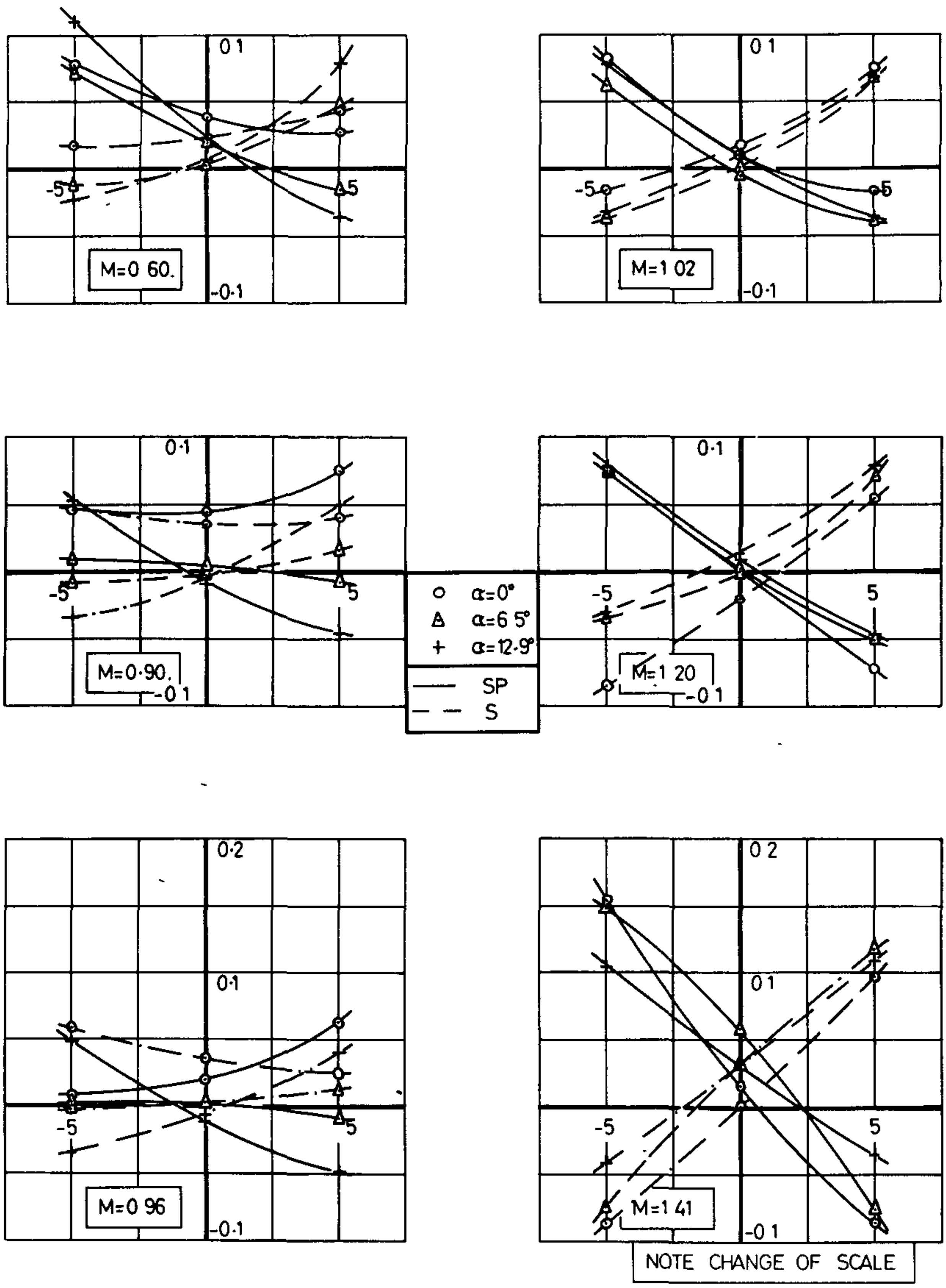

FIG. 7(e). y_s=0·30, x_s=0·50, FINS ON.

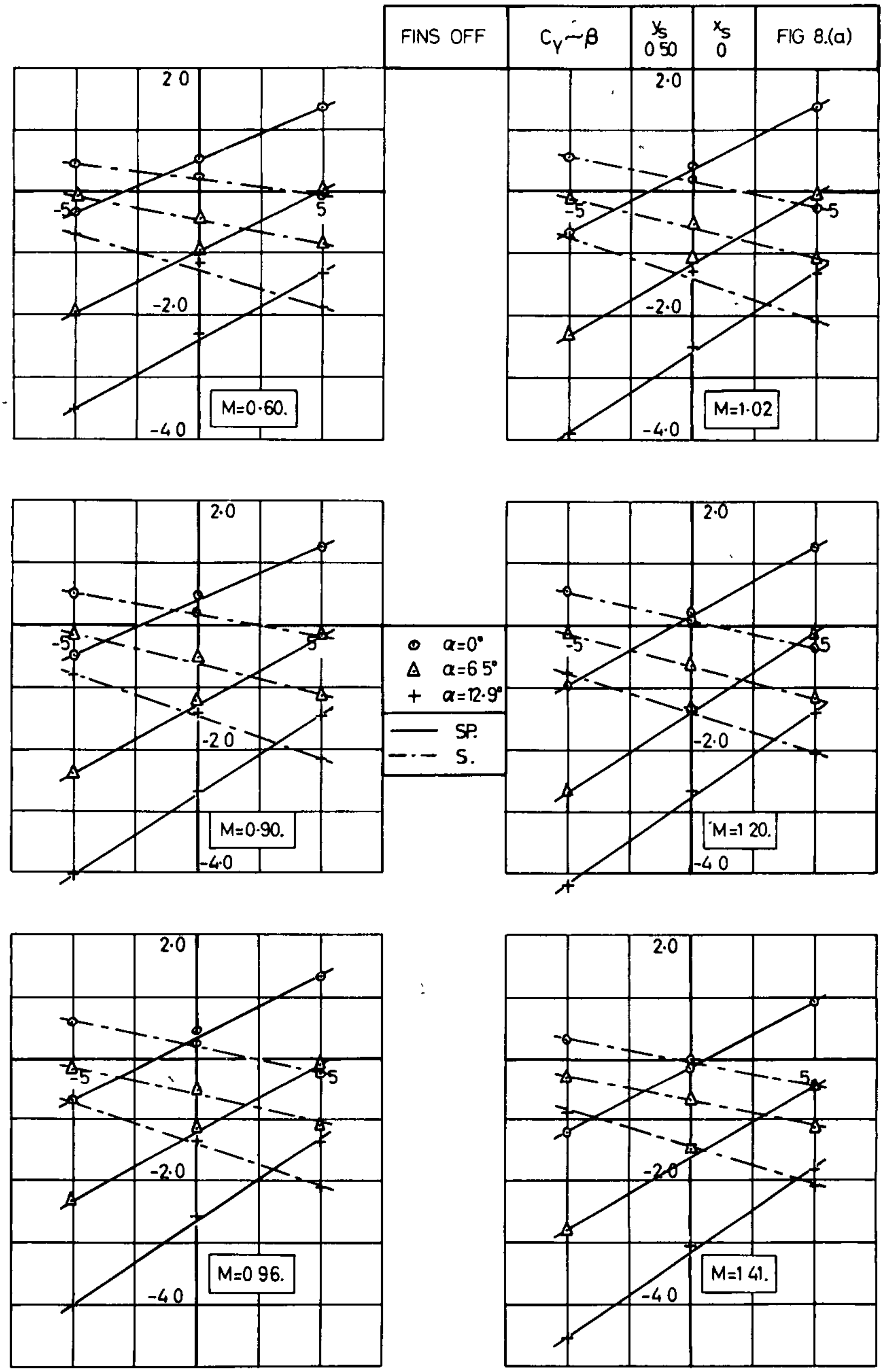

FIG. 8 (a). VARIATION OF UNFINNED STORE / PYLON SIDE FORCE WITH SIDESLIP.

$y_s=0{\cdot}50,\ x_s=0$, FINS OFF.

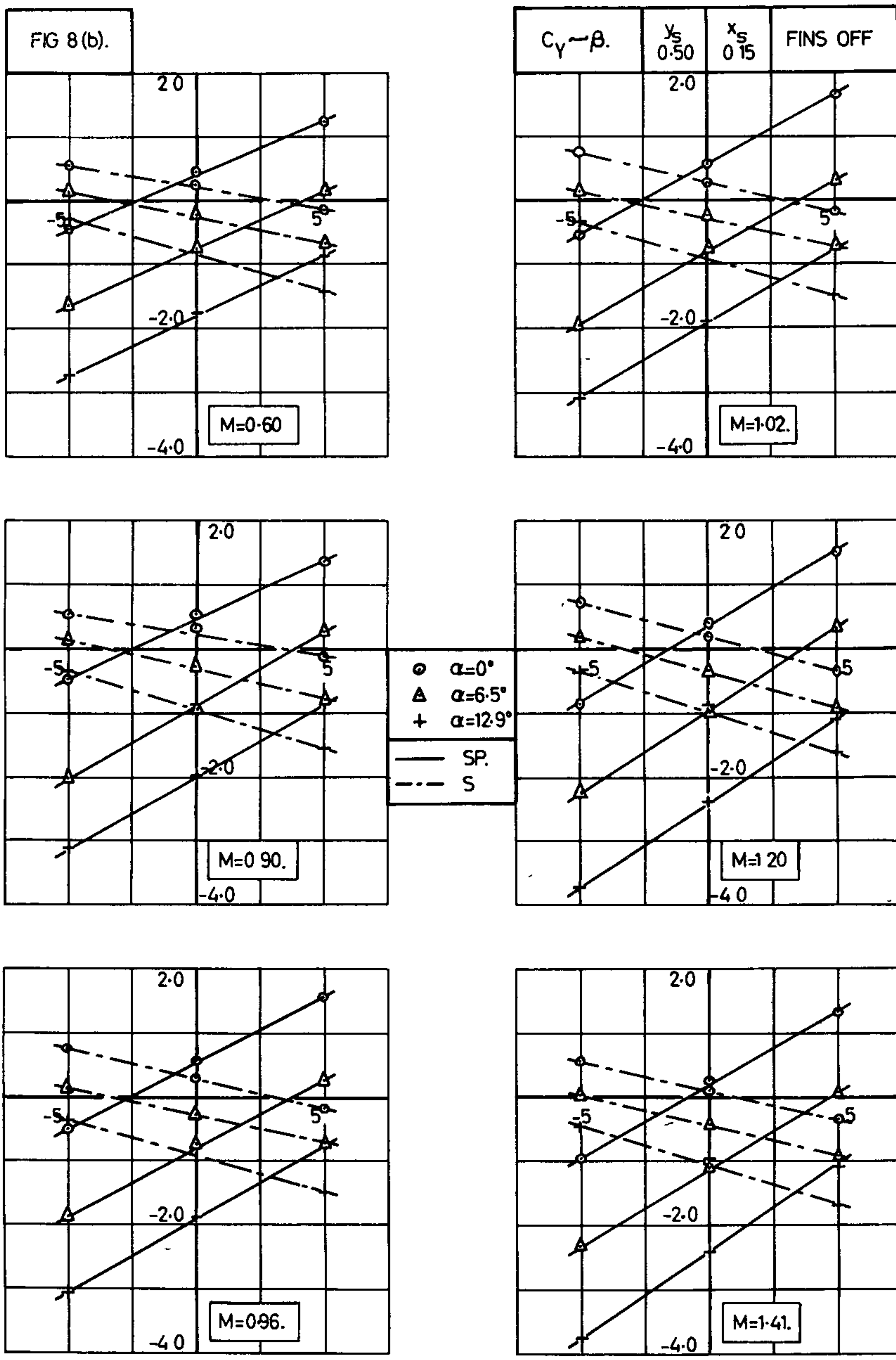

FIG. 8.(b). $y_s=0{\cdot}50$, $x_s=0{\cdot}15$, FINS OFF.

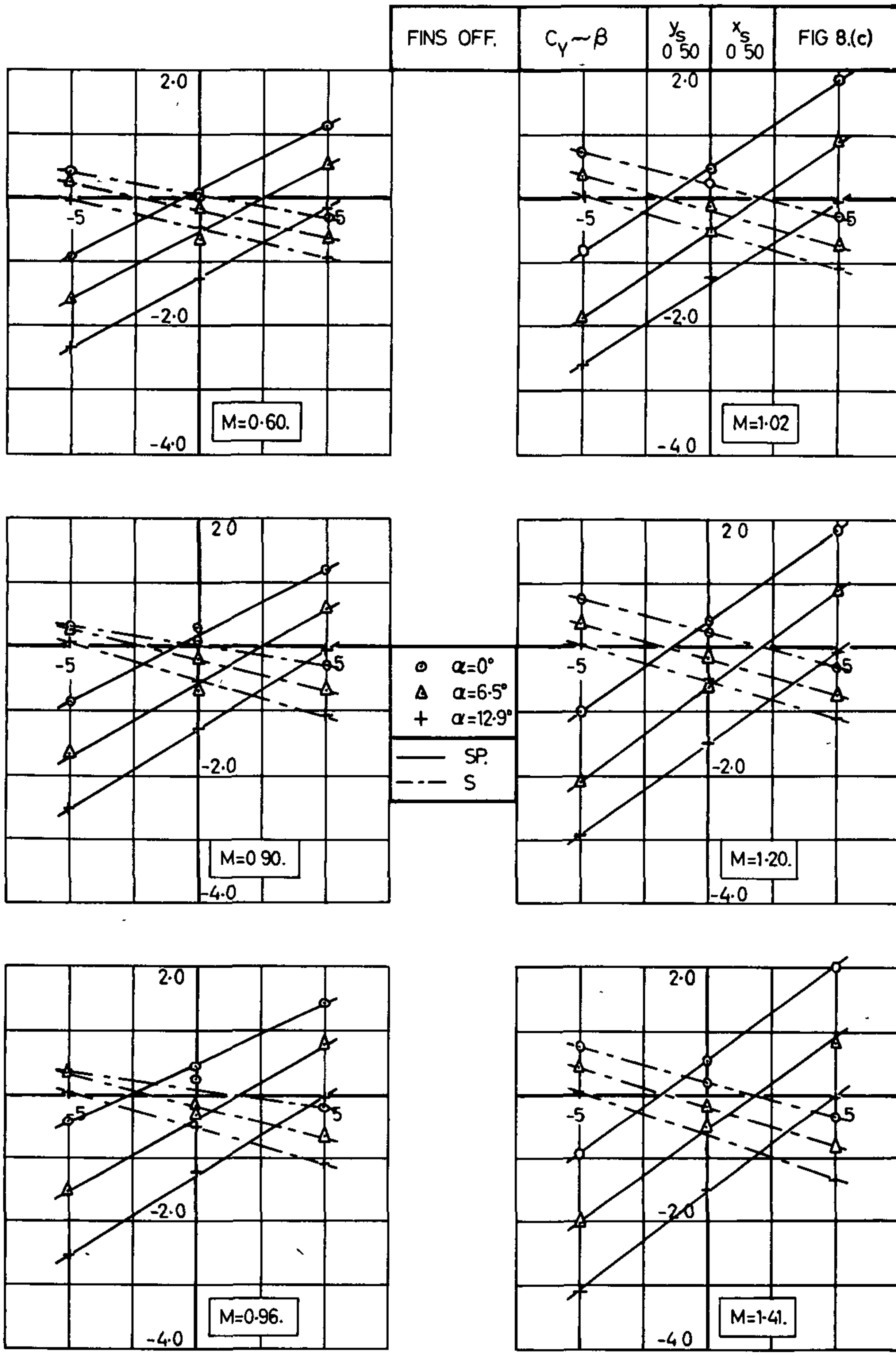

(SP)(OFF) RESULTS UNRELIABLE FOR x_s = 0 50

FIG. 8. (c). y_s = 0·50, x_s = 0·50, FINS OFF.

FIG 9(a)

$C_n \sim \beta$.	y_s 0 50	x_s 0	FINS OFF.

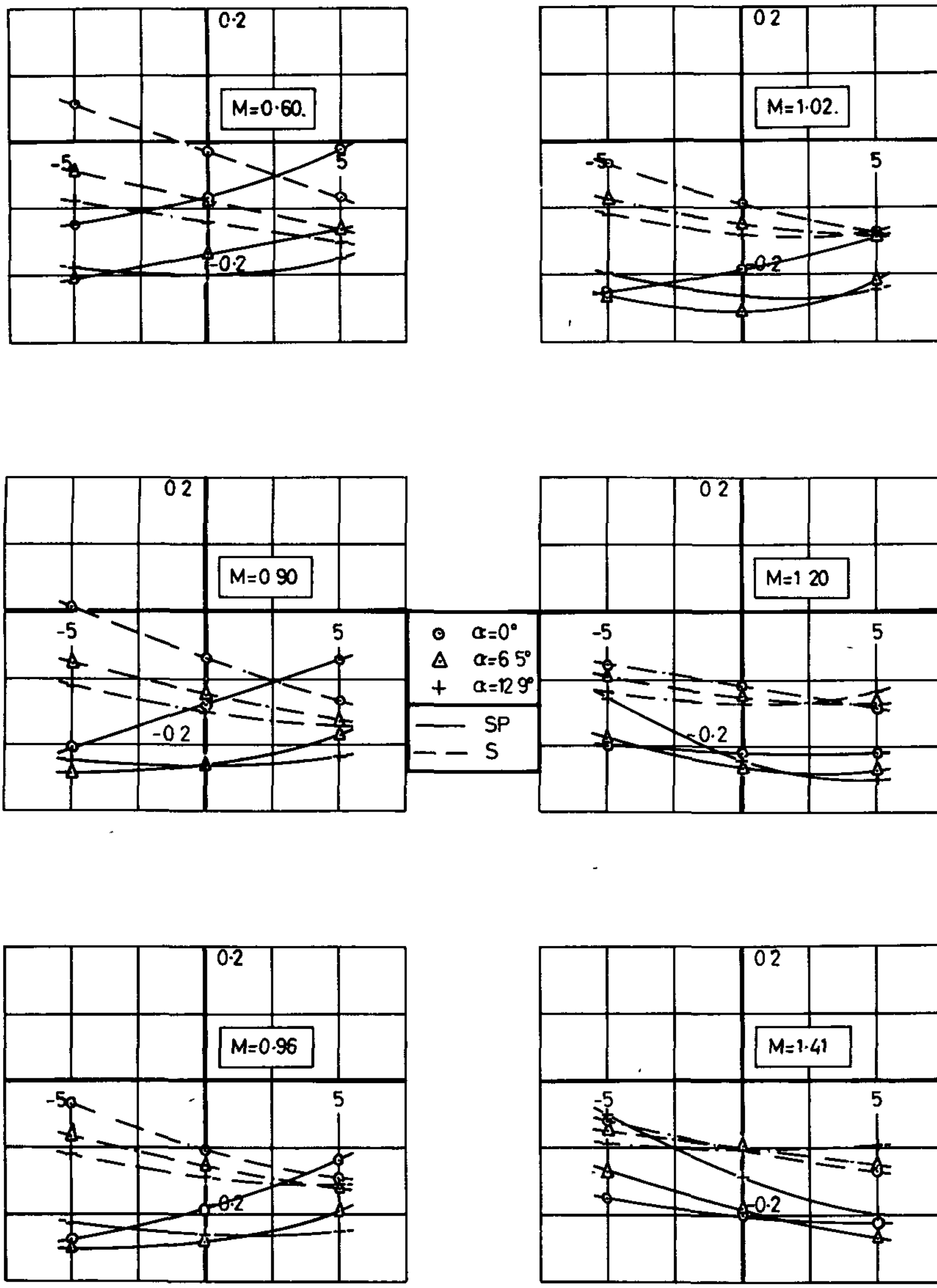

FIG. 9.(a). VARIATION OF UNFINNED STORE / PYLON YAWING MOMENT WITH SIDESLIP.

$y_s = 0{\cdot}50$, $x_s = 0$, FINS OFF.

FINS OFF	$C_n \sim \beta$.	y_s 0·50	x_s 0·15	FIG 9(b)

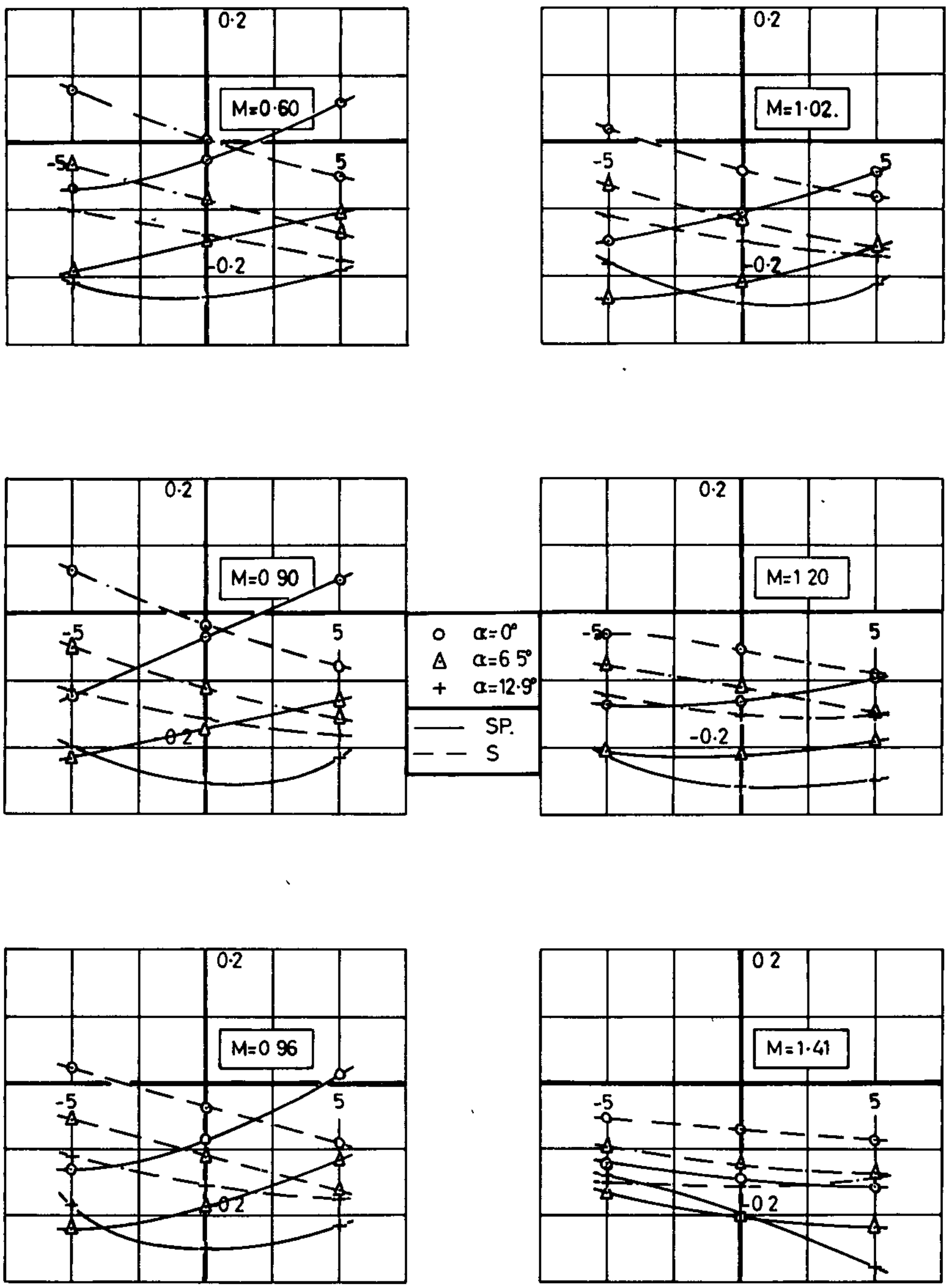

FIG. 9.(b). y_s=0·50, x_s=0·15, FINS OFF.

FIG 9 (c)

$C_n - \beta$.	$\frac{y_s}{0{\cdot}50}$	$\frac{x_s}{0{\cdot}50}$	FINS OFF.

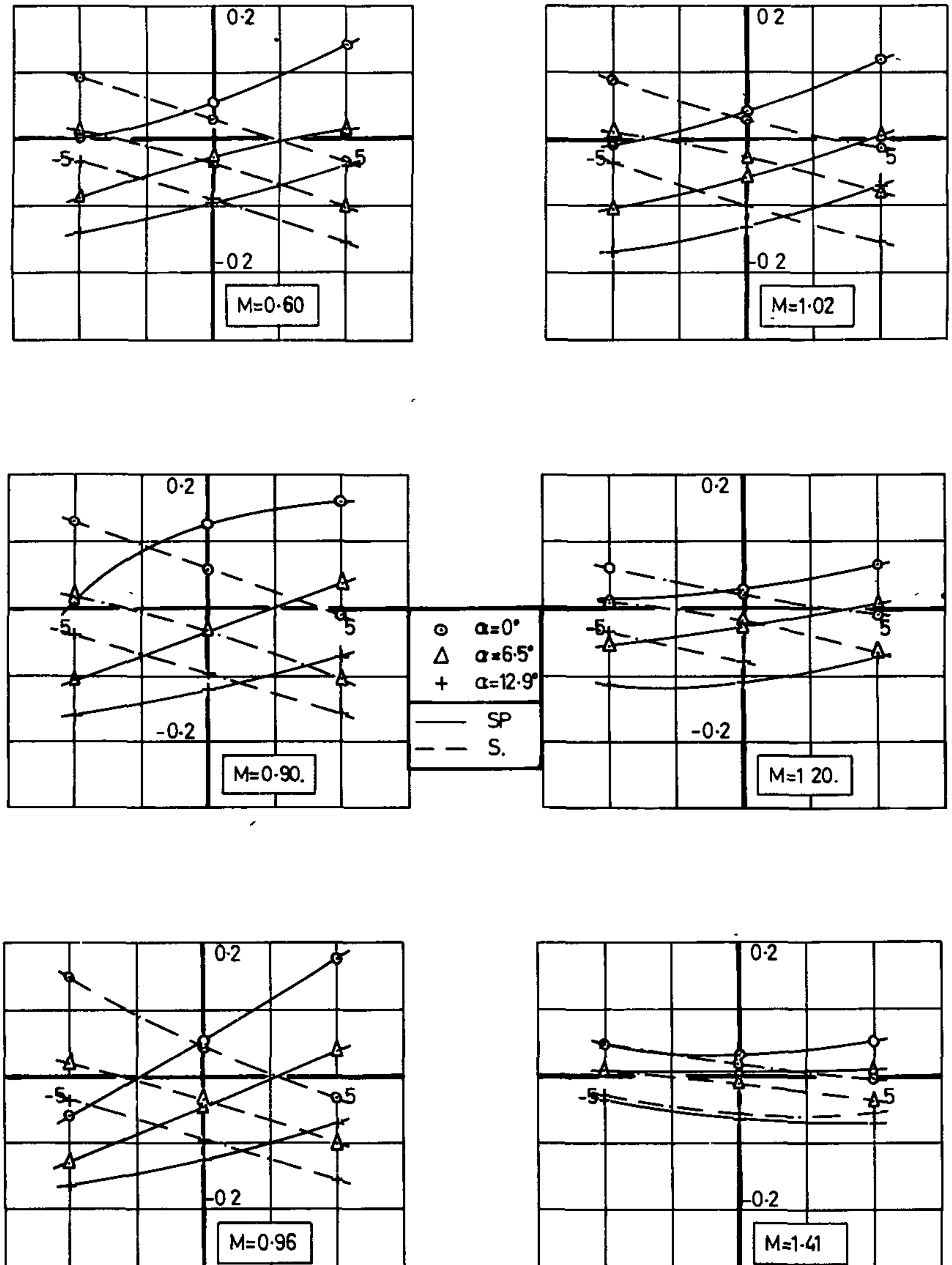

(SP)(OFF) RESULTS UNRELIABLE FOR x_s=0 50

FIG. 9.(c). y_s=0·50, x_s=0·50, FINS OFF.

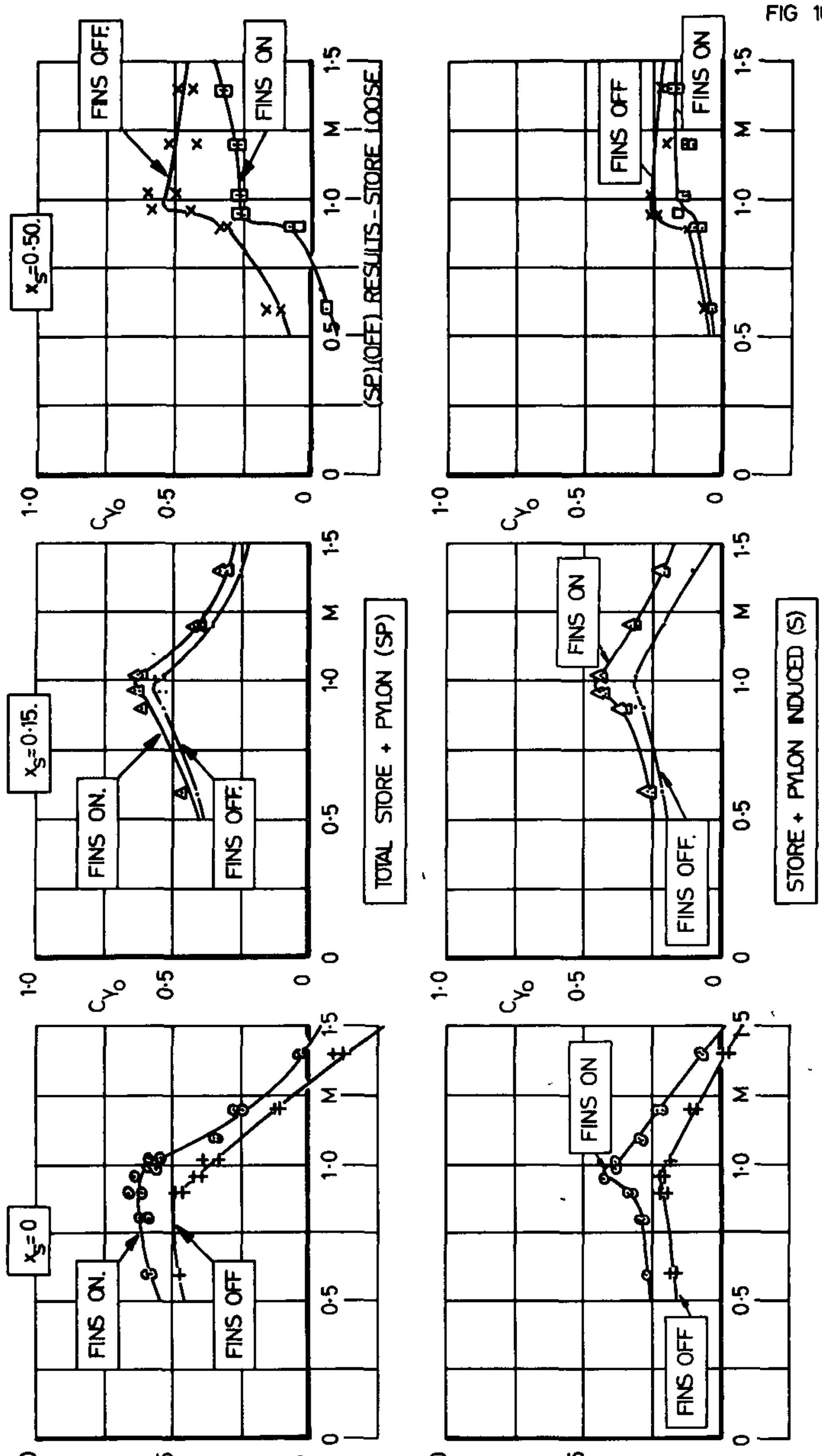

FIG. 10.(a). VARIATION OF SIDE FORCE AT ZERO INCIDENCE WITH MACH NUMBER — MIDSEMISPAN LOCATION.

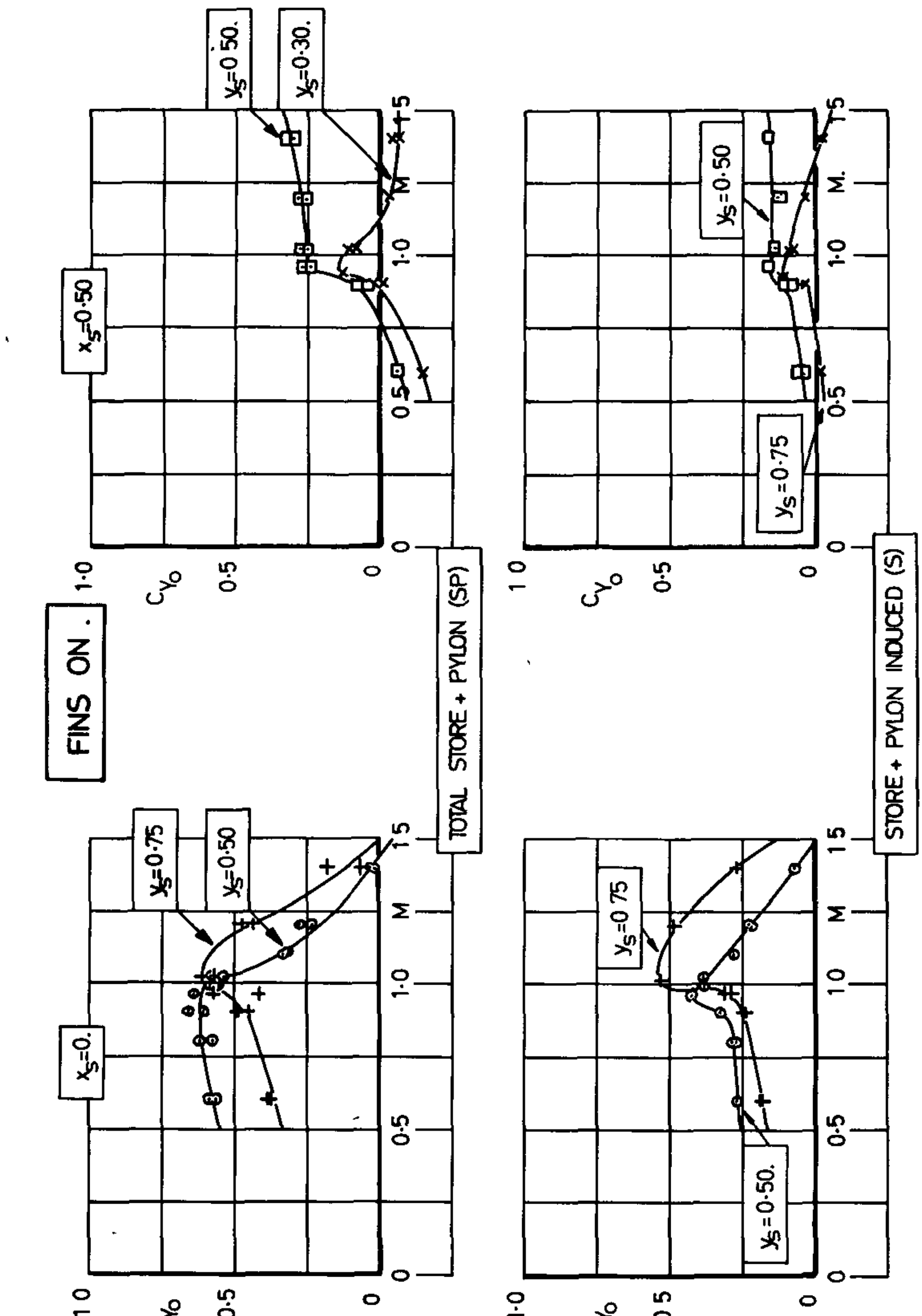

FIG. 10(b). THREE SPANWISE LOCATIONS.

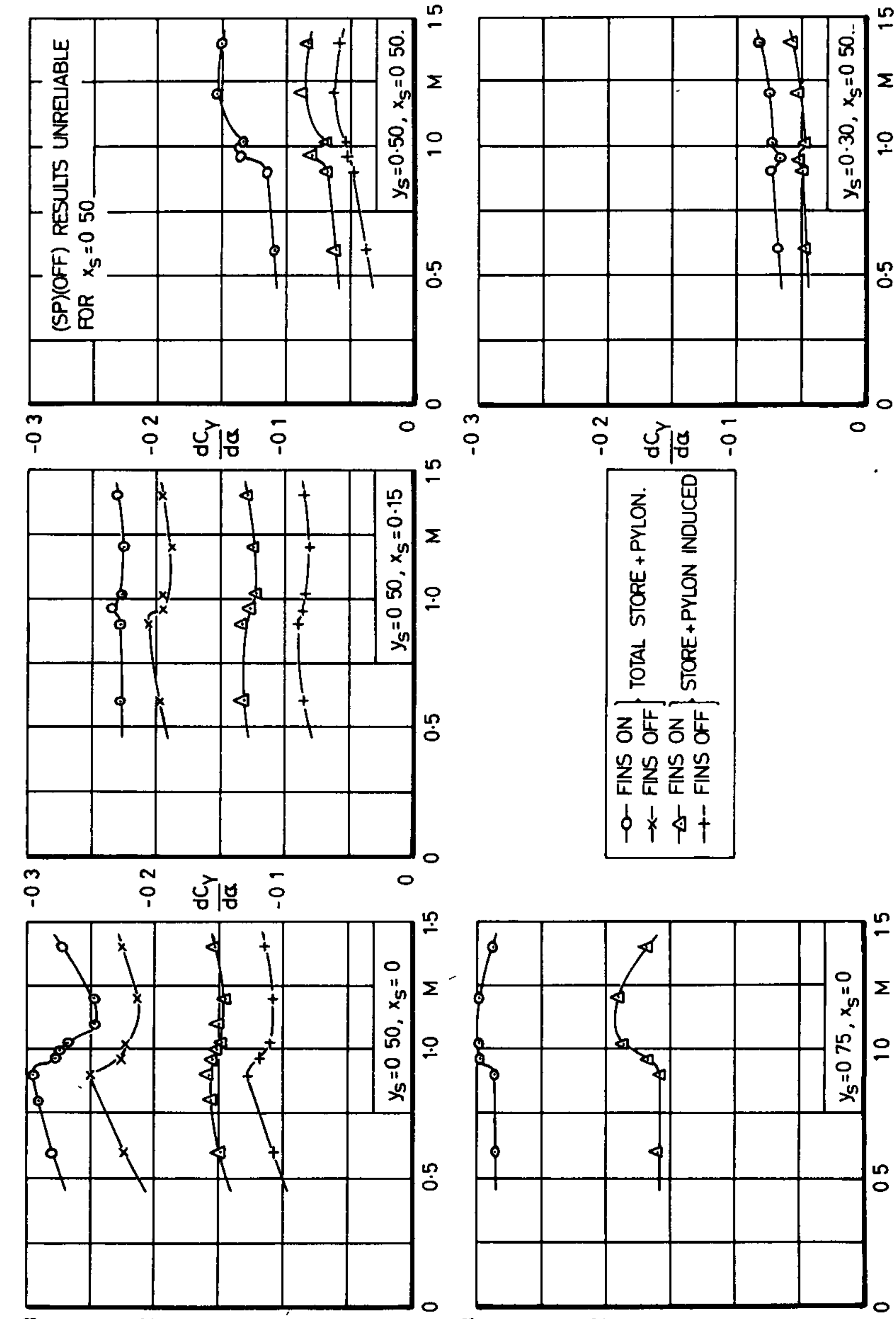

FIG. 11. VARIATION OF $\frac{dC_Y}{d\alpha}$ WITH MACH NUMBER.

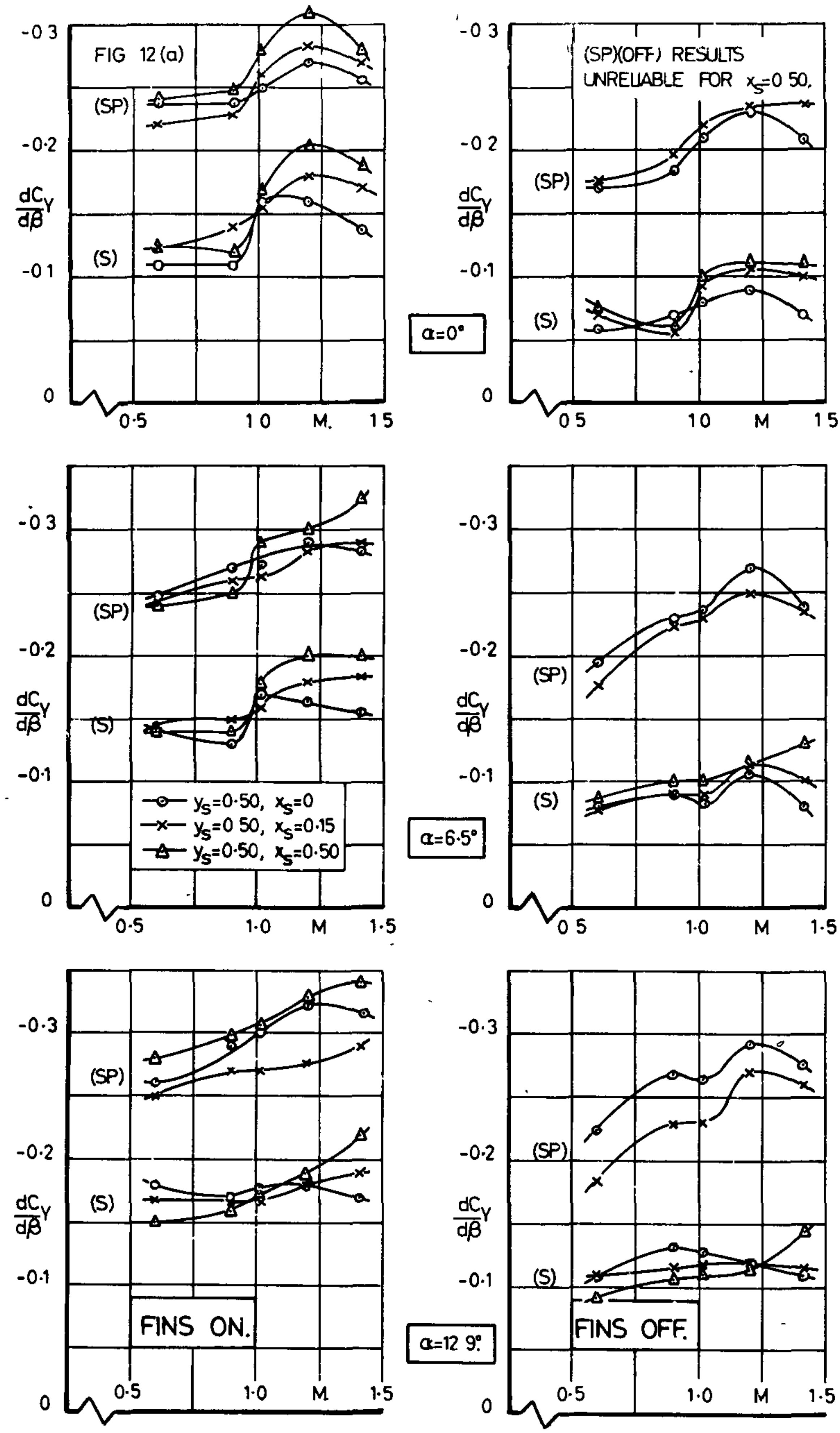

FIG. 12 (a). VARIATION OF $\frac{dC_Y}{d\beta}$ WITH MACH NUMBER.

MIDSEMISPAN LOCATION.

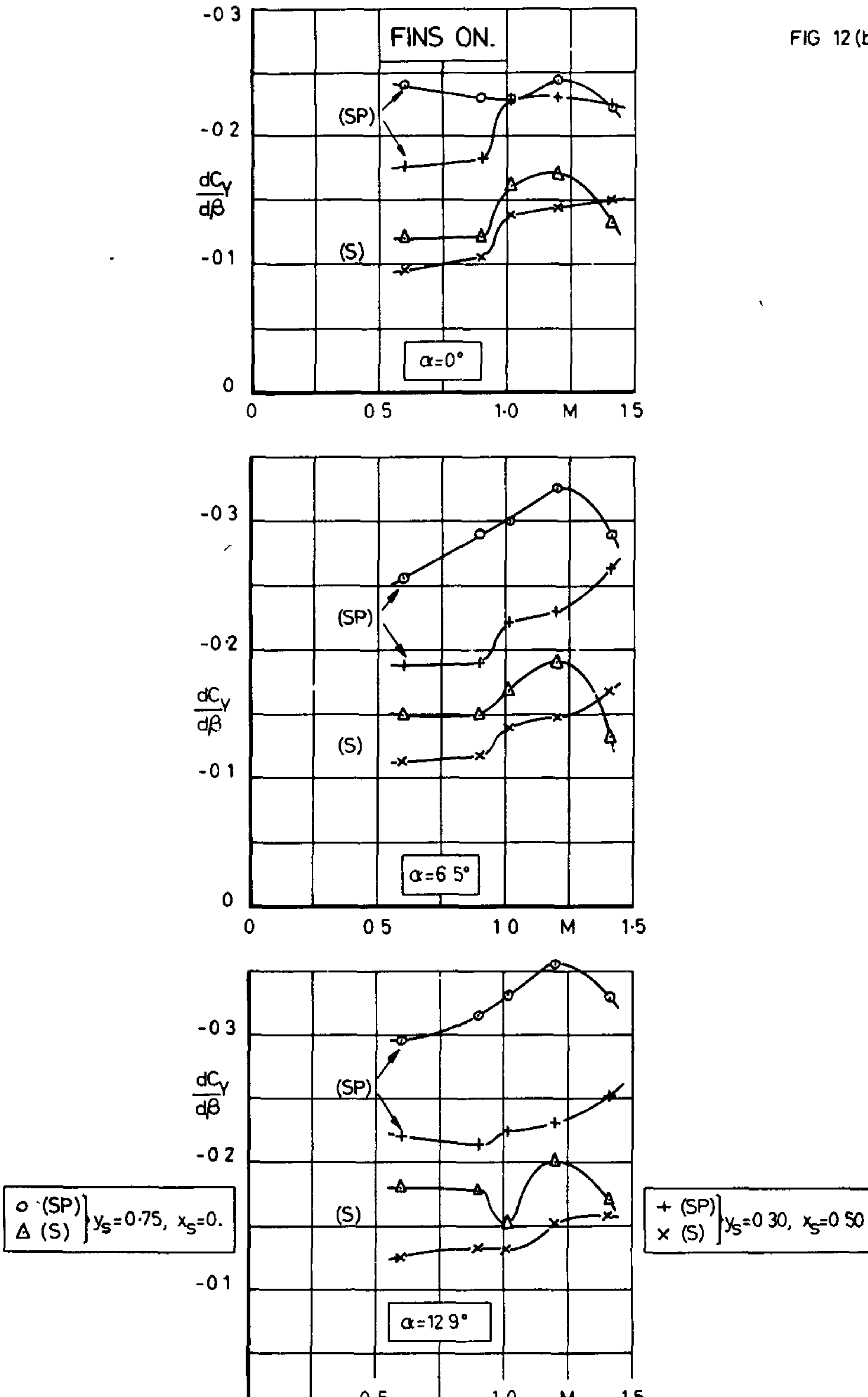

FIG. 12.(b). TWO SPANWISE LOCATIONS.

FIG. 13.(a).

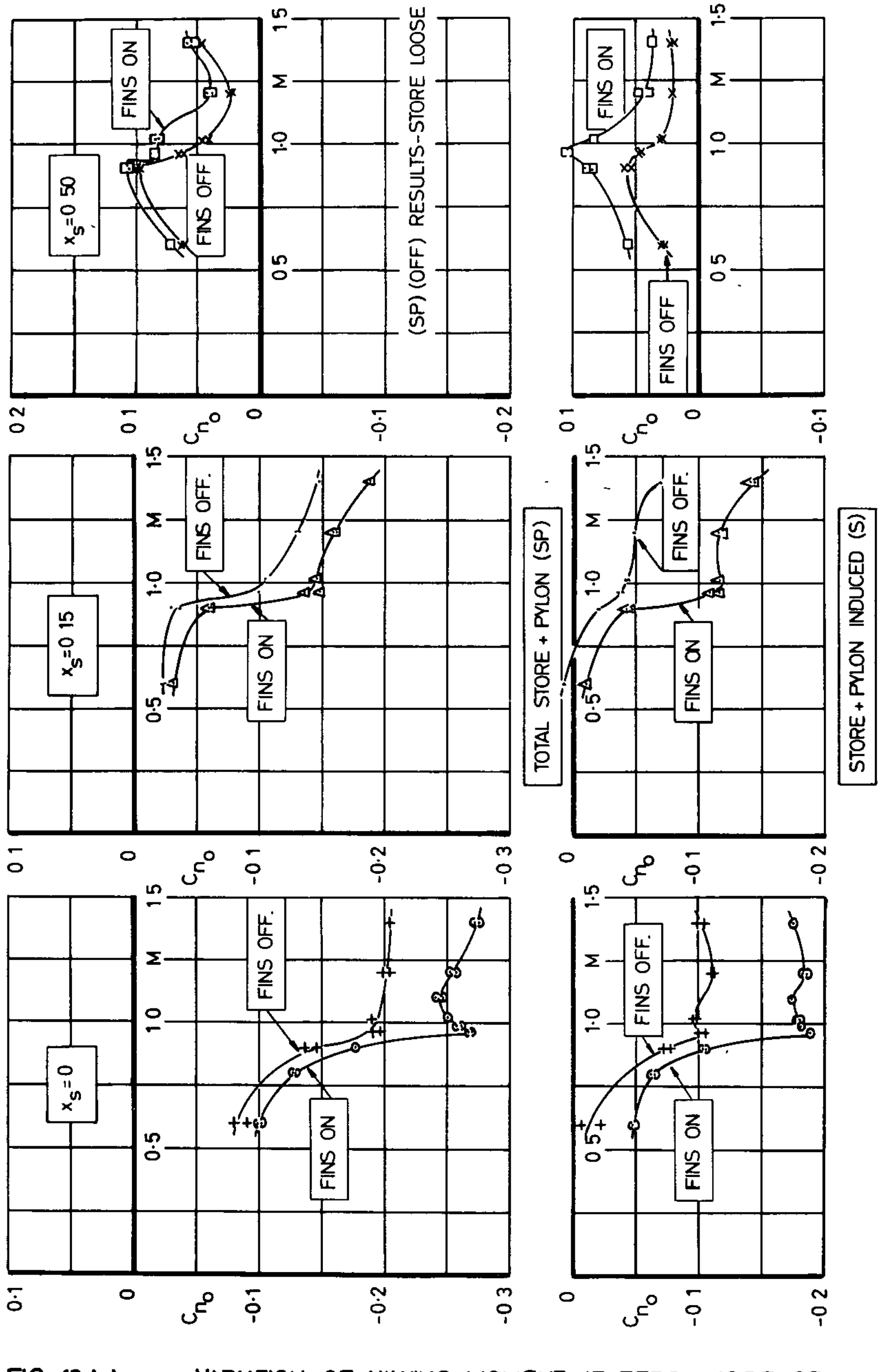

FIG. 13.(a). VARIATION OF YAWING MOMENT AT ZERO INCIDENCE WITH MACH NUMBER — MIDSEMISPAN LOCATION.

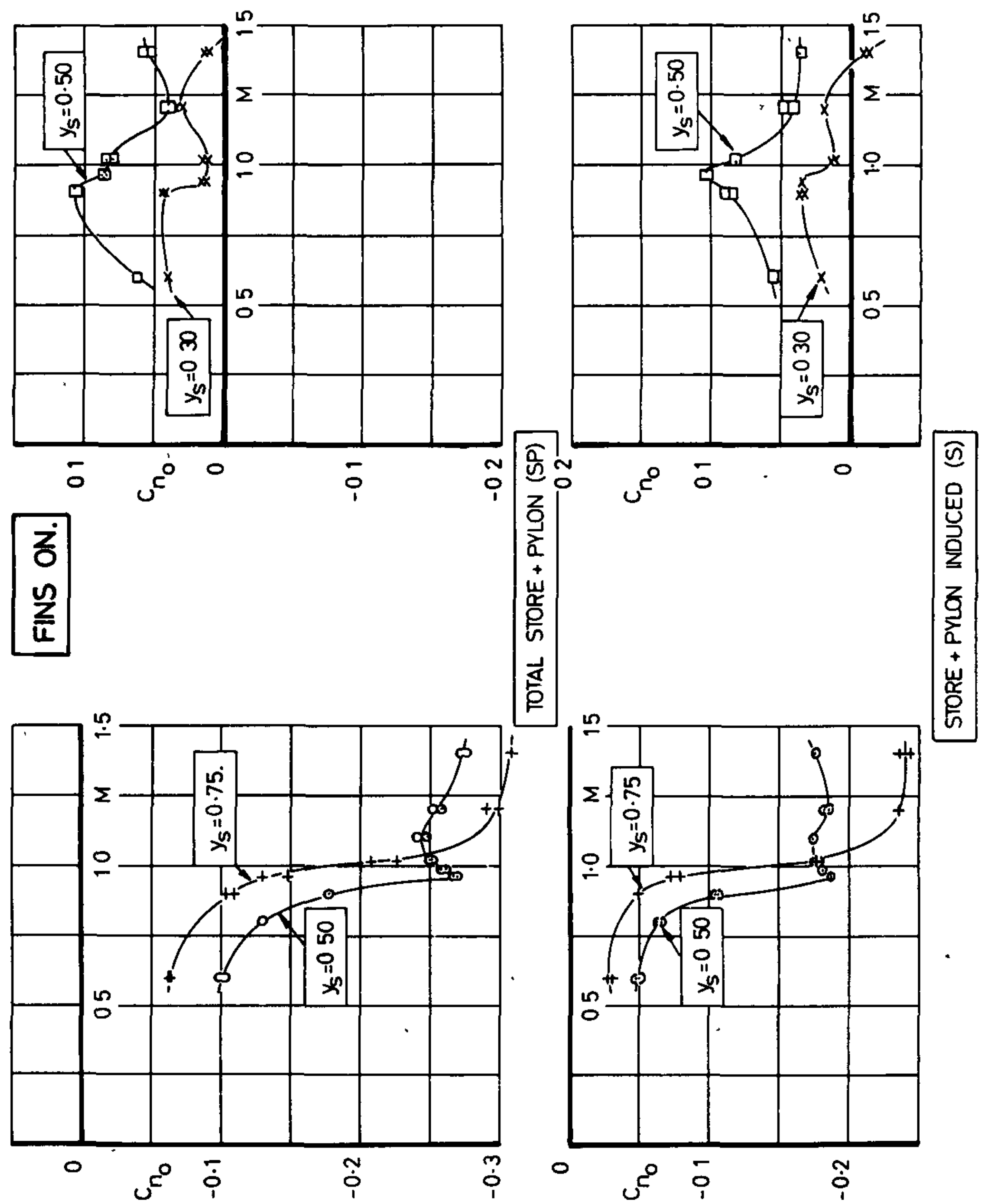

FIG. 13.(b). THREE SPANWISE LOCATIONS.

FIG 14(a)

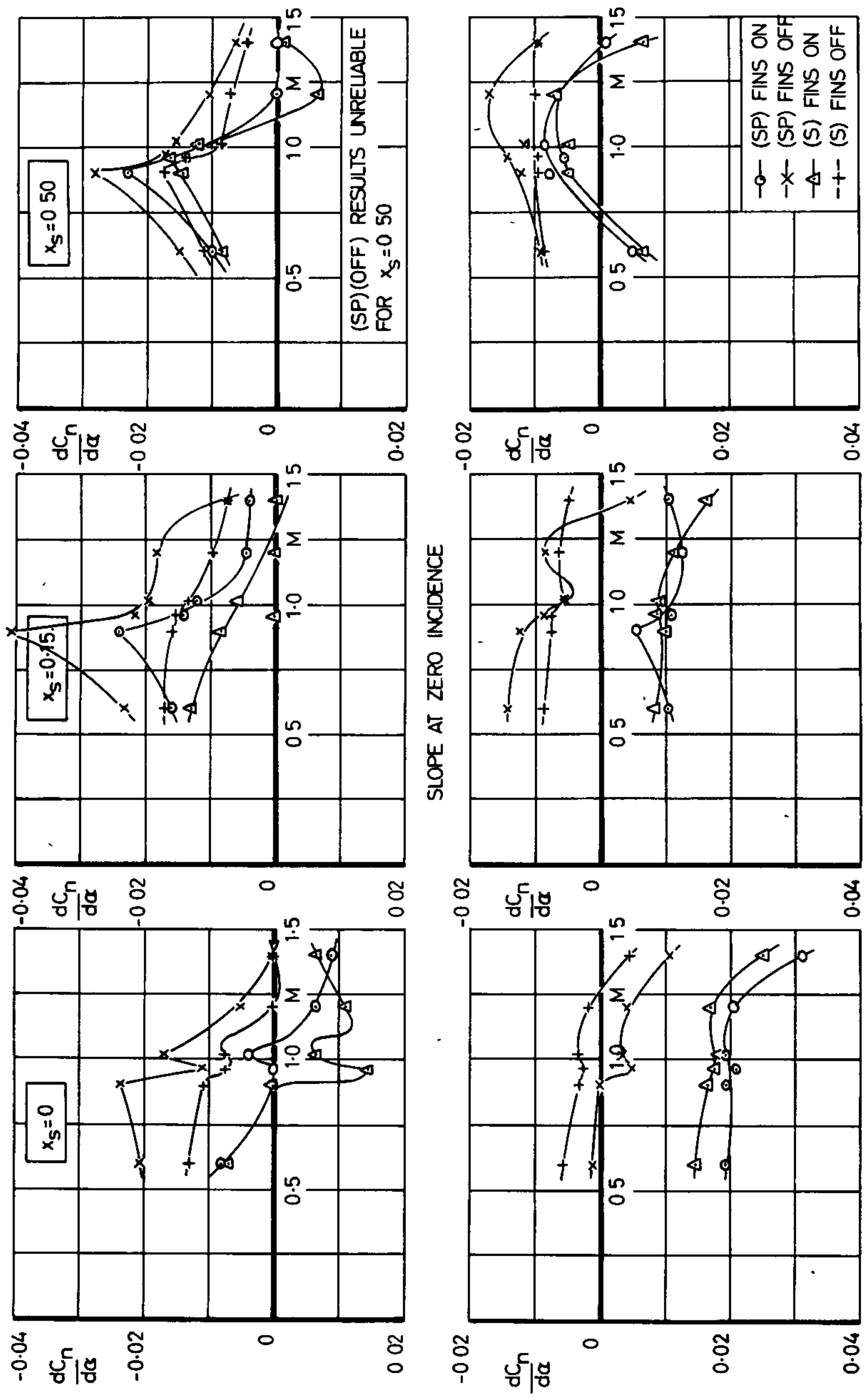

FIG. 14.(a). VARIATION OF $\frac{dC_n}{d\alpha}$ WITH MACH NUMBER.
MIDSEMISPAN LOCATION.

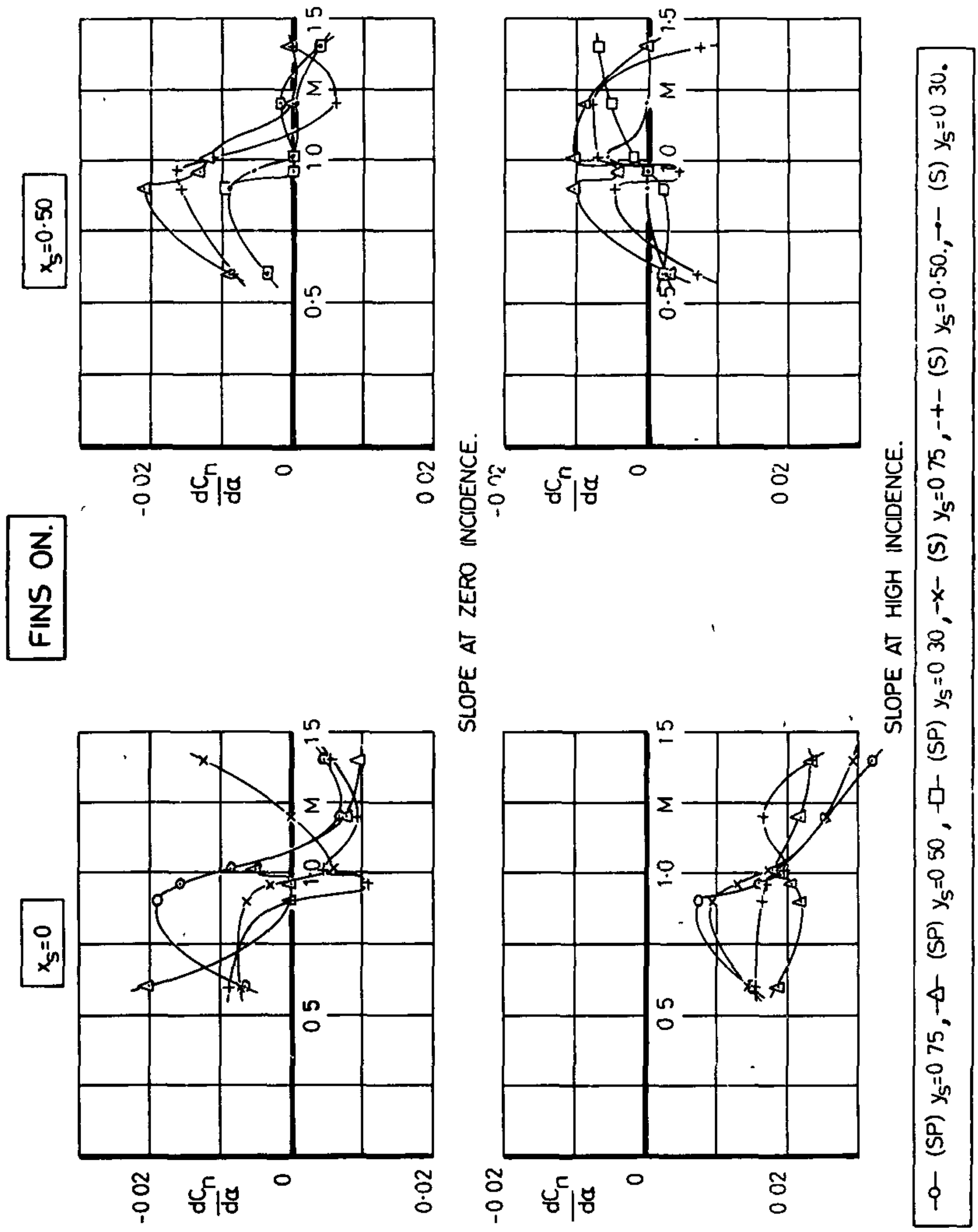

FIG. 14(b). THREE SPANWISE LOCATIONS.

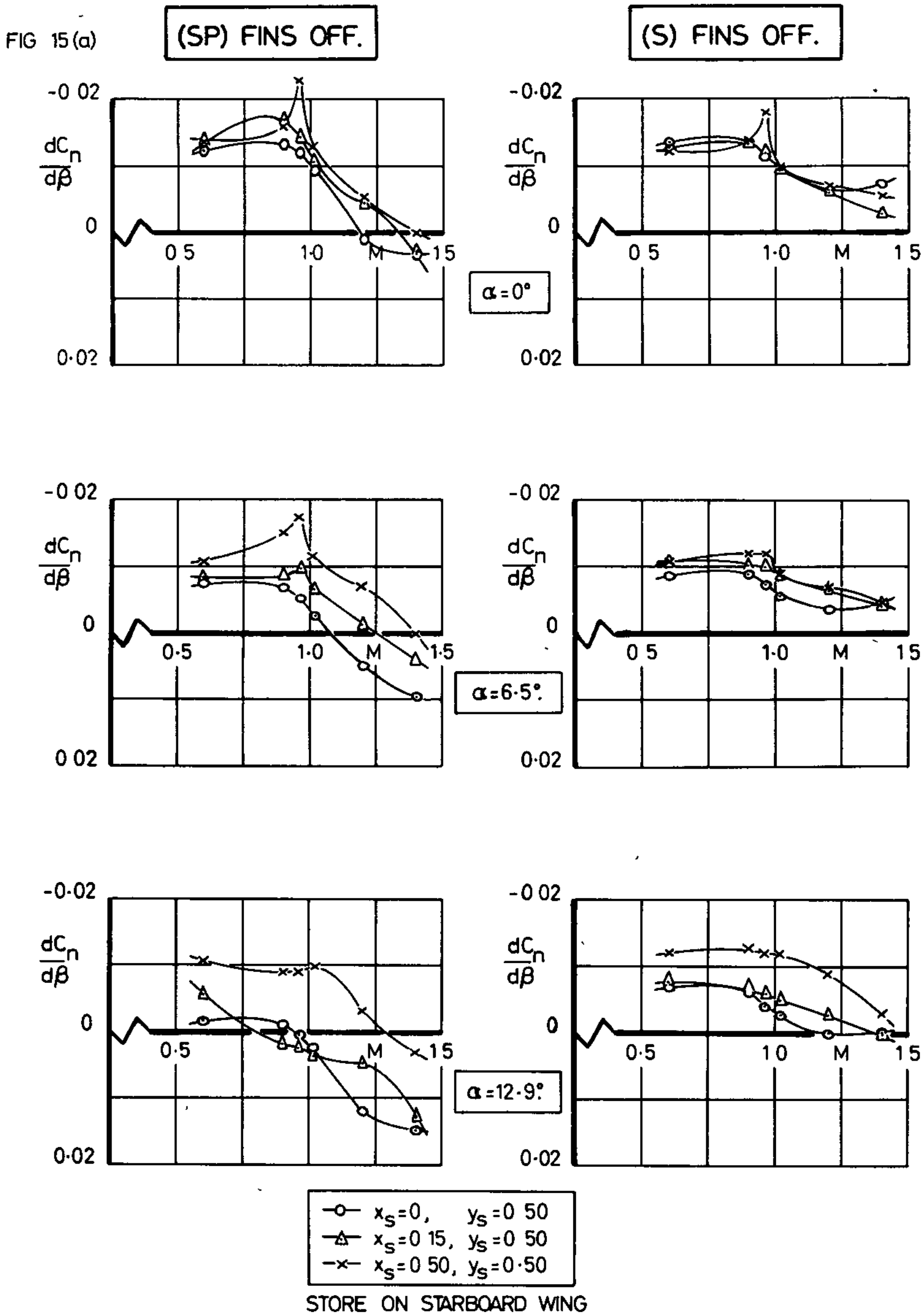

FIG. 15.(a). VARIATION OF $\frac{dC_n}{d\beta}$ WITH MACH NUMBER AT MIDSEMISPAN. FINS OFF.

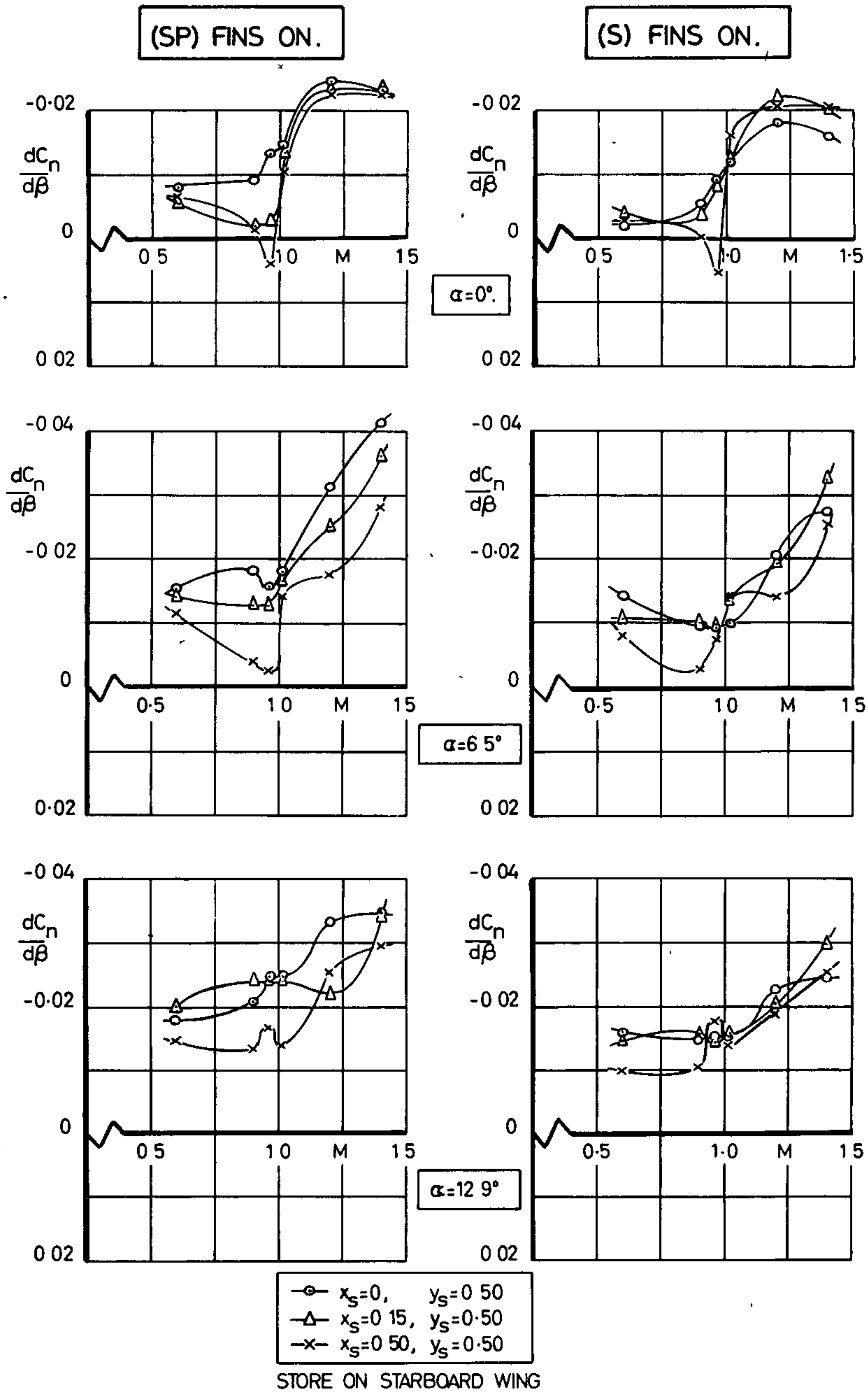

FIG. 15.(b). FINS ON.

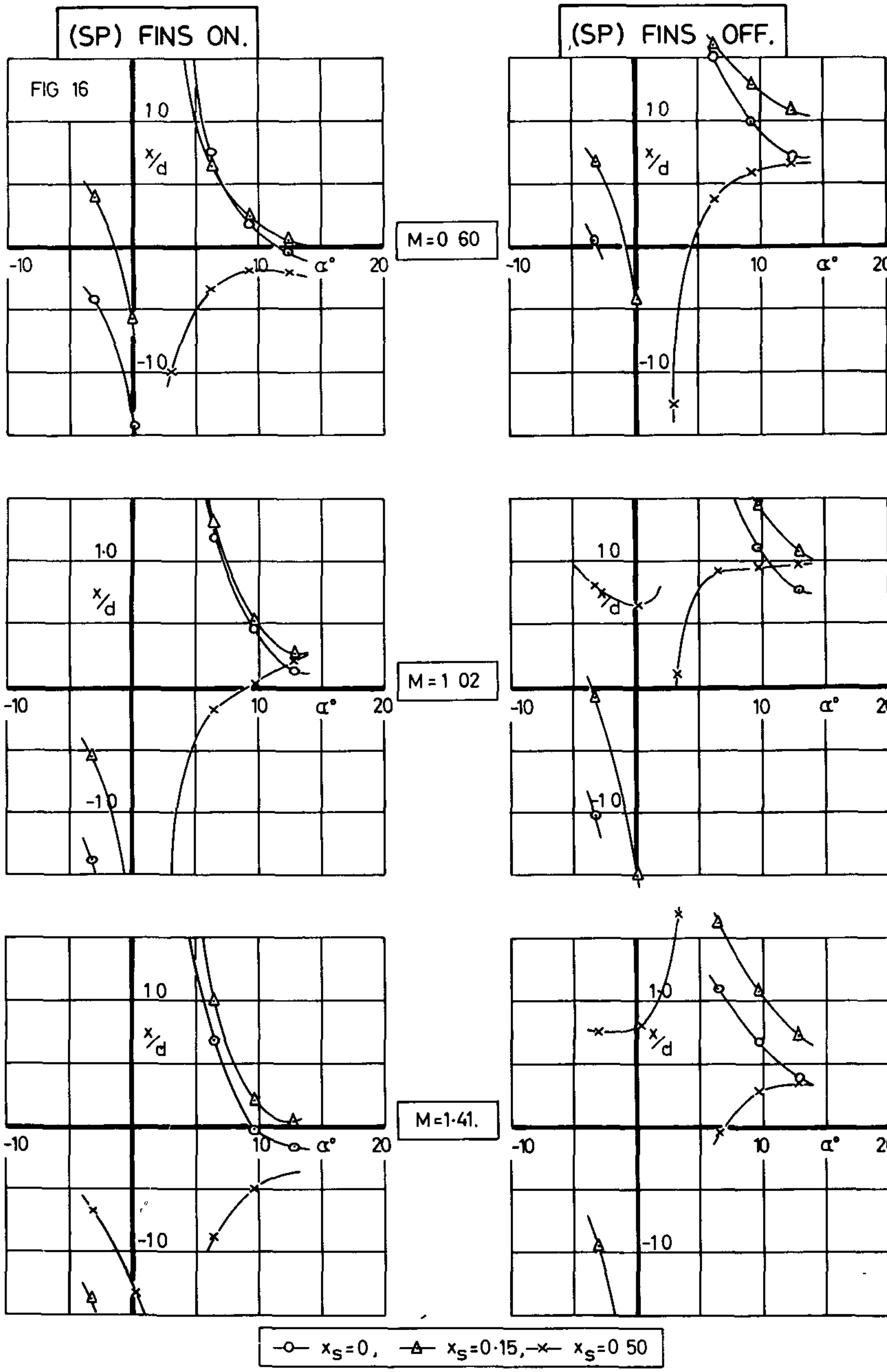

FIG. 16. VARIATION WITH INCIDENCE OF THE CHORDWISE (SP) CENTRE OF PRESSURE (x/d), AT MIDSEMISPAN.

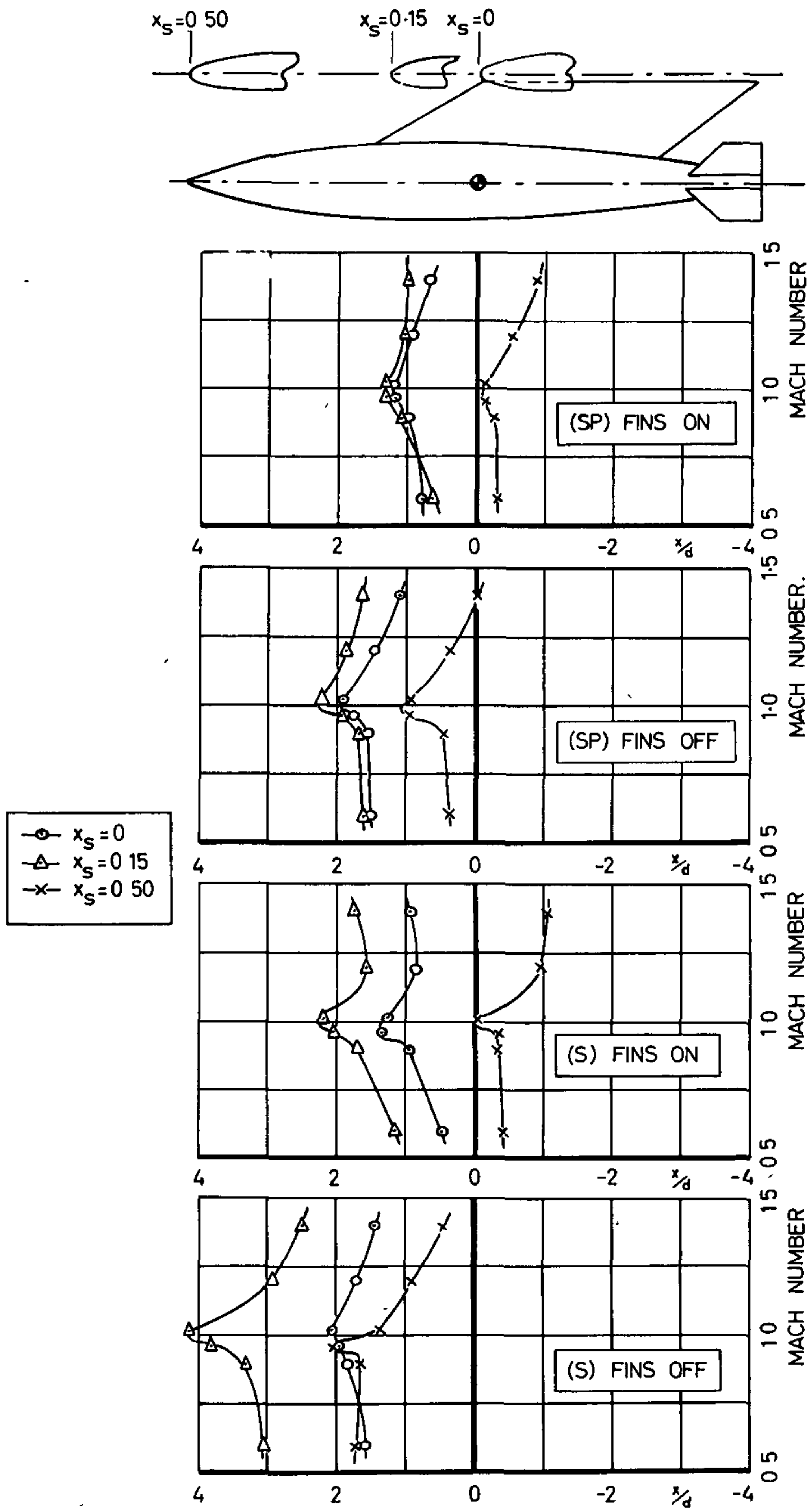

FIG. 17. VARIATION WITH MACH NUMBER OF THE CHORDWISE CENTRE OF PRESSURE AT α=6·5°, MIDSEMISPAN LOCATION.

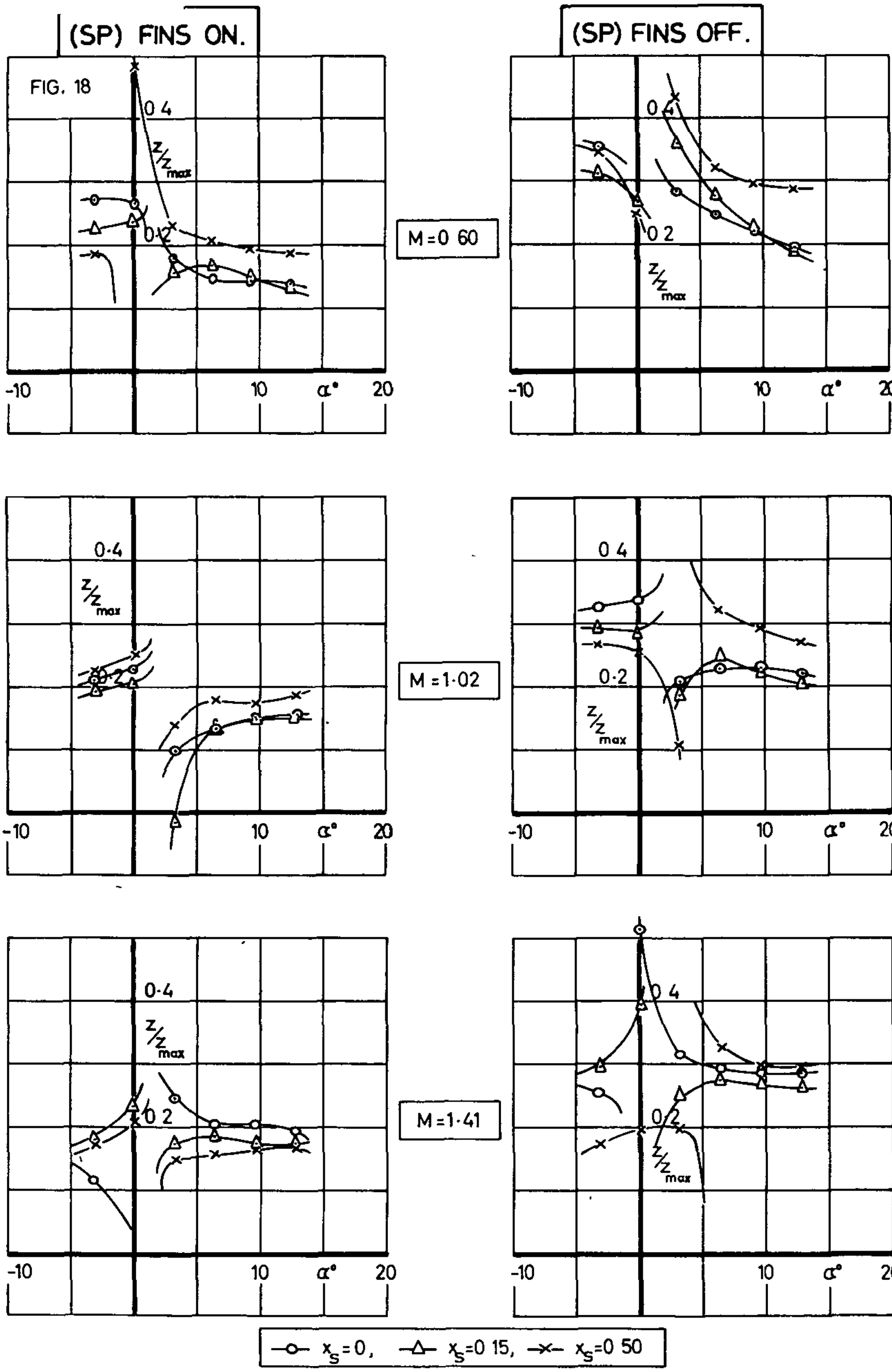

FIG. 18. VARIATION WITH INCIDENCE OF THE DEPTHWISE (SP) CENTRE OF PRESSURE (z/z_{max}), AT MIDSEMISPAN

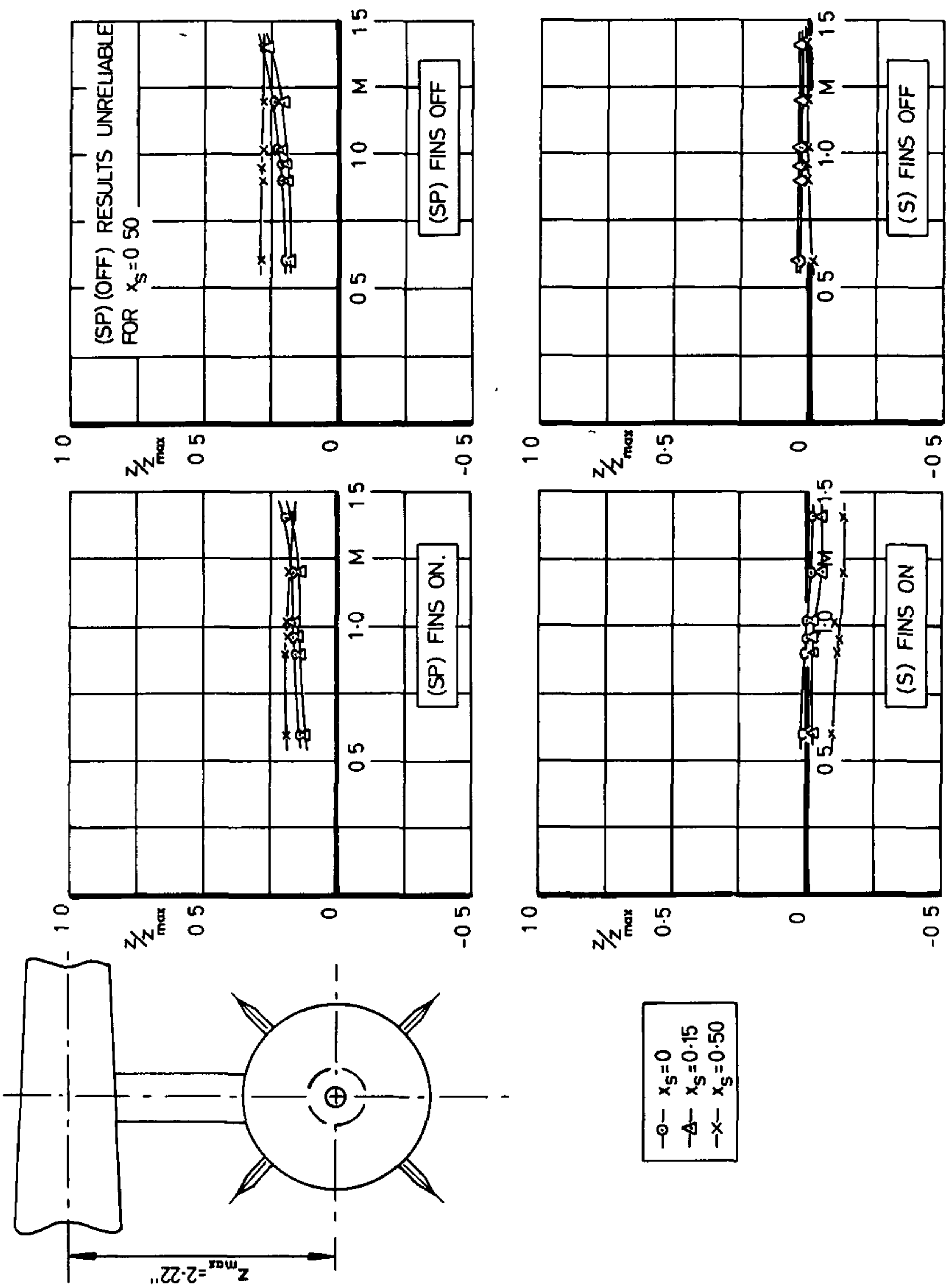

FIG. 19. VARIATION WITH MACH NUMBER OF THE DEPTHWISE CENTRE OF PRESSURE AT α=12·9°, MIDSEMISPAN LOCATION.

(a) ARA WING-FUSELAGE.

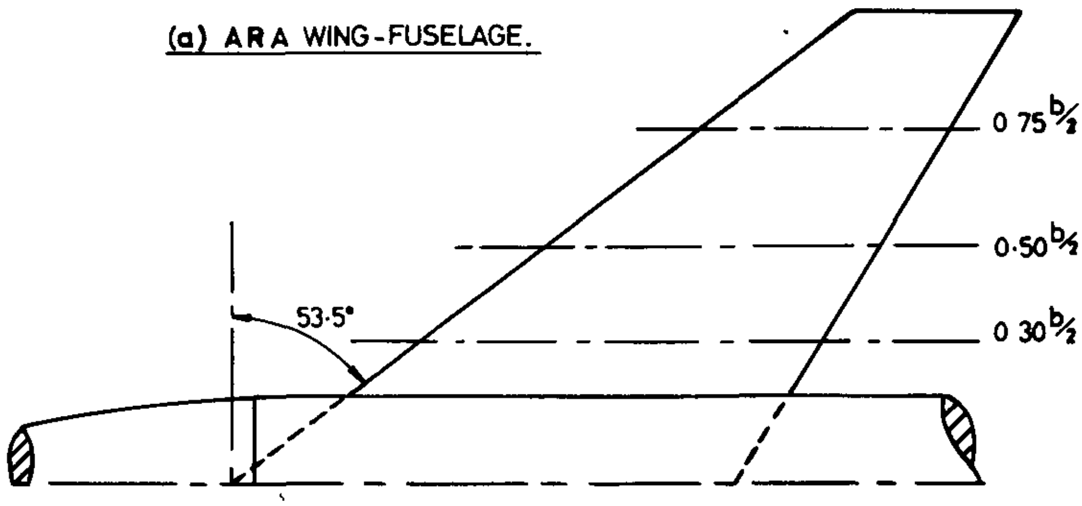

	ARA	NACA	
WING SECTION	RAE 102	NACA 65A006	
t/c %	6 0	6·0	
ASPECT RATIO.	2 82	4·0	
TAPER RATIO	0 33	0 30	
SWEEP (DEG)	45 (c/2)	45 (c/4)	
		REF 3. (SUPERSONIC)	REF 2 (SUBSONIC)
FUSELAGE STN y_S	0 186	0·115	0 139
WING POSITION	MID	HIGH	MID
NOSE OGIVE ENDS %l	0 360	0 366	0 320
L.E APEX STARTS %l	0 349	0 442	0 369
ROOT CHORD %l	0 283	0·258	0 253

(b) NACA WING-FUSELAGES.

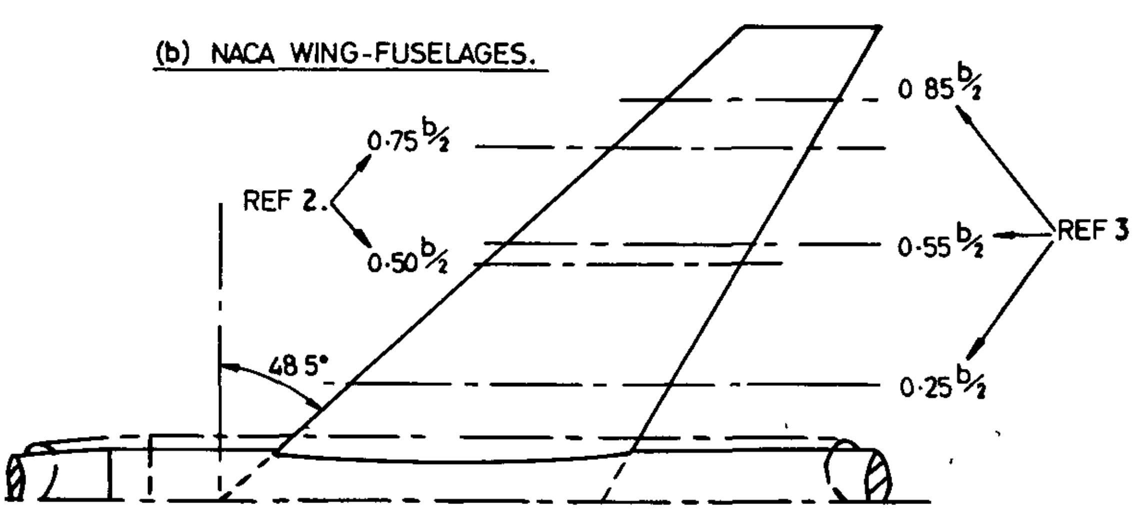

FIG. 20. ARA. AND NACA. SWEPT WING-FUSELAGE CONFIGURATIONS.

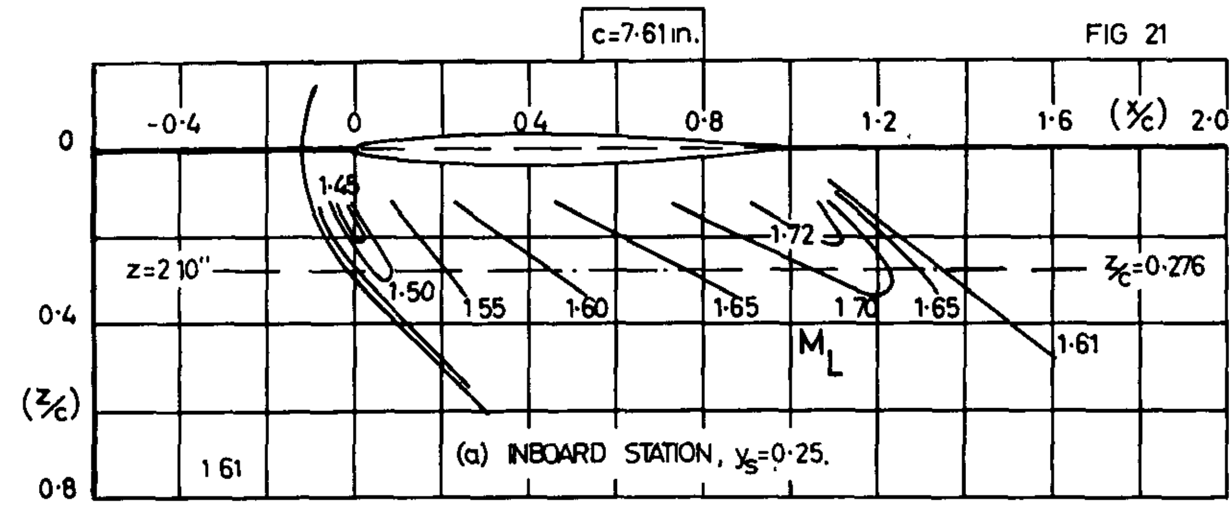

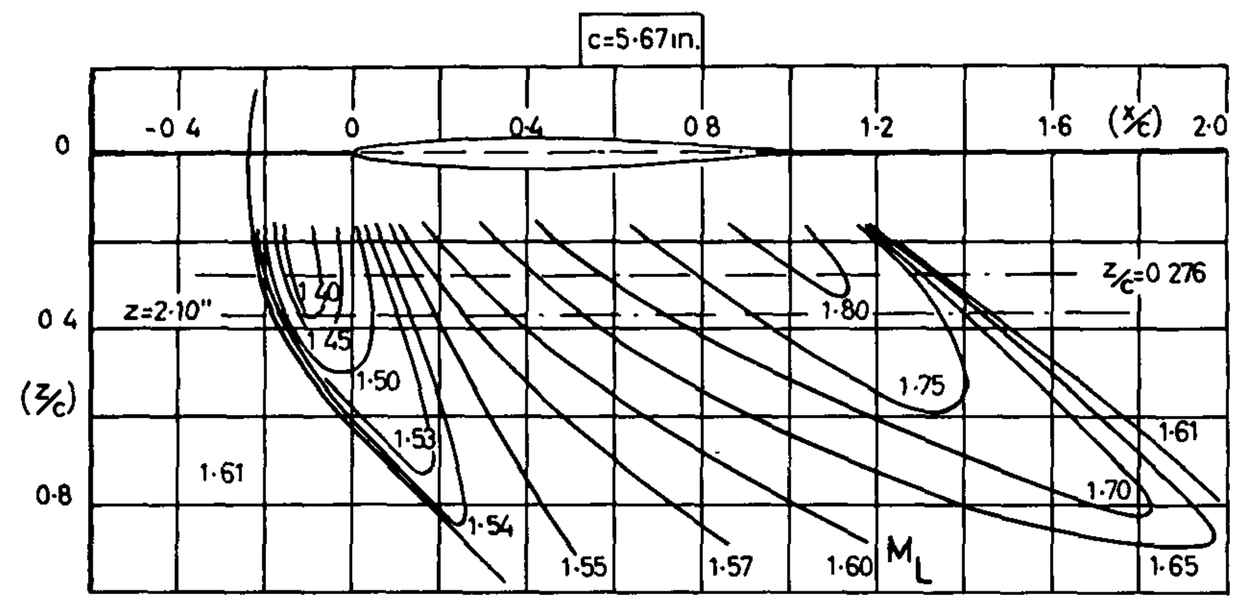

(b) MID STATION, y_s=0·55

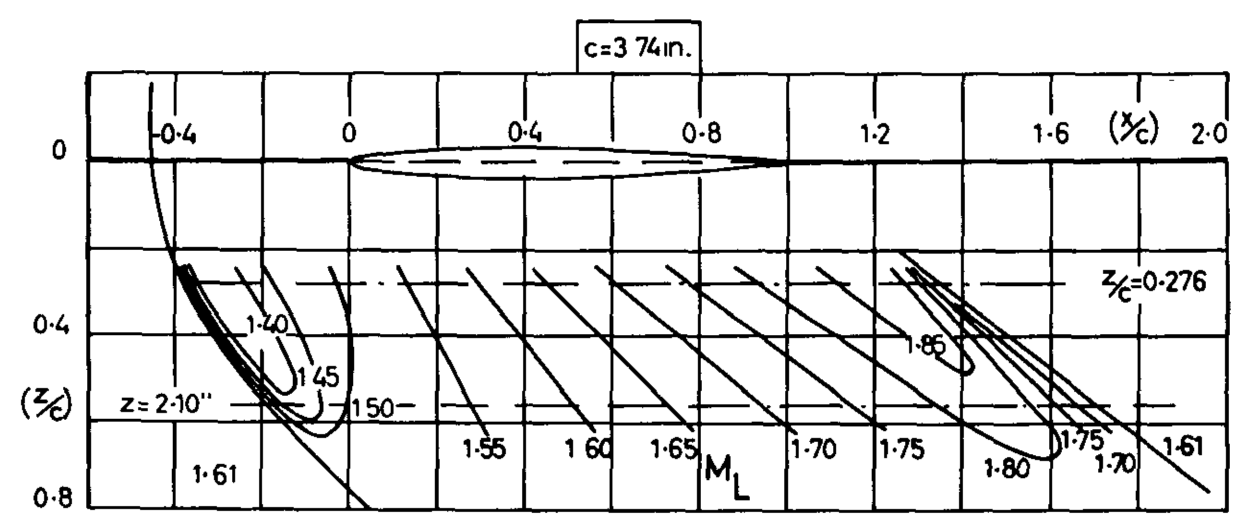

(c) OUTBOARD STATION, y_s=0·85.

FIG. 21. EXPERIMENTAL VARIATION OF LOCAL MACH NUMBER BENEATH NACA WING AT ZERO INCIDENCE FOR FREESTREAM M=1·61.

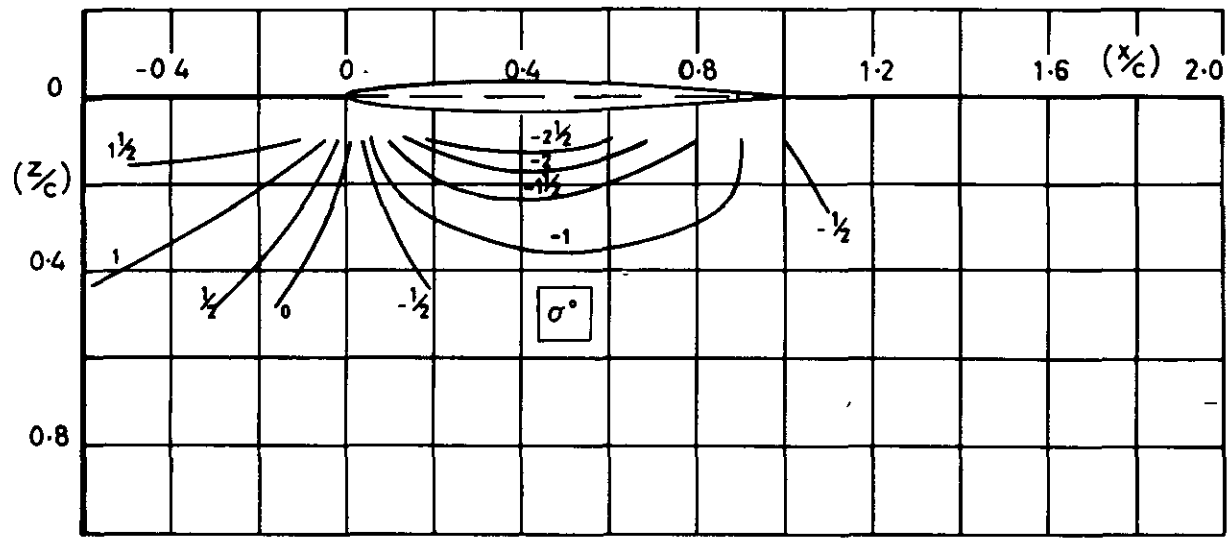

(a) LOW SUBSONIC MACH NUMBER

$y_s = 0{\cdot}50$

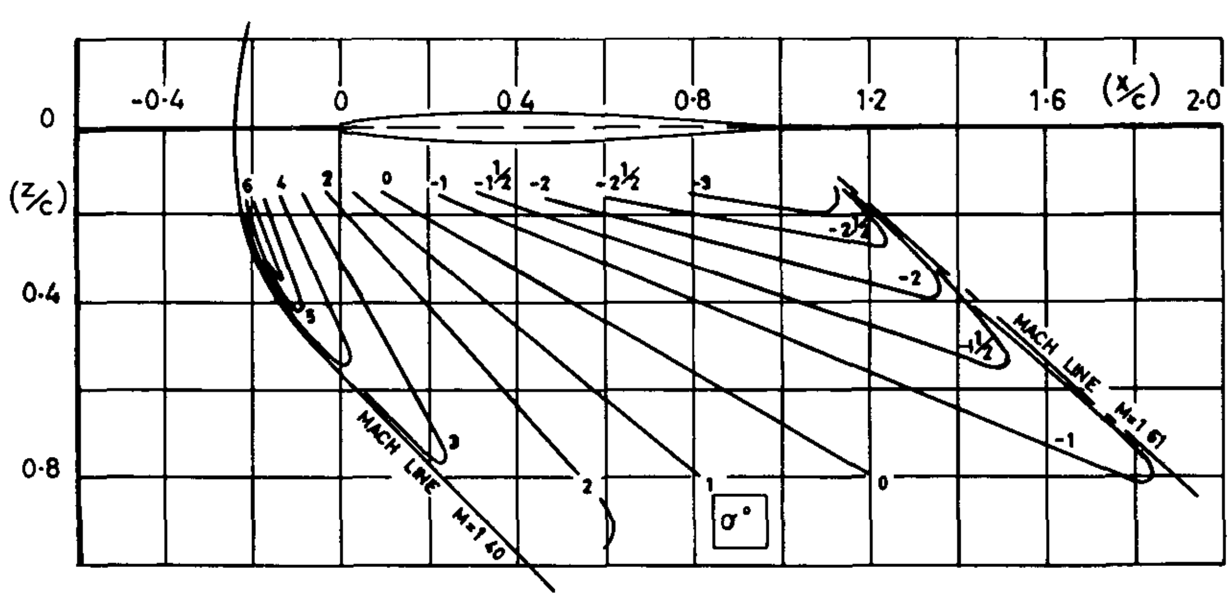

(b) SUPERSONIC MACH NUMBER

$y_s = 0{\cdot}55$, $M = 1{\cdot}61$.

FIG. 22. EXPERIMENTAL SIDEWASH CONTOURS AT ZERO INCIDENCE. VARIATION WITH CHORDWISE AND DEPTHWISE LOCATION.

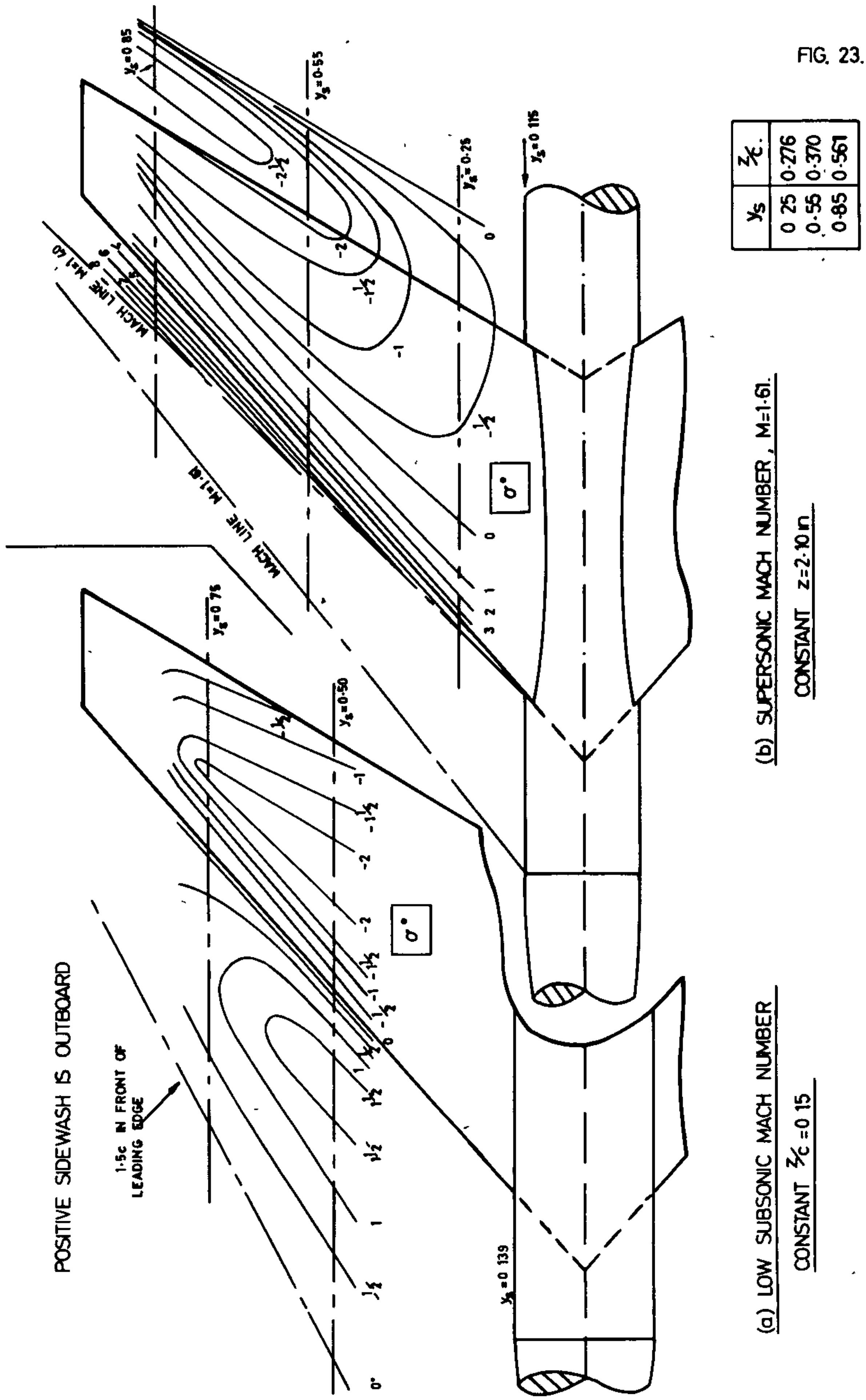

FIG. 23. EXPERIMENTAL SIDEWASH CONTOURS AT ZERO INCIDENCE. VARIATION WITH CHORDWISE AND SPANWISE LOCATION

FIG 24.

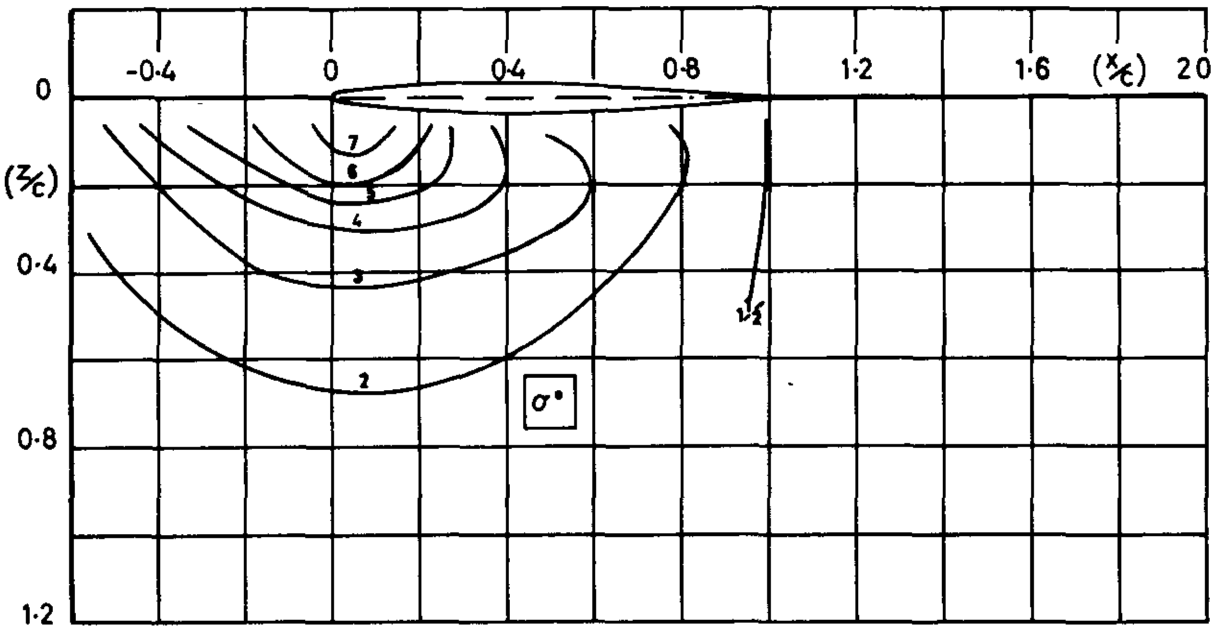

(a) LOW SUBSONIC MACH NUMBER
y_s=0 50

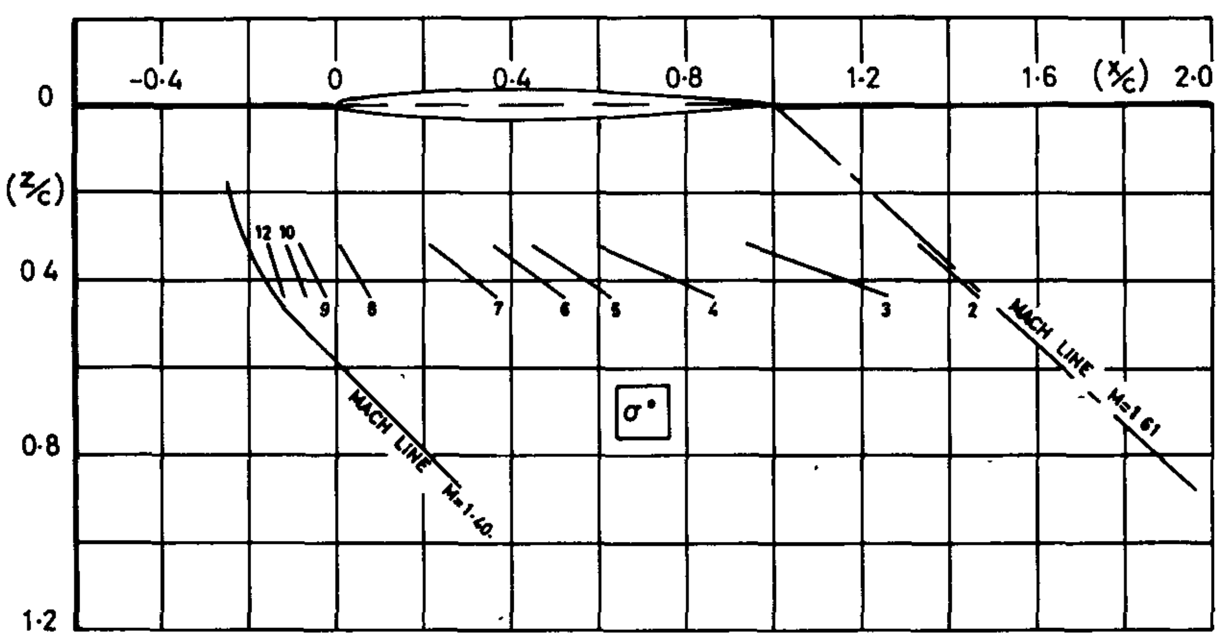

(b) SUPERSONIC MACH NUMBER
y_s=0 55, M =1·61.

FIG. 24. EXPERIMENTAL SIDEWASH CONTOURS AT 8° INCIDENCE. VARIATION WITH CHORDWISE AND DEPTHWISE LOCATION.

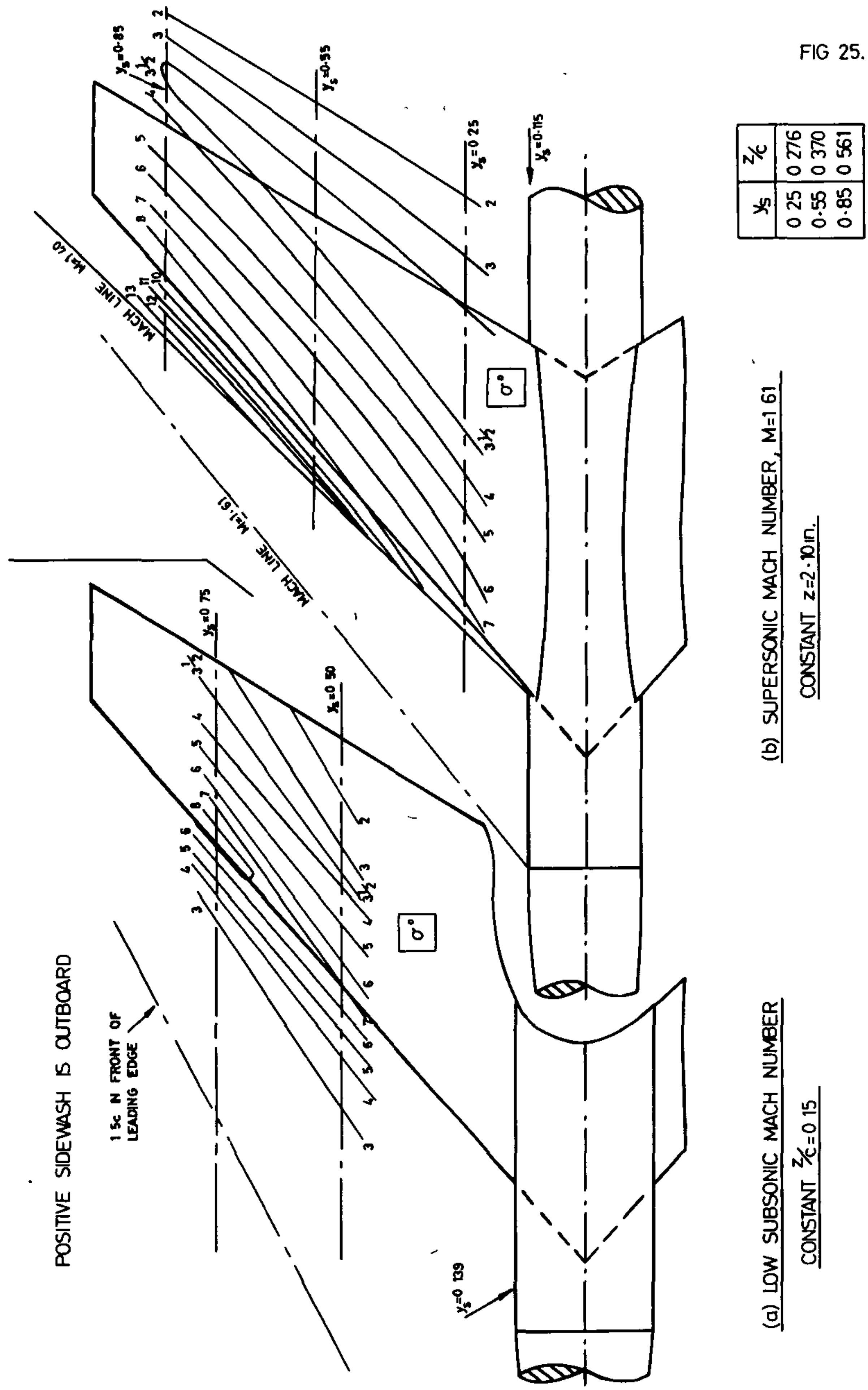

FIG. 25. EXPERIMENTAL SIDEWASH CONTOURS AT 8° INCIDENCE. VARIATION WITH CHORDWISE AND SPANWISE LOCATION.

FIG. 26

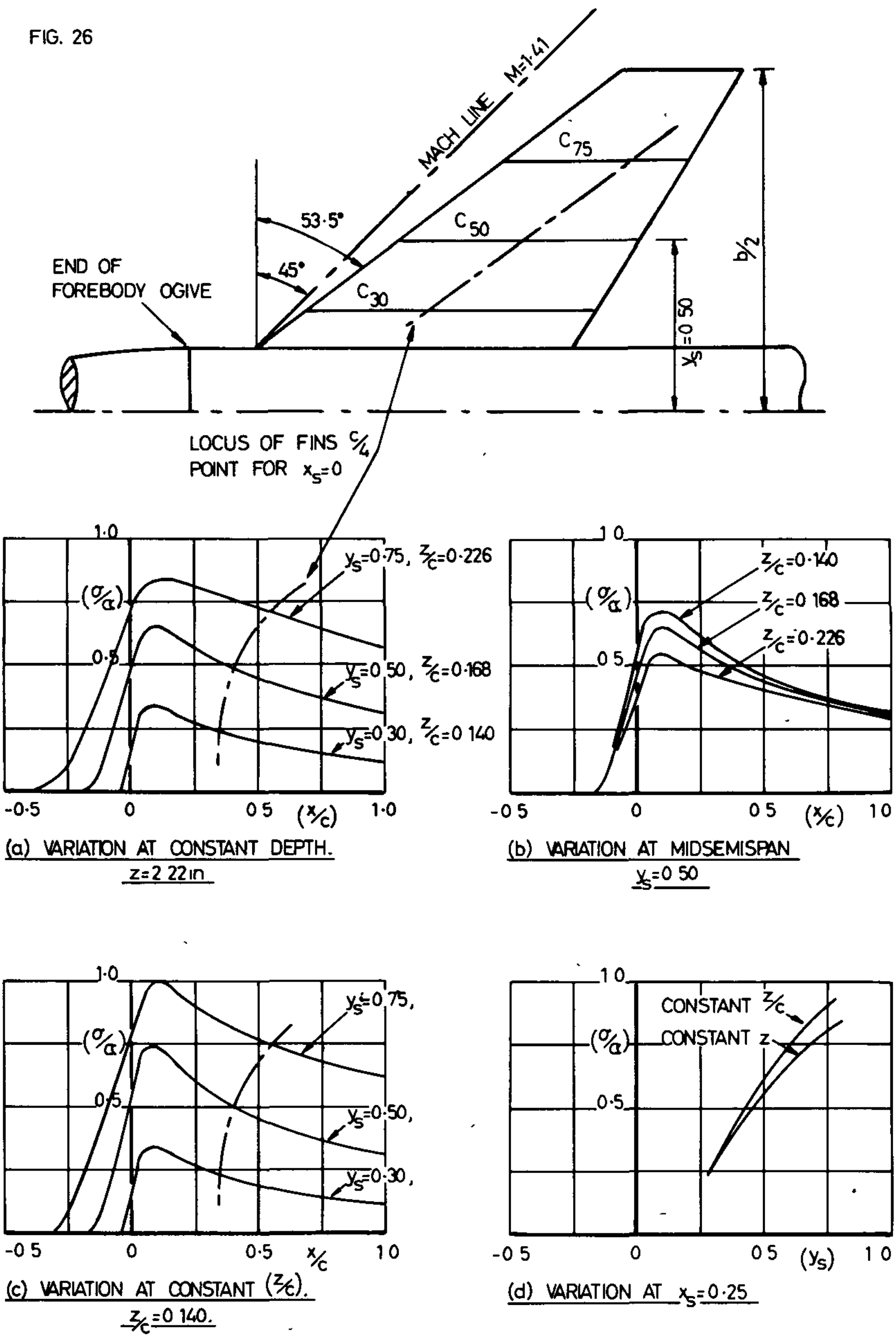

FIG. 26. VARIATION OF THEORETICAL SIDEWASH DUE TO INCIDENCE AT M=1·41, SUBSONIC LEADING EDGE, FOR A.R.A. SWEPT WING

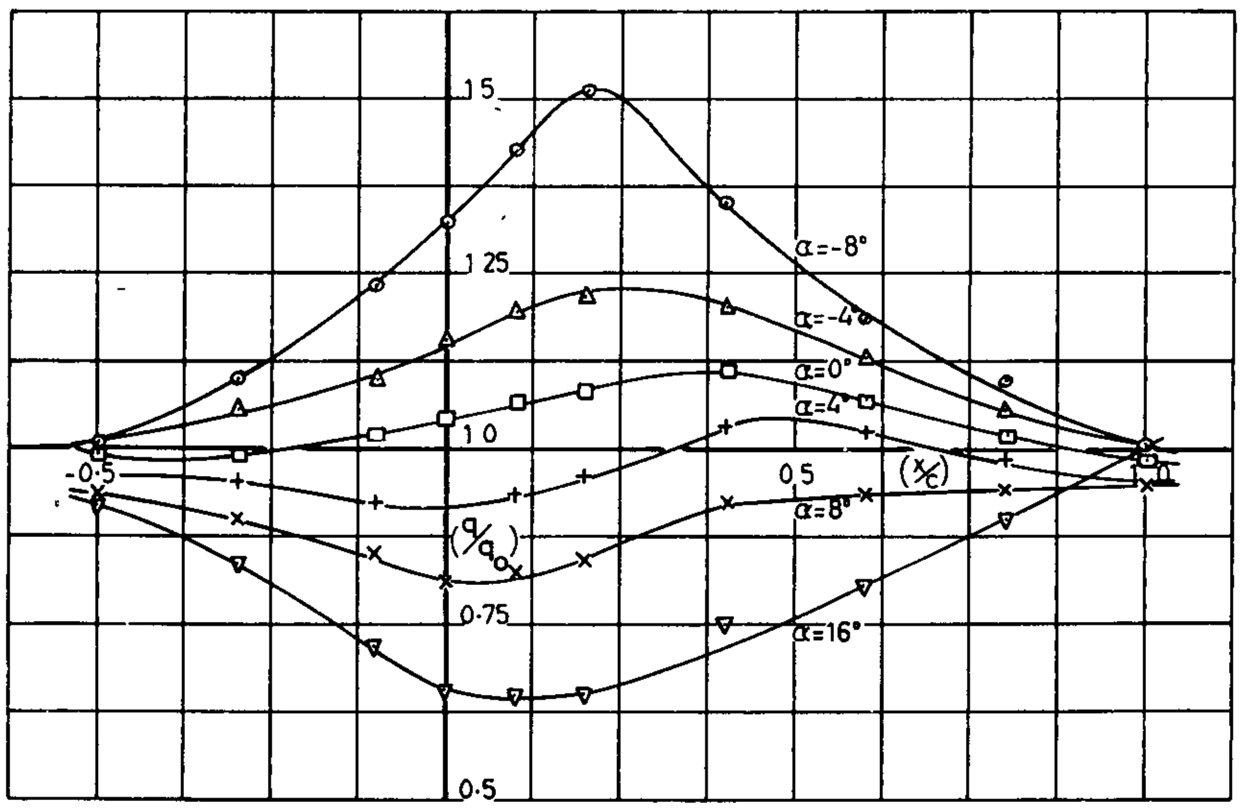

(a) VARIATION WITH INCIDENCE AT $(z/c)=0{\cdot}15$, $y_s=0{\cdot}50$

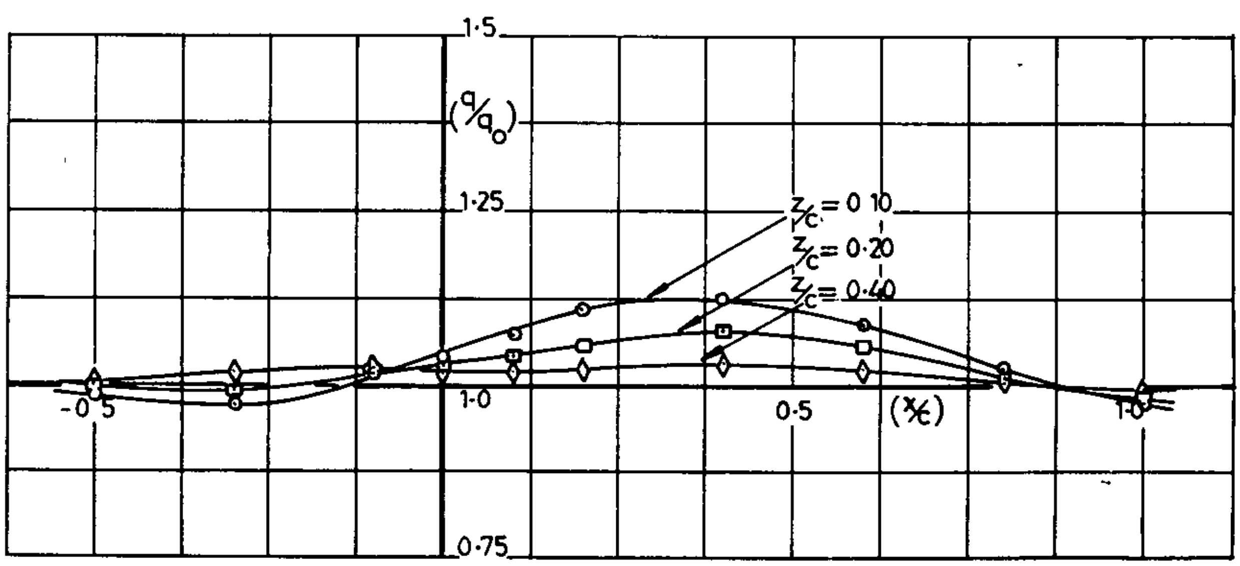

(b) VARIATION WITH (z/c) AT $\alpha=0$, $y_s=0{\cdot}50$.

FIG. 27. VARIATION OF DYNAMIC PRESSURE RATIO BENEATH NACA SWEPT WING AT LOW SUBSONIC MACH NUMBER.

FIG. 28.

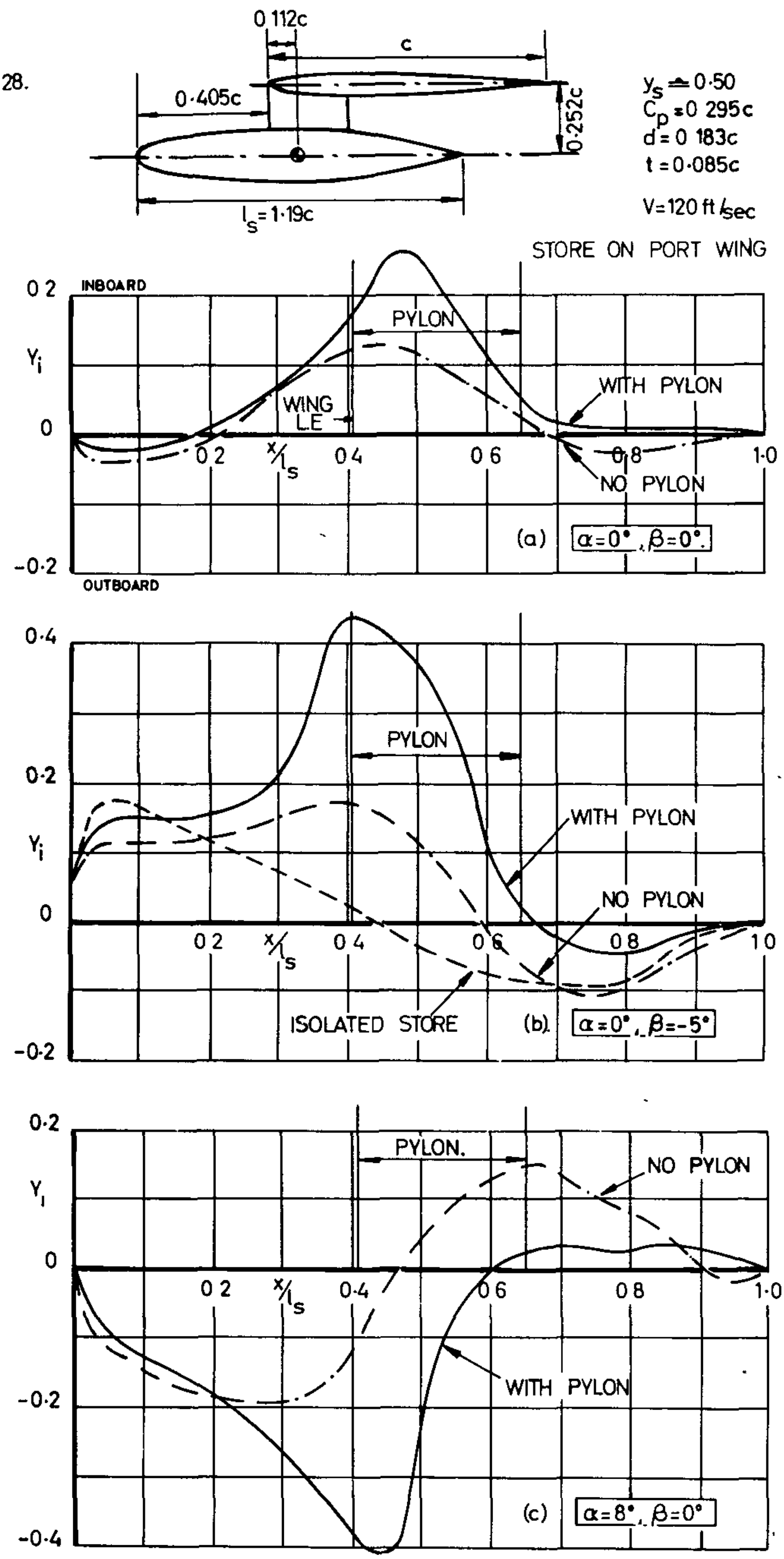

FIG. 28. EXPERIMENTAL SIDE FORCE DISTRIBUTIONS ON A STREAMLINED STORE BENEATH A 40° SWEPT WING, AT LOW SUBSONIC SPEED.

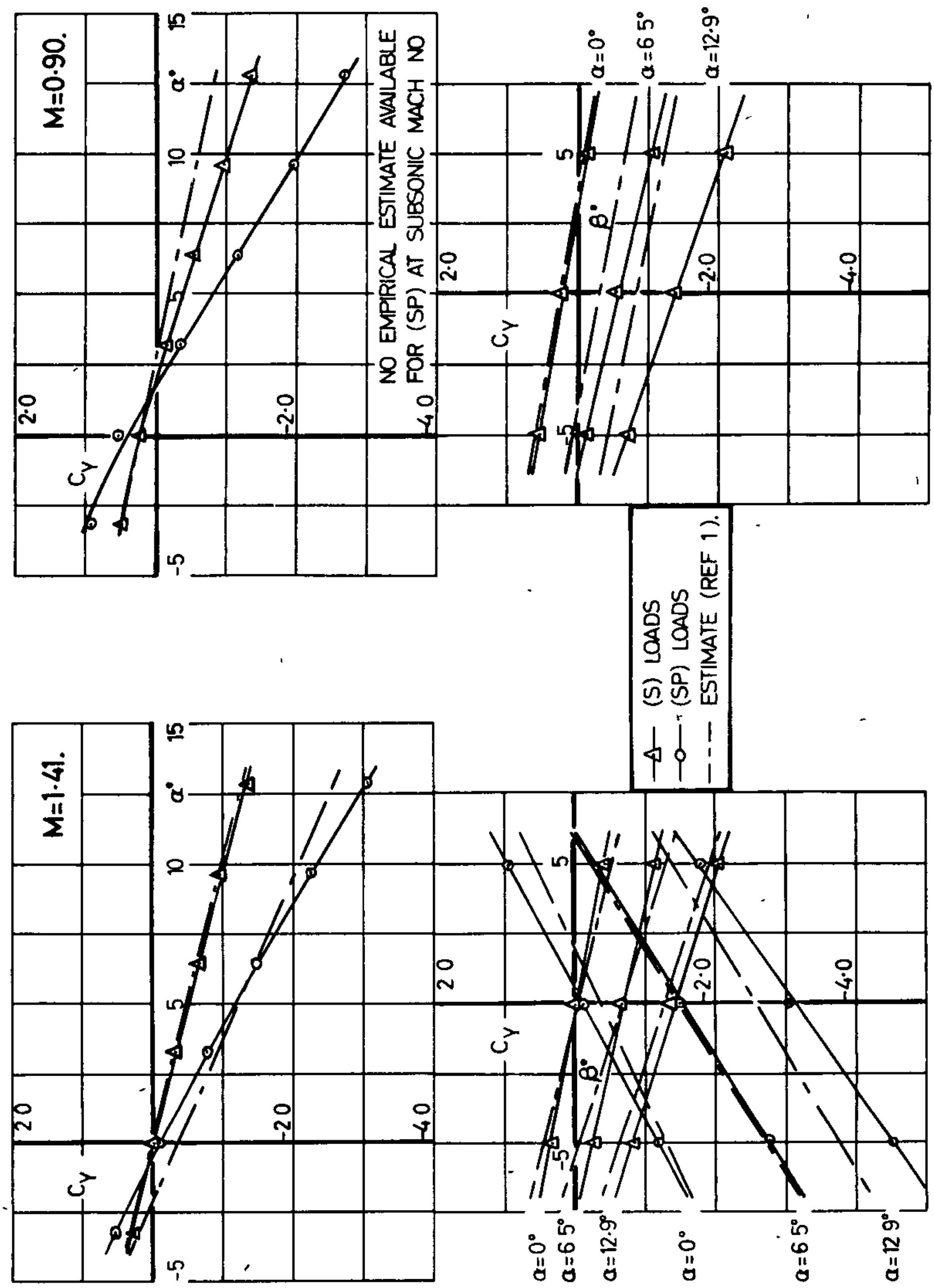

FIG. 29. COMPARISON WITH EMPIRICAL ESTIMATES.

$y_S=0{\cdot}50$, $x_S=0$, FINS OFF.

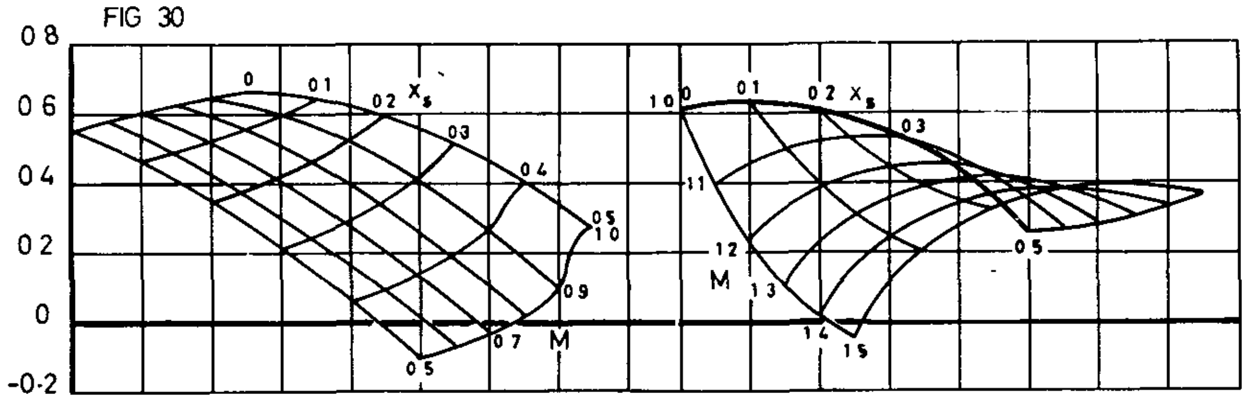

TOTAL STORE + PYLON (SP) VALUES

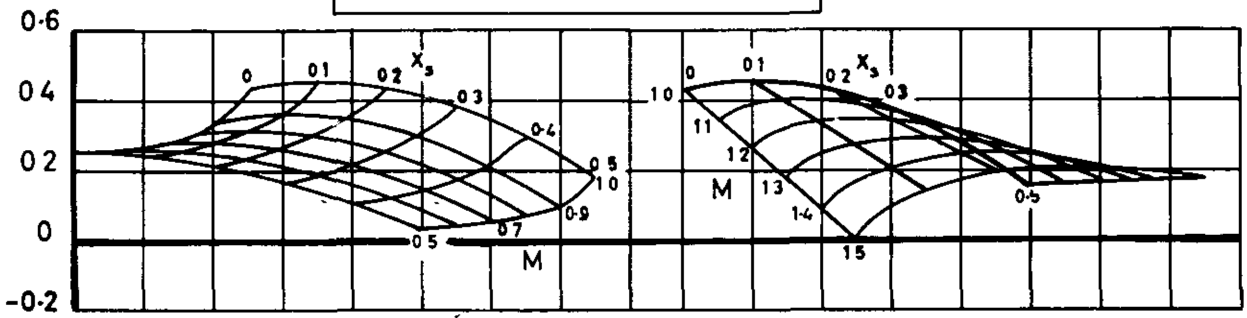

STORE + PYLON INDUCED (S) VALUES.

(a) STORE WITH TAIL FINS.

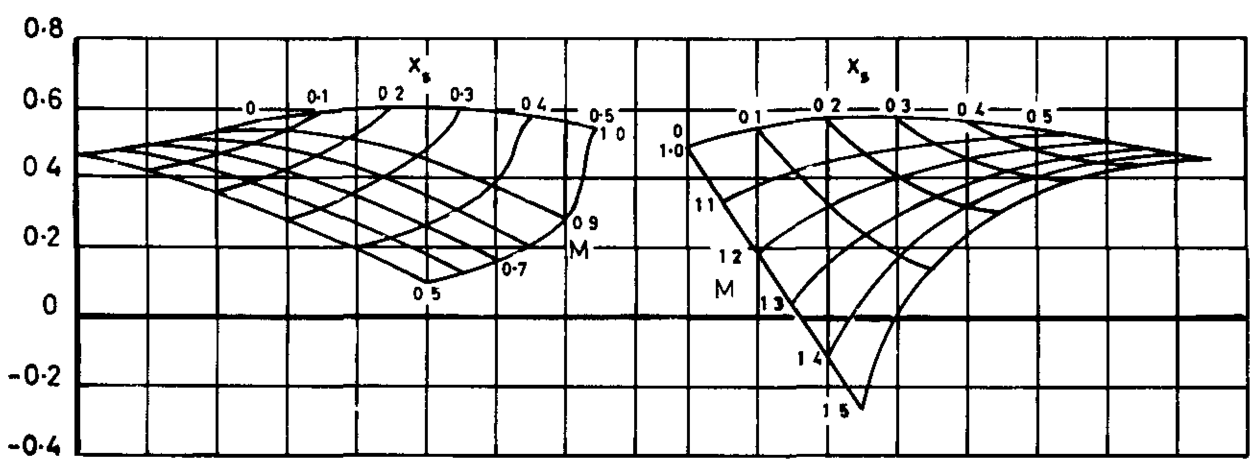

TOTAL STORE + PYLON (SP) VALUES

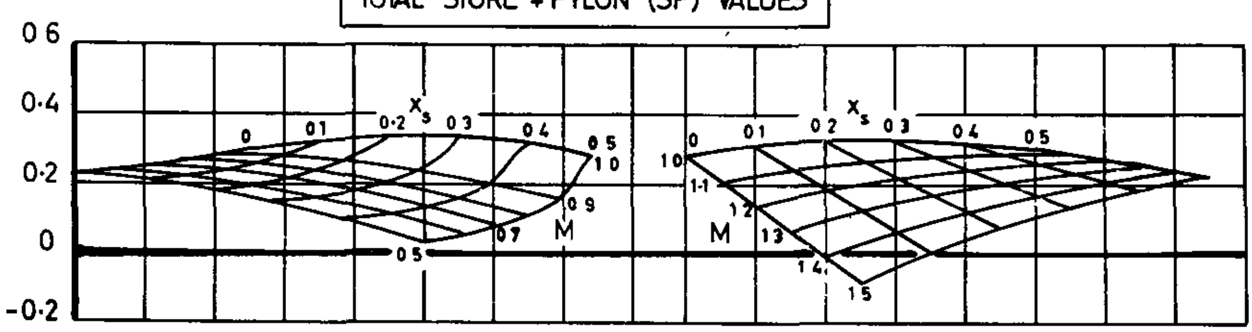

STORE + PYLON INDUCED (S) VALUES.

(b) STORE WITHOUT TAIL FINS

FIG. 30. EMPIRICAL METHOD FOR STORE/PYLON SIDE FORCE. DETERMINATION OF C_{Y_O} AT MIDSEMISPAN.

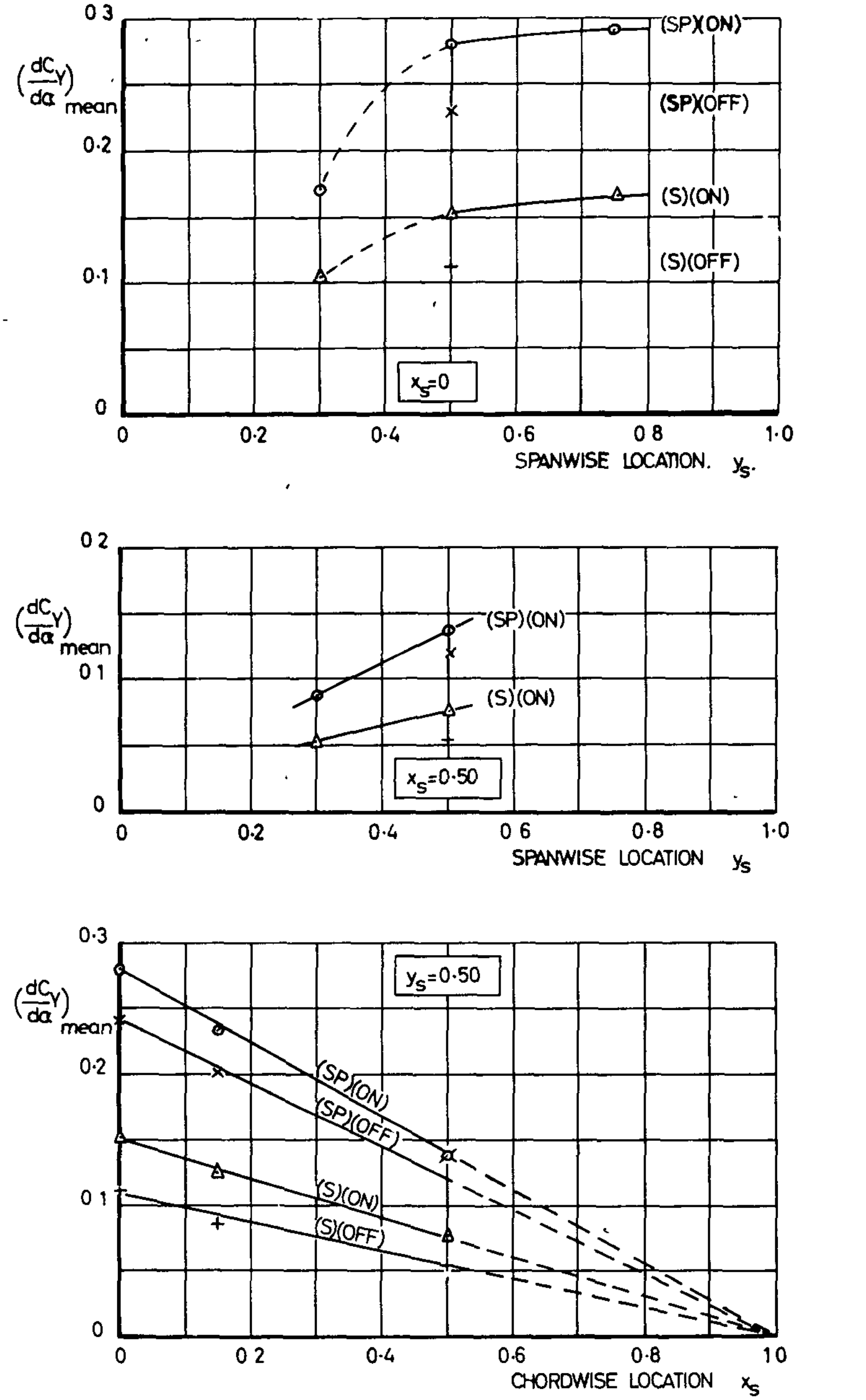

FIG 31. VARIATION OF $\left(\frac{dC_Y}{d\alpha}\right)_{mean}$ WITH SPANWISE AND CHORDWISE LOCATION.

FIG 32

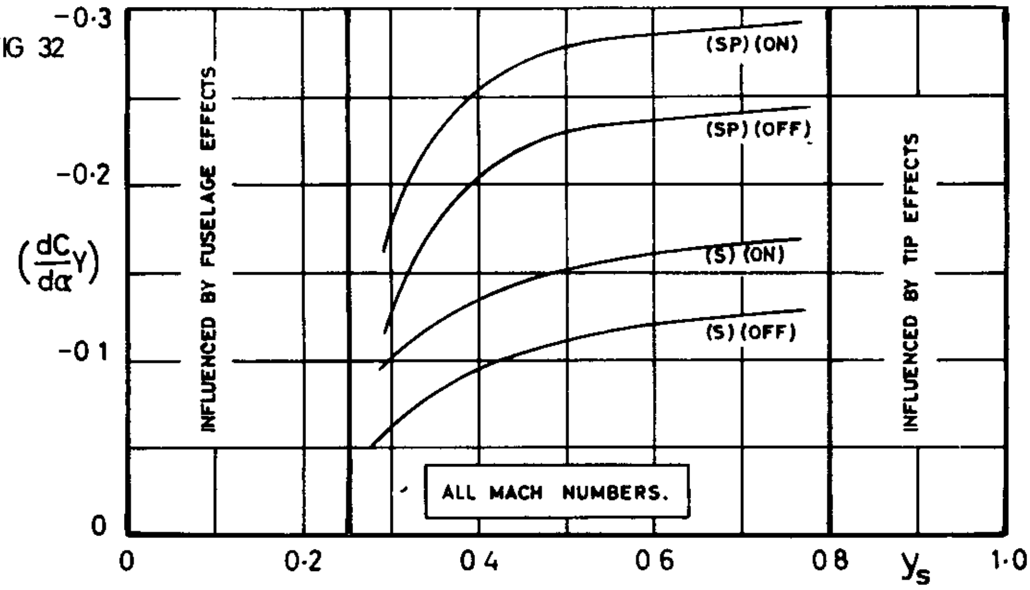

(a) VARIATION OF $\left(\frac{dC_Y}{d\alpha}\right)$ WITH SPANWISE LOCATION AT $x_s = 0$

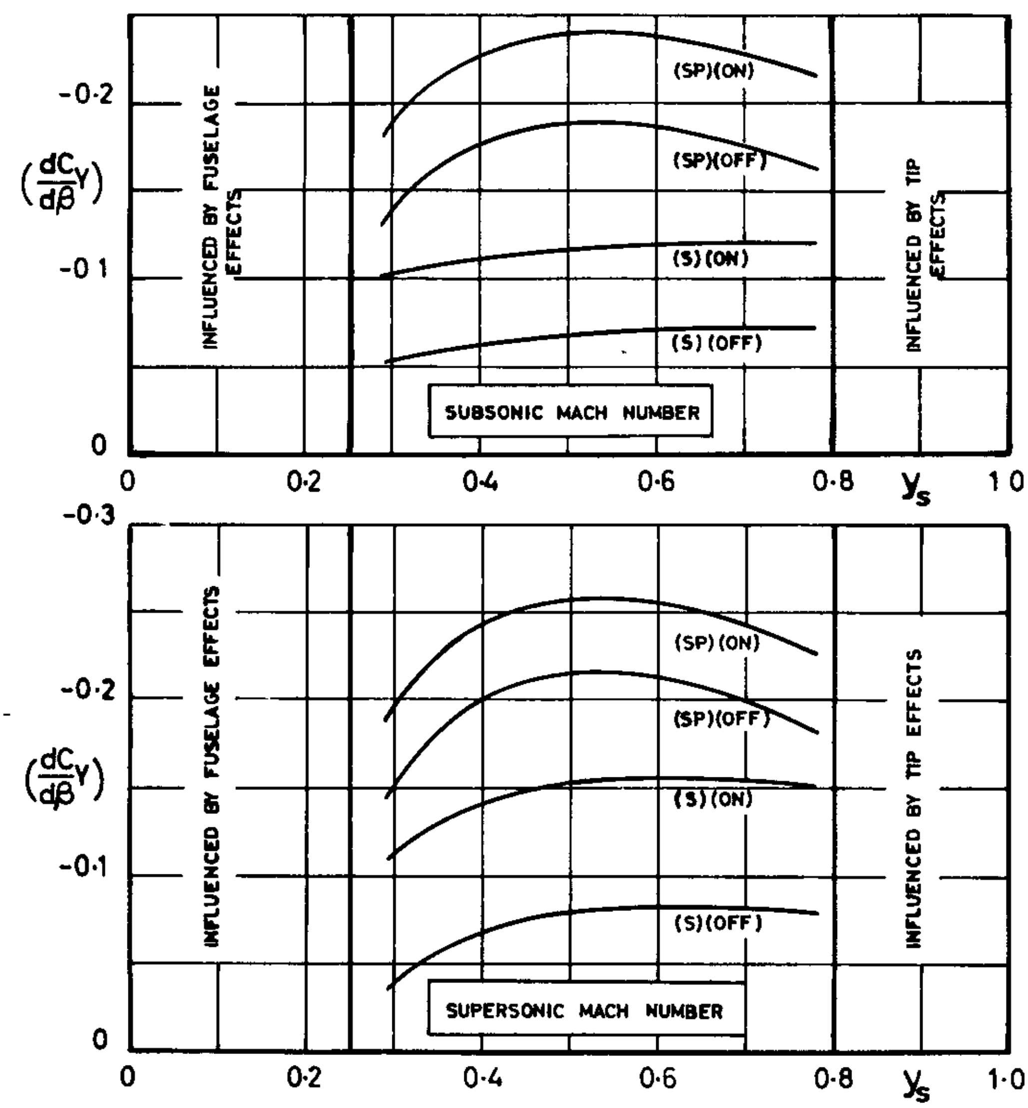

(b) VARIATION OF $\left(\frac{dC_Y}{d\beta}\right)$ WITH SPANWISE LOCATION AT $x_s = 0$

STORE ON PORT WING

FIG. 32. EMPIRICAL METHOD FOR STORE/PYLON SIDE FORCE. DETERMINATION OF $\frac{dC_Y}{d\alpha}$ AND $\frac{dC_Y}{d\beta}$ AT $x_s = 0$.

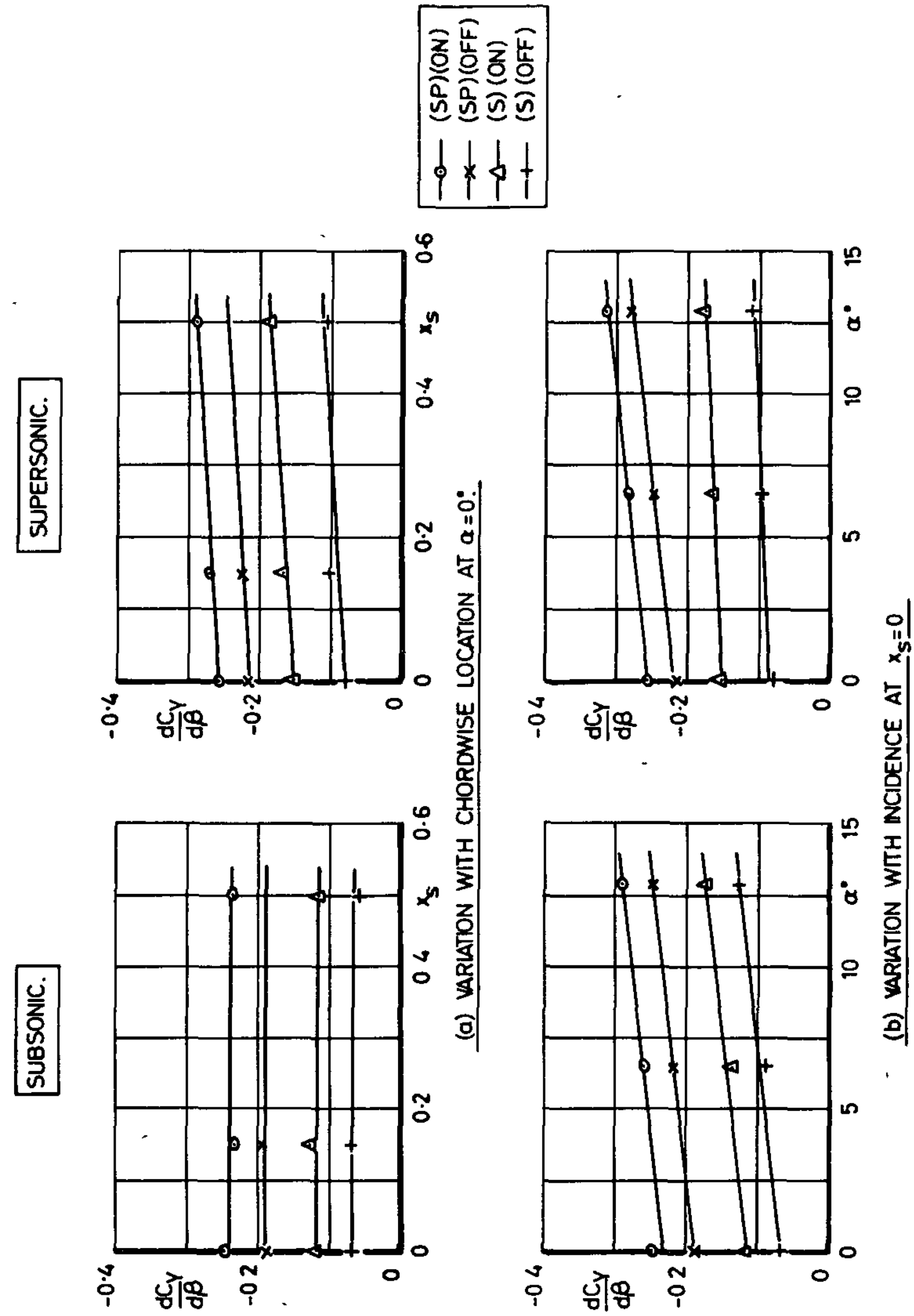

FIG. 33. VARIATION OF $\frac{dC_Y}{d\beta}$ WITH CHORDWISE LOCATION AND INCIDENCE AT MIDSEMISPAN.

FIG 34

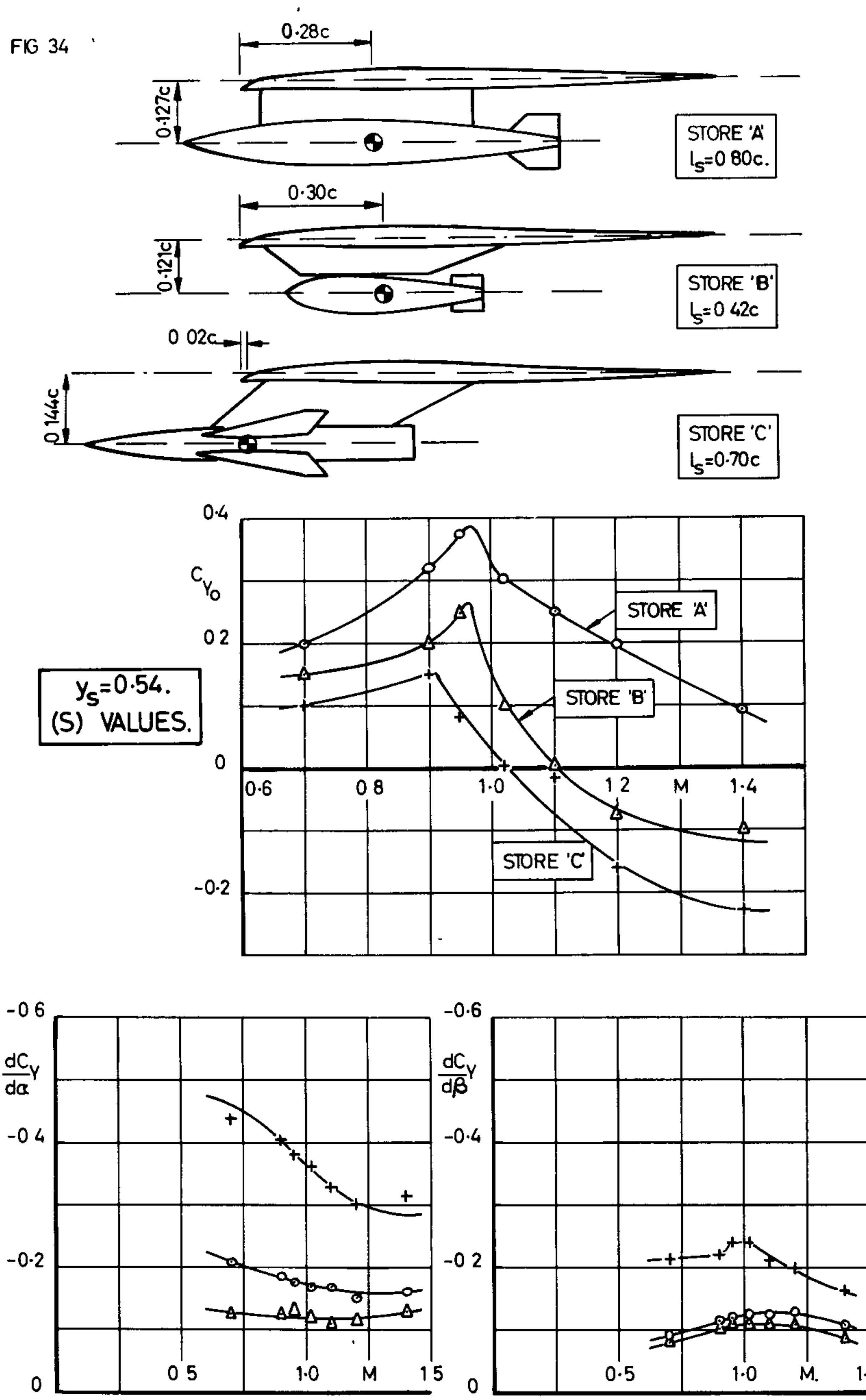

FIG. 34 SIDE FORCE TERMS FOR 3 DIFFERENT STORES UNDER A 60° DELTA WING AT TRANSONIC MACH NUMBERS.

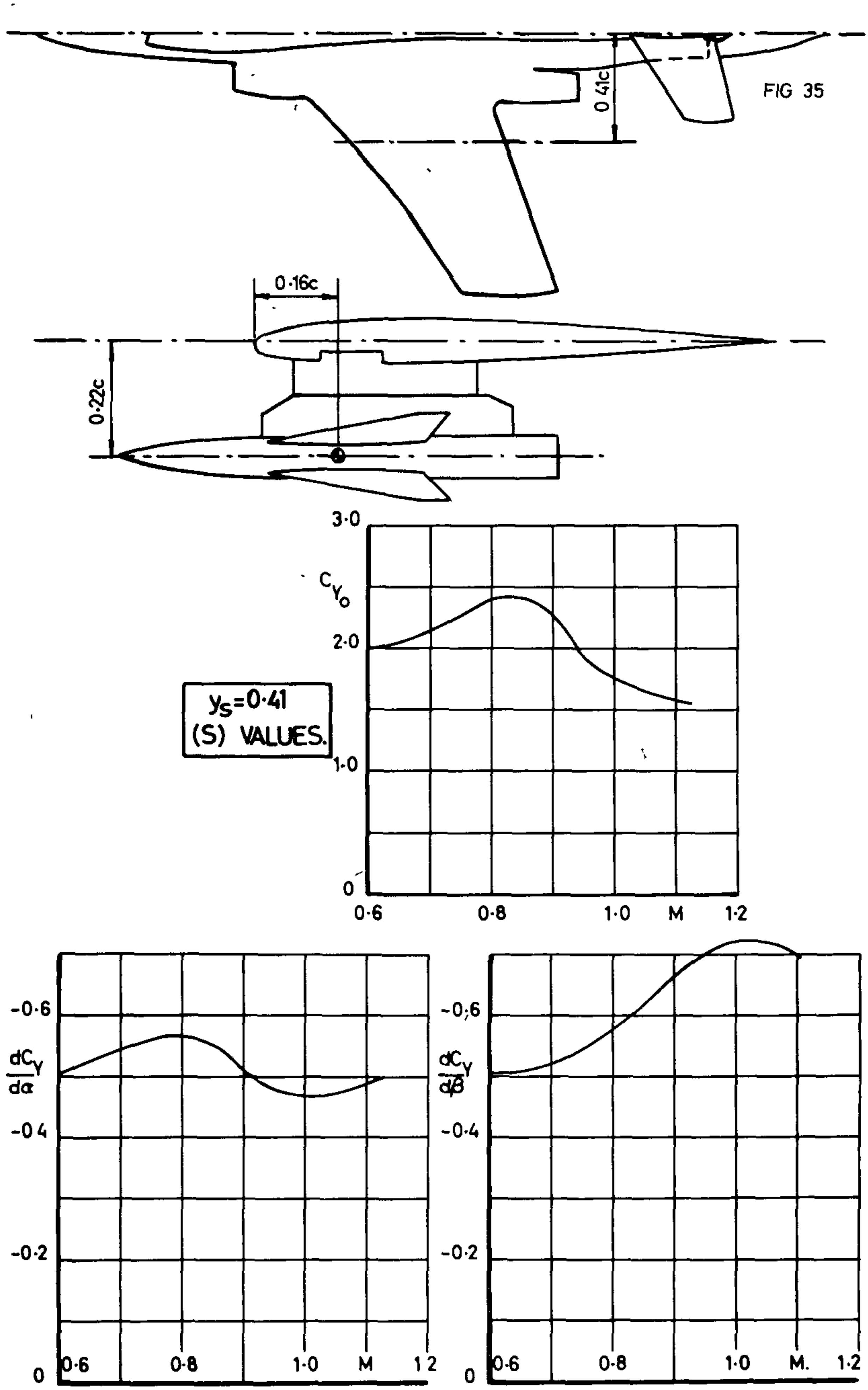

FIG. 35. SIDE FORCE TERMS FOR A WINGED STORE LOCATED CLOSE TO THE FUSELAGE BENEATH A 40° SWEPT WING.

D 88422/1/129528 K.4 6/67 CL

A.R.C C P. No 955
June, 1964.
P. Marsden and A B. Haines

MEASUREMENTS AT TRANSONIC SPEEDS OF THE SIDEFORCE AND YAWING MOMENT ON VARIOUS STORE ARRANGEMENTS MOUNTED BENEATH A 45° SWEPT WING-FUSELAGE MODEL

Test have been made in the A.R.A. 9 ft x 8 ft transonic tunnel on a streamlined store-pylon arrangement mounted in various locations beneath a 45° swept wing-fuselage model Six-component measurements of both the loads on the store including pylon-induced effects, and of the total store plus pylon loads have been obtained for Mach numbers from M = 0 60 to M = 1 41 This note presents the full sideforce and yawing moment results These are analysed in detail and related to the likely sidewash field beneath the wing at both subsonic and supersonic speeds, as obtained from other sources. The experimental sideforce results are compared with estimates based on

the/

the empirical method presented in A.R.A Report No 5 These comparisons show that certain changes in the empirical method are desirable and appropriate suggestions are made in this note, a final revision will be made when further experimental results are available showing in particular, the effects of changing the depth of the store beneath the wing

The unpublished results of some ad hoc tests at transonic speeds on winged missiles mounted beneath both a 60° delta and a 40° swept-back wing are given in order to emphasise the dangers in using the empirical method for stores which have significant wing-type lifting surfaces

C.P. No. 955

Printed and published by
HER MAJESTY'S STATIONERY OFFICE

To be purchased from
49 High Holborn, London W C 1
423 Oxford Street, London W 1
13A Castle Street, Edinburgh 2
109 St Mary Street, Cardiff
Brazennose Street, Manchester 2
50 Fairfax Street, Bristol 1
35 Smallbrook, Ringway, Birmingham 5
7 - 11 Linenhall Street, Belfast 2
or through any bookseller

Printed in England

C.P. No. 955

S O Code No 23-9017-55